DOCTORAL (PhD) DISSERTATION

KALPITA SINGH

GÖDÖLLŐ

2026

Hungarian University of Agriculture and Life Sciences

Redox control of physiological and biochemical processes in maize

Kalpita Singh

Gödöllő

2026

The PhD School

Name: Doctoral School of Agricultural and Food Sciences

Discipline: Crop and Horticulture Sciences

Head: Prof. Dr. Melinda Kovács
Professor, MTA member
Institute of Animal Physiology and Nutrition,
Hungarian University of Agriculture and Life Sciences

Supervisors: Dr. Gábor Kocsy
Scientific advisor
Agricultural Institute, HUN-REN Centre for Agricultural Research

Dr. Dávid Polgári
Assistant Professor
Hungarian University of Agriculture and Life Science

.....
Approval of the Supervisor

....

Approval of the Head of Doctoral School Approval of the Supervisor

TABLE OF CONTENTS

ABBREVIATIONS

ABA- Abscisic acid

ADC- Arginine decarboxylase

AO- Ascorbate oxidase

APX- Ascorbate peroxidase

Asc- Ascorbate

Asc-GSH cycle- Ascorbate-Glutathione cycle

BR- Brassinosteroids

CAT- Catalase

CG- Cysteinylglycine

Cys- Cysteine

DAO- Diamine oxidase

DAP- 1,3-diaminopropane

DHA- Dehydroascorbate

DHAR- Dehydroascorbate reductase

DPA- Dihydrophaseic acid

GA- Gibberellic acid

GPX- Glutathione peroxidase

GR-Glutathione reductase

GSH- Glutathione

GSSG- Glutathione disulfide

H_2O_2- Hydrogen peroxide

H_2S- Hydrogen sulfide

HPLC- High-performance liquid chromatography

IAAO- Indole-3-acetic acid oxidase

JA- Jasmonic acid

JA-LE/ILE- JA-isoleucine/ leucine

MDA- malondialdehyde

MDHA- Monodehydroascorbate

MDHAR- Monodehydroascorbate reductase

MQ- Milli-Q water

NaHS- Sodium hydrosulfide

NO- Nitric oxide

OASTL- O-acetylserine (thiol)lyase

***o*HCA**- *ortho*-hydroxycinnamic acid

PA- Phaseic acid

PAO- Polyamine oxidase

POD- Peroxidase

PPO- Polyphenol oxidase

Pro- Proline

PRXs- Peroxiredoxins

PTMs- Post-translational modifications

PUT- Putrescine

ROS-Reactive oxygen species

SA- Salicylic acid

SOD- Superoxide dismutase

SPD- Spermidine

SPDS- Spermidine synthase

SPM- Spermine

SPMS- Spermine synthase

TCA- Tricarboxylic acid cycle

TRXs- Thioredoxins

γ-EC- γ-glutamylcysteine

γ-ECS- γ-glutamylcysteine synthase

1. INTRODUCTION

Maize is utilised globally, either as a staple food, fodder crop or in the production of ethanol. Its origin can be traced back to ancient civilisations of the Mayans and Aztecs. Contrary to the earlier prevalent view, the new findings provide evidence of the mixture of two genomes of *Zea mays* ssp. *parviglumis* and *Zea mays* ssp. *mexicana* (YANG et al., 2023). Hundreds of years of domestication and selective crop breeding techniques have significantly improved maize production (YANG et al., 2023). The development and registration of the first inbred maize hybrid (Mv5) in Hungary, Europe and the release of the first commercial maize hybrid in the USA mark the milestone steps for mankind in maize improvement programmes (JÁNOSSY et al., 1957; MARTON, 2013; TROYER, 1995). A significant increase in maize production and demand has been observed over the years. However, with shifting habits to gluten-free options along with the population boom, the demand for maize has increased. This inflated demand, together with changing climate conditions, necessitates the need to develop stress-resilient crops (CGIAR, 2024).

In order to develop stress-tolerant crops, we first need to understand the signalling triggered in plants when faced with stress. Under unfavourable environmental conditions such as drought, salinity or the presence of a pathogen, stress-specific molecular sensors are activated in the cells that are in contact with the stimuli. After perceiving the stress, the message needs to be shared with the neighbouring cells and ultimately with the whole plant (LAMERS et al., 2020). Thus, to perform this, a transient Ca^{2+} wave is formed with Ca^{2+} accumulation in the cytosol. Furthermore, plants generate reactive oxygen species (ROS) at the expense of energy via the enzyme NADPH oxidase. These changes are sensed in the adjacent cells. The formed ROS wave, together with the Ca^{2+} wave, helps in primary signal transduction and triggers the downstream signalling in the whole plant (LAMERS et al., 2020). The change in cellular redox homeostasis stimulates the antioxidant system and modifies the transcriptome and metabolome. To further strengthen the stress signal perceived, a series of protein phosphorylations is initiated, including the Mitogen-Activated Protein Kinase (MAPK) cascade and sucrose non-fermenting-1-related protein kinase 2 (SnRK2) modules (ZHANG et al., 2023). It is essential to understand that instead of a single chain reaction, stress perception, signalling, and ultimately adaptation are a network of cross-communications with nodes and one molecule affecting multiple at different layers. For instance,

the ROS wave triggers the antioxidant system that initiates ROS scavenging, but at the same time stimulates hormonal production, such as abscisic acid (ABA) and jasmonic acid (JA), which further complements ROS production via NADPH and boosts antioxidant enzymes to maintain ROS balance (DEVIREDDY et al., 2021). These changes govern transcriptional reprogramming and exhibit stress adaptive responses such as the accumulation of osmoprotectants, biosynthesis of antioxidants, amino acid profile modifications, and changes in carbon and nitrogen assimilation (ZHANG et al., 2023). Therefore, understanding redox alteration and its crosstalk with other components, such as hormones, amino acids, and thiols, could provide helpful insights to not only curb the global hunger but also fight against the prevailing nutritional hunger. The focus of the present study is to understand the holistic network of simultaneous modulations in the hormonal profile, carbohydrates, organic acids, amino acids, polyamines, phenylpropanoids, and the redox system at the metabolic and genetic level by the application of two reductants (ascorbate -Asc, and sodium hydrosulfide- NaHS) and one oxidant (hydrogen peroxide- H_2O_2). The main problem addressed in the study is the influence of 3 different redox compounds on the internal redox chemistry of the plants governing metabolism and hormone interaction with the redox homeostasis to modulate seedling growth.

The present results improve our understanding of redox chemistry governing maize seedling growth, metabolism and stress-related signals. The results obtained provide useful insight for targeted metabolic engineering of maize to enhance stress tolerance and nutritional quality.

2. OBJECTIVES

- To characterise the effects of three redox compounds (Asc, H_2O_2, and NaHS) on seedling growth and cellular redox homeostasis in maize.
- To investigate the redox-modulated regulation of the central carbon and nitrogen metabolism (carbohydrates, organic acids, amino acids, and polyamines) to identify redox-sensitive metabolic pathways.
- To identify and analyse redox-dependent specific changes in the hormonal profile at the transcriptional and metabolic levels.
- To explore the interplay between redox homeostasis and holistic plant metabolism to understand the simultaneous changes in metabolic pathways in response to redox imbalance.

3. LITERATURE REVIEW

3.1. *Maize: history, consumption, and production trends*

Maize (*Zea mays* L.) is a crop with multiple uses. It is a staple food used globally, to being used as biofuel in ethanol production. The crop originated in Mexico and served as the main ingredient in the diets of ancient civilisations, such as the Mayans and Aztecs. Earlier, it was thought that maize originated from the domestication of a single wild grass, *Zea mays* ssp. *parviglumis* Iltis & Doebley, about 9,000 to 10,000 years ago (TANUMIHARDJO et al., 2020). However, a recent study published in Science challenged this theory as they provided the evidence that 15– 25% of the genetic material in the present-day maize is contributed by a second highland teosinte - *Zea mays* ssp. *mexicana* (YANG et al., 2023). Based on genetic screening of more than 5000 varieties of maize and related species, the study concluded that about 4000 years after the initial domestication, gene flow from the second teosinte occurred in *Zea mays* ssp. *parviglumis* Iltis & Doebley. This resulted in the mixture of these two genomes, with *Zea mays* ssp. *mexicana* alleles affecting traits such as flowering time, circadian clock, kernel size, and disease resistance (YANG et al., 2023). For hundreds of years, scientists around the globe have been developing maize hybrids, with the first commercially sold in the USA, resulting in an additional $300 million in annual income from maize breeding (TROYER, 1995). In Europe, it was the Martonvásár research institute, Hungary, that released the first inbred maize hybrid in 1953. Dr. Endre Pap developed the first inbred maize hybrid in 1953 by breeding and registered it as Martonvásári 5 (Mv 5), contributing significantly to enhancing maize production in Hungary (JÁNOSSY et al., 1957; MARTON, 2013).

From the dawn of civilisation to the present day, maize cultivation and consumption have increased significantly. It witnessed a dramatic growth of +97% from 2000 to 2022, with the highest production of approximately 1.2 billion tonnes in the year 2022, compared to other cereals such as wheat, rice, barley or sorghum (FAOSTAT, 2023). The Consortium of International Agricultural Research Centres (CGIAR) predicts a steady increase in maize demand, with expectations to be almost double by 2050 compared to 2010. This hike in demand is propelled by population growth, changing lifestyles, and the need for animal feed (CGIAR, 2024). However, the same report also highlighted a downward projection in maize production, with climate change and declining land and water resources as the main driving factors (CGIAR, 2024). We already witnessed such a

decline, as maize production dropped by 44 million tonnes (4%) from 2021 to 2022 due to drought in major maize-producing European countries, with war and weather conditions further affecting (37%) maize production in Ukraine (FAOSTAT, 2023). Therefore, in the current scenario of constantly increasing demand and declining production, it is vital to understand the molecular mechanisms to develop stress-resilient crops.

3.2. *Reactive oxygen species and the redox system*

Reactive Oxygen Species (ROS) are the signalling molecules containing reactive oxygen that can readily donate or transfer an electron. This ability of transferring excited energy to another molecule works as a two-edged sword. On one hand, when ROS levels are below a certain threshold, they act as signal transducers, involved in a quick and agile response to various external stimuli. On the other hand, if their levels exceed this threshold, they induce oxidative stress, often leading to damaged DNA, RNA, and lipids and causing cell death in severe cases. However, a point to mention here is that there are certain biological processes which involve an 'imposed oxidative state', as they are crucial for the maintenance of quiescence and stem cells, and even seed germination. Nevertheless, plants maintain a complex system comprising antioxidant enzymes and compounds to scavenge these ROS and keep their levels in check (MITTLER et al., 2022). A complete list of these ROS in plants is compiled by MITTLER et al. (2022). In this work, we mainly focus on hydrogen peroxide (H_2O_2).

Plants produce ROS, such as H_2O_2, either as a by-product of the metabolic reactions, including photosynthesis, respiration, or polyamine degradation. Their formation is also possible at the expense of energy via the dedicated enzymes, such as respiratory burst oxidase homologues (RBOHs) **(Fig. 1)** (Mittler et al., 2022). Chloroplasts are the primary source of ROS as they are produced during photosynthesis (light-dependent reactions and Mehler reaction); in mitochondria, during aerobic respiration; in peroxisomes, during photorespiration and breakdown of lipids; and various other environmental conditions also trigger ROS formation **(Fig. 1)**.

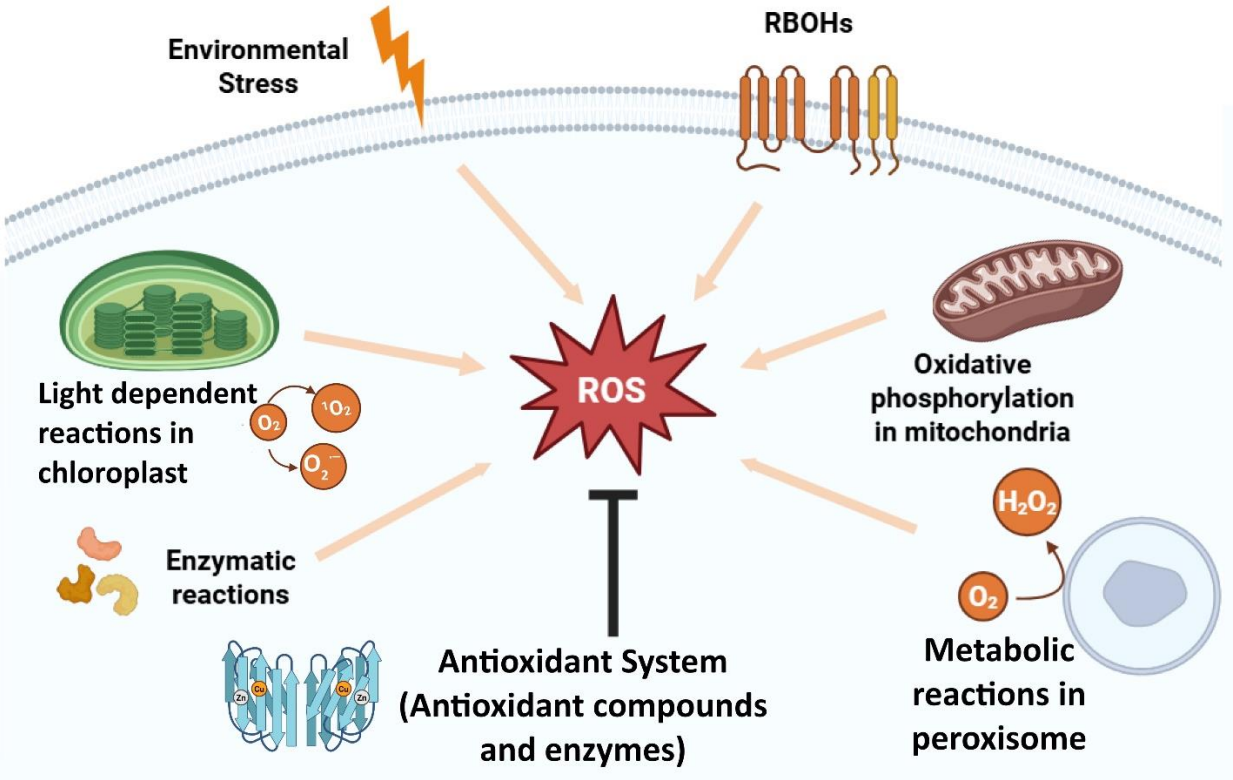

Figure 1: An overview of various sources of ROS formation in plants. Respiratory burst oxidase homologues (RBOHs) are the dedicated enzymes for ROS formation. In mitochondria, ROS are formed by the electron leakage from the electron transport chain. In peroxisomes, the ROS are formed as a consequence of lipid breakdown and photorespiration. Other enzymatic processes, such as polyamine oxidation also release H_2O_2 as a by-product. Chloroplasts are the primary source of ROS formed during the process of photosynthesis. Other external environmental conditions (such as drought, salinity, and high light) also trigger ROS formation. The antioxidant system, comprising the antioxidant compounds such as ascorbate, glutathione, phenols, and enzymes including superoxide dismutase, catalase, ascorbate peroxidase, etc., is responsible for scavenging accumulating ROS and keeping the levels in check.

Interestingly, the ROS are evolutionarily conserved and can be found from unicellular organisms to mammalian cells, serving as a signalling and communication mechanism between cells (FICHMAN et al., 2023). Furthermore, H_2O_2 is one of the most stable ROS. Its ability to cross the plasma membrane via aquaporins, along with the interaction with various transcription factors, makes it an excellent signalling molecule (ALI et al., 2023). The role of these ROS is diverse and indispensable. For instance, they not only regulate plant growth via cell division and differentiation but are also crucial for the induction of calcium and hormonal signalling. In addition, they regulate root development, flowering, senescence, and epigenetic response (FOYER AND KUNERT,

2024). Moreover, ROS signalling is vital for cell-to-cell and even plant-to-plant communication. This is achieved by activating the RBOHs in the cell that is directly in contact with the stimulus. Receptors such as HPCA1 (H_2O_2-induced Ca^{2+} increase 1) further facilitate this process. The receptors of the adjacent cell sense the H_2O_2 production, which in turn triggers its own ROS formation. This propagates and amplifies the received signal, ultimately leading to heightened ROS accumulation and thereby forming a ROS wave. This ROS wave eventually facilitates the long-distance signalling throughout the plant. Thus, inducing adaptive responses under stressful conditions, such as hormonal modification and gene expression changes (FOYER AND KUNERT, 2024).

ROS are important components of the redox system of plant cells in which the various redox reactions occur. These reactions involve the transfer of electrons from the donor molecules (acting as reductants) to the acceptor molecules (acting as oxidants), thereby helping to maintain a delicate balance of cellular redox homeostasis. Synthesising the energy coins, such as NAD^+/NADH and $NADP^+$/NADPH, comes at an unavoidable cost of generating H_2O_2. Thus, the whole metabolism is linked with redox state and vice versa (MITTLER AND JONES, 2024). This idea of metabolism regulating redox and redox homeostasis, in turn, regulating metabolism, is elucidated by GEIGENBERGER AND FERNIE (2014). The article summarises that the redox state is mediated by NAD(H)/NADP(H) and thiol/disulfide across organelles like chloroplasts, mitochondria, and peroxisomes. They generate redox signals through processes like respiration and photorespiration, affecting not only their own metabolism but also coordinating across compartments (GEIGENBERGER AND FERNIE, 2014). Thus, the redox system becomes an indispensable part of plant metabolism and understanding it becomes even more important to develop stress-resilient crops.

3.3. *Antioxidant system and the ascorbate-glutathione cycle*

It is vital to understand that plants counteract ROS accumulation actively by either transporting or scavenging them. As discussed earlier, the antioxidant system consists of enzymes and compounds that exhibit scavenging activity to protect cells from oxidative damage by inhibiting ROS **(Fig. 1)**. Broadly, the antioxidant enzymes consist of superoxide dismutase (SOD), catalase (CAT), ascorbate peroxidase (APX), glutathione reductase (GR), monodehydroascorbate reductase (MDHAR), dehydroascorbate reductase (DHAR), glutathione peroxidase (GPX), glutathione S-transferase (GST), and thioredoxins (TRXs). Non-enzymatic antioxidants include ascorbate (Asc),

glutathione (GSH), phenolic compounds, alkaloids, flavonoids, carotenoids, certain amino acids and α-tocopherols. Apart from them, various vitamins (vitamin B and E) and minerals (copper, iron and zinc) also act as cofactors of antioxidant enzymes. Their absence can even severely hinder antioxidant activity (MEHLA et al., 2017). Of these, the Asc, GSH and related enzymes form the antioxidant cycle known as the Ascorbate-Glutathione cycle (Asc-GSH cycle) (**Fig. 2**). It detoxifies H_2O_2 and converts it into water (FOYER AND KUNERT, 2024). It was first described in the chloroplast by FOYER AND HALLIWELL (1976), and thus is often called the Foyer-Halliwell-Asada pathway. The enzymes of the cycle are present in various intracellular compartments, and enzymes like APX and DHAR have been localised in the apoplast as well. Firstly, superoxide anion (O_2^-) is acted upon by the enzyme SOD and is converted to a less reactive H_2O_2. Then, APX transforms H_2O_2 to H_2O by utilising reduced Asc as the electron donor. As a result of electron loss, Asc changes to monodehydroascorbate (MDHA). It is an unstable radical; therefore, it can either undergo spontaneous dismutation and form Asc and dehydroascorbate (2MDHA → Asc + DHA) or can be directly converted to Asc by MDHAR using NADH, thus replenishing the Asc pool. DHA is the fully oxidised form of Asc, and to maintain the redox homeostasis, it needs to be reduced again. Therefore, the enzyme DHAR utilises reduced GSH as the electron source and converts DHA to Asc, thus further replenishing the Asc pool by the redox reaction as DHA + 2GSH → Asc + GSSG. However, during this reaction, GSH loses an electron and is converted to its oxidised form, glutathione disulfide (GSSG). This is recycled back to GSH using NADPH as the electron source by the enzyme GR (FOYER AND NOCTOR, 2013; SINGH et al., 2024). Interestingly, the ability of Asc and GSH to exist in both oxidised and reduced forms is not only beneficial in the Asc-GSH cycle for detoxifying H_2O_2, but also acts as a redox sensor, helping to sense environmental changes and initiate stress-specific downstream signalling (SINGH et al., 2024).

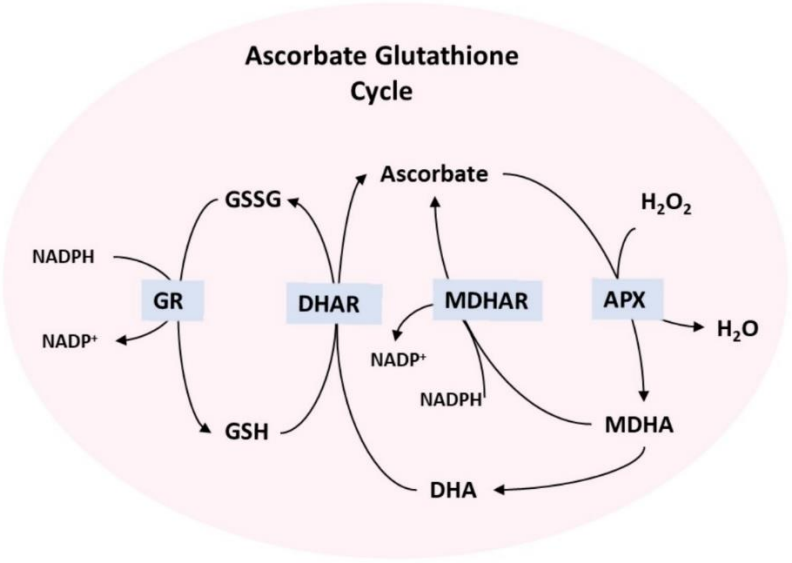

Figure 2: The Ascorbate-Glutathione cycle (Asc-GSH cycle). GR: Glutathione reductase; GSSG: Glutathione disulfide; GSH: Reduced glutathione; DHAR: Dehydroascorbate reductase; DHA: Dehydroascorbate; MDHAR: Monodehydroascorbate reductase; MDHA: Monodehydroascorbate; APX: Ascorbate peroxidase; H_2O_2: Hydrogen peroxide; H_2O: Water.

As described in the previous sections, the enzymes APX, MDHAR, DHAR, and GR are an integral part of the Asc-GSH cycle. The following section discusses these enzymes in detail.

APXs are classified as Class I heme peroxidases within the peroxidase-catalase superfamily that mainly deal with ROS detoxification. It is the haem iron cycling between Fe^{3+} and Fe^{4+} oxidation states that enables electron transfer from Asc to H_2O_2 (Foyer and Kunert, 2024). There are five isoforms of the enzyme known in plants- mitochondrial, cytosolic, chloroplastic, and peroxisomal/glyoxysomal isoforms. Limited substrate availability often results in lower stability of the enzymes with lessened activity (MEHLA et al., 2017). Interestingly, the cytosolic APX of *Oncidium* orchid species (OgcytAPX1) can utilise both GSH and Asc as substrates, though with different active sites. For GSH oxidation, OgcytAPX1 relies on the amino acid residues Pro63, Asp75, and Tyr97, whereas the equivalent positions in *Arabidopsis* do not support GSH binding. Apart from OgcytAPX1, recombinant cytosolic APX isoforms from maize and rice have been elucidated to oxidise GSH. In addition, the enzyme activity is also regulated by post-translational

modifications such as S-nitrosation, tyrosine nitration, and S-sulfhydration (CHIN et al., 2019; FOYER AND KUNERT, 2024).

MDHARs are single polypeptide chains, flavin adenine dinucleotide (FAD)-dependent oxidoreductase enzymes. The bound FAD cofactor is essential for electron transfer from NAD(P)H and reduces FAD to $FADH_2$. The reduced $FADH_2$ then donates an electron to MDHA, converting it back to Asc. The enzyme, thus, replenishes the Asc pool and maintains the efficiency of APX. MDHARs can be classified into chloroplastic/mitochondrial enzymes, peroxisomal membrane-bound, and cytosolic/ peroxisomal classes. In addition, chloroplast-localised MDHARs are known to be activated by TRXs. For instance, plastidial MDHAR in Arabidopsis are specifically regulated by TRXy2 (VANACKER et al., 2018). Moreover, MDHARs can also utilise organic radicals and recycle oxidised forms of phenols, and MDHAR6 can even react with xenobiotics such as 2,4,6-trinitrotoluene (TNT). In general, *MDHAR* overexpression usually corresponds with elevated Asc levels and stress tolerance. In contrast, loss-of-function mutants (as in *MDHAR4* in *Arabidopsis*) exhibit a lower Asc/DHA ratio but maintain the overall Asc pool. Thus, highlighting the importance of MDHAR in maintaining redox homeostasis, but not acting as the sole determinant of Asc content (FOYER AND KUNERT, 2024).

Another vital enzyme of the Asc-GSH cycle that contributes to the Asc pool is DHAR. It uses reduced glutathione to regenerate Asc from DHA. RAHANTANIAINA et al. (2017) confirmed its localisation in the cytosol and chloroplast, along with the cooperative function with salicylic acid (SA) in oxidative stress response. The study further concluded the role of cytosolic DHARs in linking intracellular H_2O_2 scavenging to GSH oxidation, which in turn influences redox-dependent regulation of SA accumulation. In addition, Asc levels remain largely unaffected even when DHAR activity is reduced to minimal levels. The possible explanation for this could be the option of other available paths to maintain the Asc pool by non-enzymatic reduction of DHA by GSH and reducing MDHA by chloroplast ferredoxin or by NAD(P)H-dependent reductase (RAHANTANIAINA et al., 2017). However, these results were in contrast to other studies, where the loss of *DHAR* significantly affected the Asc pool state (CHEN AND GALLIE, 2006; NOSHI et al., 2017, 2016). Hence, it is evident that DHARs, though important, are not the sole determinant for Asc regeneration, with other, as yet uncharacterised potential proteins might exhibit DHAR activity (FOYER AND KUNERT, 2024).

GR contributes to maintaining the glutathione pool by recycling the oxidised glutathione to its reduced state at the expense of NADPH. It is a flavoprotein oxidoreductase NAD(P)H-dependent antioxidant enzyme. It mainly converts GSSG back to its reduced form (GSH) and maintains the reduced GSH pool. Under stressful conditions, the enzyme is responsible for maintaining the GSH/GSSG ratio. It is mainly identified in the chloroplast (70–80%), but its presence is noted in mitochondria and cytosol as well (GILL et al., 2013). *GR1* encodes the enzymes that are localised in the cytosol and peroxisomes, while *GR2* encodes the mitochondrial and chloroplastic form. It also exhibits a key role in stress signalling via its interaction with glutaredoxins (GRX) and TRX to modulate the hormonal pathway, and ultimately the stress response (FOYER AND KUNERT, 2024; RAI et al., 2023).

3.4. *Redox control of physiological and biochemical processes*

3.4.1. *Redox modulation of growth and development*

Plants developed a complex signalling hub integrating the ROS and antioxidant system to sense the environmental stimuli and initiate the specific response. They utilise this redox control to govern nearly all biological processes, ranging from the regulation of metabolism to gene expression. For instance, GRXs regulate meristem growth in maize by modifying the redox state of the target proteins. These enzymes alter the redox state by either breaking disulfide bonds or by adding glutathione to the target protein. A CC-type GRX- Male Sterile Converted Anther1 (MSCA1), along with ZmGRX2 and ZmGRX5, regulates the transcription factor Fasciated Ear4 (FEA4; involved in preventing excessive inflorescence meristem growth that forms flowers and ears in maize). Knockout mutant plants lacking all three GRXs had shorter height, stunted meristem, ear, and tassel development. Thus, the study concluded that GRXs alter the redox state of FEA4, which in turn affects its DNA binding and gene expression (YANG et al., 2021). Likewise, cellular redox state regulates cell cycle and proliferation. The stem cells in the quiescent centre of the roots are arrested at the G1 phase by maintaining a highly oxidised environment (low accumulation of GSH and Asc) along with auxin maxima. However, when these cells were supplemented with reduced Asc and GSH, the cells started to transit from G1 to the S phase of the cell cycle. In addition, the movement of GSH from the cytosol to the nucleus creates a redox gradient with an oxidised cytosol and a reduced environment in the nucleus, thus safeguarding it during arrested growth (FOYER AND NOCTOR, 2013). Moreover, subcellular redox changes

regulating growth in plants are well documented by KOCSY et al. (2013), with CEJUDO et al. (2021) and VAN AKEN (2021) elucidating the redox metabolism in chloroplasts and mitochondria, respectively. Furthermore, redox balance regulating root growth and architecture (ZHANG et al., 2024), kernel development (ZHANG et al., 2021), organ initiation and shoot meristem maintenance (ZHONG et al., 2025), hormone signalling (SINGH et al., 2025), normal reproduction (JIANG et al., 2022), and pollen development (XIE et al., 2022) in maize are further evidence that redox balance acts as a fundamental regulator of growth, development, and reproduction. Therefore, these observations highlight the central role of redox status in regulating growth and development.

The redox signalling for stress response is achieved by the stress-induced accumulation of ROS. Whenever there are unfavourable changes in the immediate environment, such as heat stress, salinity, or even insect feeding, superoxide and H_2O_2 generation is triggered by plasmalemma-localised NADPH oxidases and peroxidases. They create a sudden oxidative burst and an oxidised environment in the apoplast, whereas the cytosol remains reduced. In addition, ascorbate oxidase (AO) enzyme in the apoplast rapidly utilises reduced Asc to convert oxygen to water, thus changing the Asc redox state as well. This differential redox gradient regulates proteins at the cell surface, along with specific receptors and ion channels. Furthermore, this redox change of the apoplast is sensed by the cytosol, and it triggers downstream signalling, such as the upregulation of the Asc-GSH cycle, formation of secondary metabolites and the modulation of hormones (FOYER AND NOCTOR, 2013; SINGH et al., 2024). These hormones, being modulated by ROS, also contribute to ROS generation to amplify the oxidative burst and strengthen the stress response, while simultaneously regulating the Asc-GSH to scavenge the excess ROS.

As the balance between reductants and oxidants governs almost all biological processes, photosynthesis is also closely related to ROS. The process of photosynthesis generates abundant ROS, not only serving as signalling molecules but also maintaining the flow of electrons from the donor to acceptor molecules. Thus, the process of photosynthesis perfectly integrates ‘energy metabolism and redox balance’ as the central hub. Light reactions in the chloroplast generate ATP, reduced ferredoxins, and NADPH, which are then utilised for carbon fixation. Plants fine-tune the supply of ATP and NADPH, as well as the activity of carbon-assimilating enzymes, via the thiol-disulfide exchange system, which is modulated by TRXs (FOYER, 2018). Also, the proteins inside the thylakoid lumen are redox-regulated. For instance, the immunophilin FKBP13, polyphenol

oxidase, and violaxanthin de-epoxidase are modulated by the oxygen release from photosystem II, creating an oxidative environment (BUCHANAN AND LUAN, 2005). Interestingly, the cell machinery involved in utilising inorganic components to generate a source of reducing power and energy with organic compounds and oxygen is well equipped to prevent redox imbalance, such as the cysteine (Cys)-based redox system and antioxidant enzymes in chloroplasts (RIAZ et al., 2022). Other components of the protective machinery include Asc, which is synthesised in mitochondria and transported to chloroplasts (RIAZ et al., 2022).

3.4.2. *Thiols and redox signalling*

Thiols are organic sulfur-containing compounds with the functional -SH group attached to an alkyl or other organic substituent. In plants, they are synthesised from inorganic sulfate, being sequentially reduced to sulfide, leading to their incorporation into the amino acid Cys via the enzyme O-acetylserine(thiol)lyase (OASTL). Cys serves as the fundamental block for other sulfur-containing molecules, such as GSH, methionine (Met), vitamins and enzymes (PIVATO et al., 2014). Due to the property of Cys to be protonated and deprotonated at different pH levels, it serves as a nucleophile and is involved in redox reactions. Furthermore, the ability to form disulfide bonds (in some cases, reversible disulfide bond formation) not only helps in protein folding but also forms the fundamentals of redox maintenance and enzymatic activity.

The major site for Cys synthesis is the cytosol, with concentrations reaching more than 300 μM, whereas other cell compartments have less than 10 μM. Notably, Cys concentration is highly regulated, as concentrations higher than the threshold are toxic due to its strong reactivity. For instance, it can reduce ferric ions, thereby facilitating oxidative damage through the Fenton reaction. Therefore, the delicate balance is maintained by the coordinated function of the biosynthetic enzyme (OASTL) and degradative enzyme (L-Cysteine Desulfhydrase; DES1) to regulate plant metabolism and stress response (ROMERO et al., 2014). The post-translational modifications of the proteins (especially of the transcription factors) can alter their DNA binding capacity, their stability and subcellular localisation, phase separation, and protein-protein interactions (ZHOU et al., 2023). During the post-translational modifications (PTMs), the Cys can form S-sulfenylated, S-nitrosated, or persulfidated residues through its reaction with H_2O_2, NO, and H_2S. For instance, the enzyme plastidial triosephosphate isomerase, involved in glycolysis and the Calvin cycle, contains a Cys residue at position 74. Under salt stress, H_2O_2 accumulation reversibly modifies (S-sulfenylates) this Cys74 to inhibit its activity, leading to the accumulation

of methylglyoxal. This accumulated methylglyoxal, in turn, acts as a signal for more H_2O_2 production, creating a self-amplifying loop to trigger a stronger stress response (BOUTIN et al., 2024). Furthermore, Cys availability is the rate-limiting step in the biosynthesis of GSH.

GSH not only acts as a low-molecular-weight antioxidant but also serves as a signal in sensing stimuli and initiating a stress response. The multiple roles of GSH are in the biosynthesis of glucosinolate and phytochelatins, metabolism of glyoxylate and formaldehyde, and sulphur assimilation, in maintaining cellular redox homeostasis and related signalling, in primary metabolism, and in plant defence. These functions are further elucidated in the review articles of NOCTOR et al. (2011,2012) and SZALAI et al. (2009). GSH is a tripeptide composed of 3 amino acids- glutamic acid, Cys, and glycine. GSH is mostly present in the reduced state. Its oxidised form, GSSG, is reduced by the enzymes GRs, which catalyse the reduction of disulfide bonds (NOCTOR et al., 2011). Interestingly, overexpressing *chloroplastic γ-glutamylcysteine synthase* (*γ-ECS*) in tobacco caused oxidative stress, leaf senescence, and lesion formation, primarily due to the failure of the redox-sensing process in the chloroplast (CREISSEN et al., 1999). On the contrary, other studies report the beneficial effects of overexpressing *chloroplastic γ-ECS* and observing resistance to heavy metal stress, herbicides, and drought stress (LU et al., 2021; NOCTOR et al., 2012). GSH also acts as the major form of sulfur for transportation via the phloem. It is present in high concentrations in mitochondria, cytosol, and chloroplasts, while lower concentrations are observed in the apoplast. GSH transport from the plasmalemma is facilitated by the oligopeptide transporter family, which can transport GSH, GSSG and other peptides. Other transporters include the Chloroquine Resistance Transporter-Like (CLT) family across the chloroplast and the Multidrug Resistance-Associated Protein (MRP) into the vacuoles (NOCTOR et al., 2011). It is interesting to note that leaf mitochondria lack GSH biosynthesis machinery yet have a very high concentration of it. Therefore, transportation is facilitated to maintain the organelle redox balance.

3.4.3. *Regulatory role of hormones and their interactions with the redox system*

Plant hormones or phytohormones regulate all the critical aspects of plant life, from seed germination to the transition from vegetative to reproductive stages. They control cell division, elongation, coordinate the growth of organs, respond to environmental stress, and regulate the life cycle events as well. The classical phytohormones - auxin, gibberellins (GA), cytokinins, ABA, and ethylene- are considered central regulators, but additional hormones- SA, JA, brassinosteroids

(BR), and strigolactones are also considered as integral parts of the regulatory network (DAS et al., 2025). These phytohormones exhibit crosstalk with each other and with the redox system to fine-tune growth and life cycle transitions. For instance, ABA and GA coordinate seed germination via redox signalling (**Fig. 3**) (CONSIDINE AND FOYER, 2014). ROS are essential for breaking the endosperm barrier during seed germination. However, during seed dormancy, ABA maintains a high antioxidant capacity and a low level of ROS, keeping the cell wall intact so that the radicle cannot break through. Thus, it inhibits seed germination and promotes seed dormancy. In contrast, GA stimulates germination by breaking dormancy. This is achieved by lowering antioxidant ability and promoting DELLA protein accumulation (DELLA represents the names of five specific, highly conserved amino acids found at the N-terminal of the protein- aspartic acid, glutamic acid, leucine, leucine and alanine) degradation, allowing ROS accumulation. This build-up, in turn, causes cell wall loosening and aids in germination (**Fig. 3**) (CONSIDINE AND FOYER, 2014). Another phytohormone, ethylene, is known to influence GSH accumulation in potatoes. The ETHYLENE RESPONSE FACTOR 10 is identified to be a transcriptional activator of the gene *Glutamate-Cysteine Ligase* (*StGSH1*) in potatoes in response to low phosphorus. The study concluded that the StERF10-StGSH1 module plays a vital role in enhancing GSH accumulation, which in turn, boosts antioxidant ability to scavenge ROS and protects the membrane stability under phosphorus starvation in potatoes (TIAN et al., 2026). Likewise, increasing cytokinin levels by silencing the negative regulator *CYTOKININ OXIDASE/DEHYDROGENASE5* (*MdCKX5*) in apples exhibited higher drought stress tolerance and lower accumulation of ROS in juvenile plants. In contrast, when *MdCKX5* was overexpressed, the root vitality decreased, and ROS accumulation increased. Thus, indicating a crosstalk between the phytohormone and redox balance to mediate plant growth and stress response (JIA et al., 2025). The crosstalk of other phytohormones, including brassinosteroids and strigolactones, with ROS and redox homeostasis is thoroughly reviewed by JARDIM-MESSEDER et al. (2025). However, the current study focuses mainly on SA, ABA, and JA. Their detailed interactions with the redox system are discussed below.

SA is mainly associated with biotic stress defence response; however, studies are elucidating its role in abiotic stress as well. For example, ALI et al. (2023) concluded that the exogenous application of SA could mitigate the negative effects of drought and salinity stress in *Brassica* plants. It improved physiological parameters, lowered malondialdehyde (MDA), improved proline, sugar content and antioxidant ability, along with minimising the damage on the ultra-

structures. Interestingly, SA signalling inhibits apoplastic ROS signalling. A fine balance is needed in the ROS levels, as too little ROS would not allow stress signalling, but too much can cause death. This counterbalance is provided by SA, which fine-tunes the ROS levels and helps in the specific response (**Fig. 3**) (Xu and Brosché, 2014). Likewise, VÁSQUEZ et al. (2015) provided a detailed overview of the crosstalk between the redox system (ROS and GSH) and SA in signalling. Initial ROS burst triggers SA biosynthesis and signalling. This activated SA signalling, which in turn modulates redox homeostasis via the Asc-GSH cycle. Thus, showing a close interaction and dependency on the redox homeostasis.

Auxin is the first discovered phytohormone that is essential for cell elongation and apical dominance (especially in shoots), root initiation, tropisms, and fruit development (PARVEEN et al., 2023). Auxin exhibits crosstalk with other phytohormones and signalling molecules at multiple levels, including biosynthesis, transport, and the regulation of gene expression. Redox signalling and auxin incorporate environmental stimuli to modulate growth and initiate the stress-specific responses if needed. For instance, NO and H_2O_2 are involved in auxin-induced adventitious root formation in *Chrysanthemum* cuttings. A dose-dependent synergistic and independent effect of H_2O_2 and NO was noted on the adventitious root formation via the activation of the enzymes polyphenol oxidase (PPO) and indole-3-acetic acid oxidase (IAAO) (LIAO et al., 2010). Moreover, an oxidised cellular environment can alter PIN-formed (PINs) transcription, leading to an altered auxin gradient, transport and localisation. Thus, exhibiting redox regulation in plant development via the regulation of auxin (CONSIDINE AND FOYER, 2014). Other redox compounds, such as Asc and GSH, also modulate auxin sensitivity and signalling to regulate organ development and stress response (PASTERNAK, 2025; PASTERNAK et al., 2020).

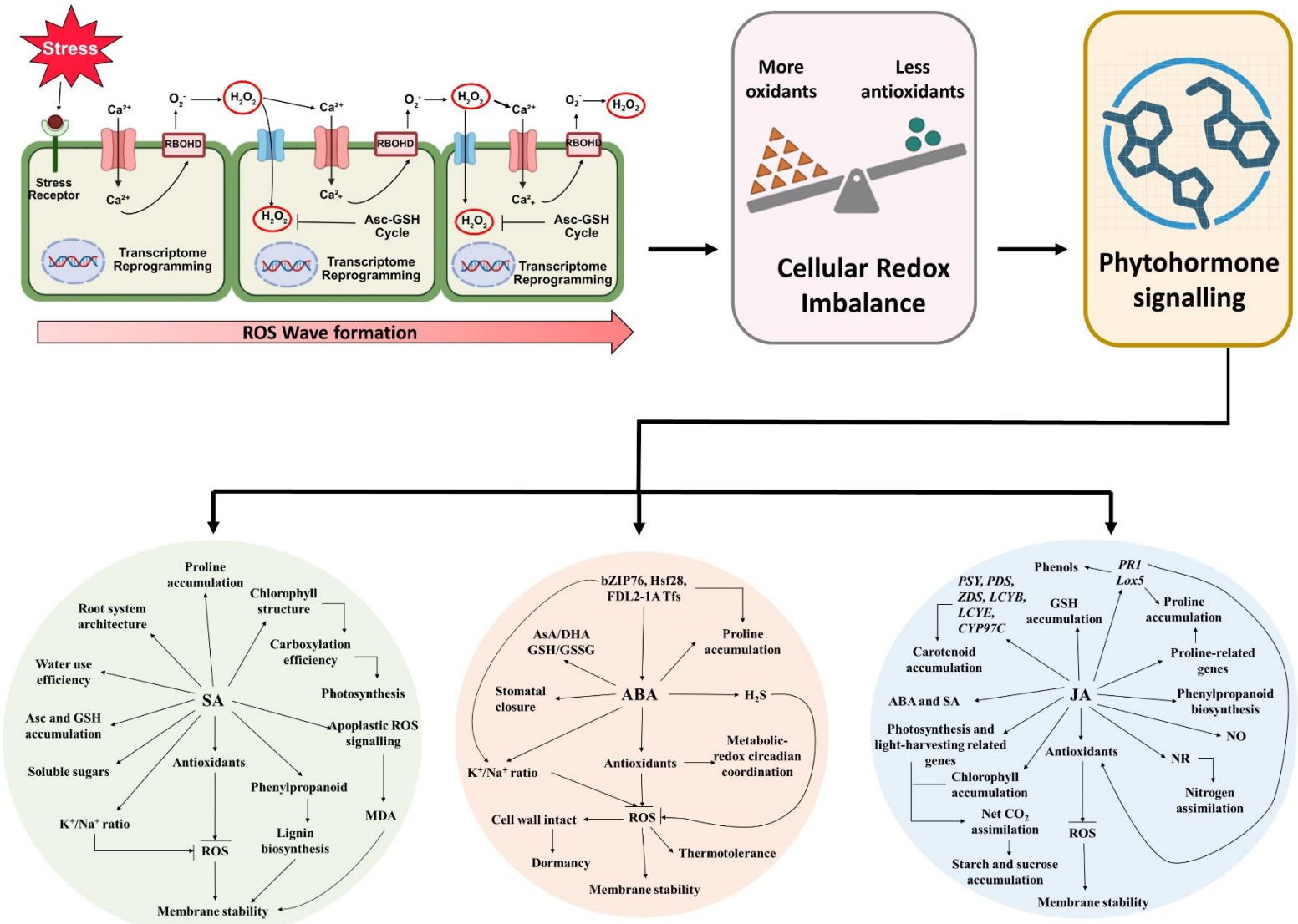

Figure 3: The overview of reactive oxygen species (ROS) wave formation and the crosstalk with the phytohormones. The stress is sensed by receptors, which trigger Calcium influx into the cytosol. This acts as a signal for RBOHs to produce superoxide. This superoxide is converted to H_2O_2 by the superoxide dismutase enzyme. The generated H_2O_2 is sensed by the adjacent cell, and it reaches the cytosol via aquaporins. This further creates calcium ion influx and triggers further ROS formation, thus propagating and amplifying the ROS wave. Elevated ROS levels act as a signal for the activation of the Asc-GSH cycle and the phytohormones. Salicylic acid (SA), jasmonic acid (JA), and abscisic acid (ABA) differently affect ROS levels and antioxidant machinery to modulate growth and stress response. RBOHD: respiratory burst oxidase homolog, H_2S: hydrogen sulfide, Asc: ascorbate, GSH: glutathione, MDA: malondialdehyde, Tfs: transcription factors, NR: nitrate reductase, *PSY*: *phytoene synthase, PDS: phytoene desaturase, ZDS: carotene desaturase, LCYB: lycopene β-cyclase, LCYE: lycopene ε-cyclase, CYP97C: cytochrome P450, PR1: pathogenesis-related protein, LOX5: lipoxygenase 5*, NO: nitric oxide.

ABA was initially associated with senescence, but subsequent studies confirmed its diverse roles. Its crosstalk with other phytohormones and signalling molecules is well-documented in model and crop plants, directing physiology, metabolism and stress adaptation (JIANG et al., 2025; SINGH et al., 2025). A recent study analysed the effect of combined stress (low temperature and drought stress) on quinoa and the beneficial role of ABA application in mediating stress tolerance. Exogenous ABA application induced stress tolerance via the PYR/PYL-PP2C-SnRK2 module. ABA accumulation upregulates the activity of SOD, POD, and CAT, stress-responsive genes, and increases the sugar-to-starch ratio (**Fig. 3**). The study concluded that ABA coordinates molecular pathways that integrate redox homeostasis, carbohydrate metabolism, and circadian regulation to enhance plant tolerance to combined stress (LU et al., 2025). Likewise, the study by DAS et al. (2024) elucidated the crosstalk of ABA and redox metabolism under salt stress in rice. Pre-treatment with ABA improved relative water content, K^+/Na^+ ratio, membrane stabilisation, lower accumulation of ROS (O_2^- and H_2O_2), reduced activity of NADP-oxidase, and active redox turnover. Thus, they demonstrated the active role of ABA in modulating ROS metabolism and oxidative stress signalling to impart tolerance in rice seedlings (**Fig. 3**) (DAS et al., 2024).

JA is another phytohormone derived from linolenic acid and was first identified in jasmonate oils from jasmine. It regulates root growth, seed germination, senescence, tuber formation, and reproductive development. Furthermore, under stressful conditions, it triggers the production of secondary metabolites such as alkaloids and terpenoids. It is mainly associated with defence response against insects, necrotrophic fungi and wounding. However, studies have investigated its role in abiotic stress as well. It orchestrates a networking signal with other phytohormones, including ABA and SA, as well as redox compounds (LIU AND TIMKO, 2021; SINGH et al., 2025). Redox homeostasis and JA signalling together have been shown to contribute to induce cadmium stress tolerance (**Fig. 3**). For instance, the exogenous application of methyl jasmonate (MeJA) in spinach reduced the uptake of cadmium, improved growth parameters, photosynthetic pigments, stomatal conductance, gas exchange, enzymatic activity of SOD, CAT, POD/GPX, and membrane stability under cadmium stress (HAQUE et al., 2025; MONDAL et al., 2025). Likewise, JA and GSH coordinatively induce high light stress tolerance in Arabidopsis. Excessive ROS formation and build-up are observed even after a short exposure to high light. This ROS accumulation disturbs the redox homeostasis and causes oxidative stress. As a response, the

oxylipin/ JA pathways are activated at the genetic and metabolomic levels. These JA-related genes and endogenous levels of JA remain high during the recovery phase. This helps in restoring the GSH/GSSG ratio, Asc/DHA ratio, and maintaining antioxidant enzyme activity, thus enabling a quick recovery. The theory was supported by the performance of *coronatine-insensitive 1* (*coi1*) mutants in which JA perception is hindered. The study concluded that JA, together with GSH, coordinate the plant recovery from high light. Thus, it exhibits the co-dependency of redox metabolism and phytohormone signalling in maintaining plant physiology and metabolism (KILIÇ et al., 2025).

All the above-presented studies not only focus on the explicit role of phytohormones in steering plant growth during stressful conditions but also point out the redox regulation of these phytohormones and vice versa.

3.4.4. *Redox modulation and the role of phenols*

Phenolic compounds are the secondary metabolites consisting of flavonoids and phenylpropanoids (CUONG et al., 2018). They serve as the backbone for plant physiology and biochemistry. They are derived from amino acids such as phenylalanine and tyrosine (Tyr) via the shikimate pathway, and contribute to the formation of pigments, antioxidants, defence molecules, lignins, and even phytohormones (DIAS et al., 2021). Due to their chemical structure and the ability to donate electrons, they also act as the scavengers of ROS (**Fig. 4**).

Phenolic compounds can directly scavenge ROS and can also chelate redox-active metals such as Fe^{2+} and prevent oxidative damage via the Fenton reaction. Interestingly, the changes in the cellular environment trigger their formation and accumulation. A close connection exists between the redox system and phenols. For instance, on one hand, ROS act as a signal to promote phenylpropanoid metabolism via transcription factors like MYB, bHLH, and WRKY. Whereas, on the other hand, these phenolic compounds act as ROS scavengers (LIU et al., 2015). Of the secondary phenolic compounds, *p*-coumaric acid not only possesses antioxidant ability but can also promote the accumulation of compatible osmolytes like proline (**Fig. 4**). When applied exogenously, it can improve growth parameters, accumulate chlorophyll and carotenoids, and positively influence proline, glycine betaine, and SOD activity (NKOMO et al., 2019). Cinnamic acid plays a central role in lignin formation, influences root growth, and mediates stress response via ROS signalling and its levels (**Fig. 4**) (SINGH et al., 2013). Another phenolic compound,

ferulic acid, is also documented to regulate the antioxidant system, cell wall formation, boost photosynthesis and related enzyme activity (**Fig. 4**). Furthermore, it is identified to be a potent antioxidant that scavenges ROS and prevents oxidative damage under stressful conditions (KHAN et al., 2024).

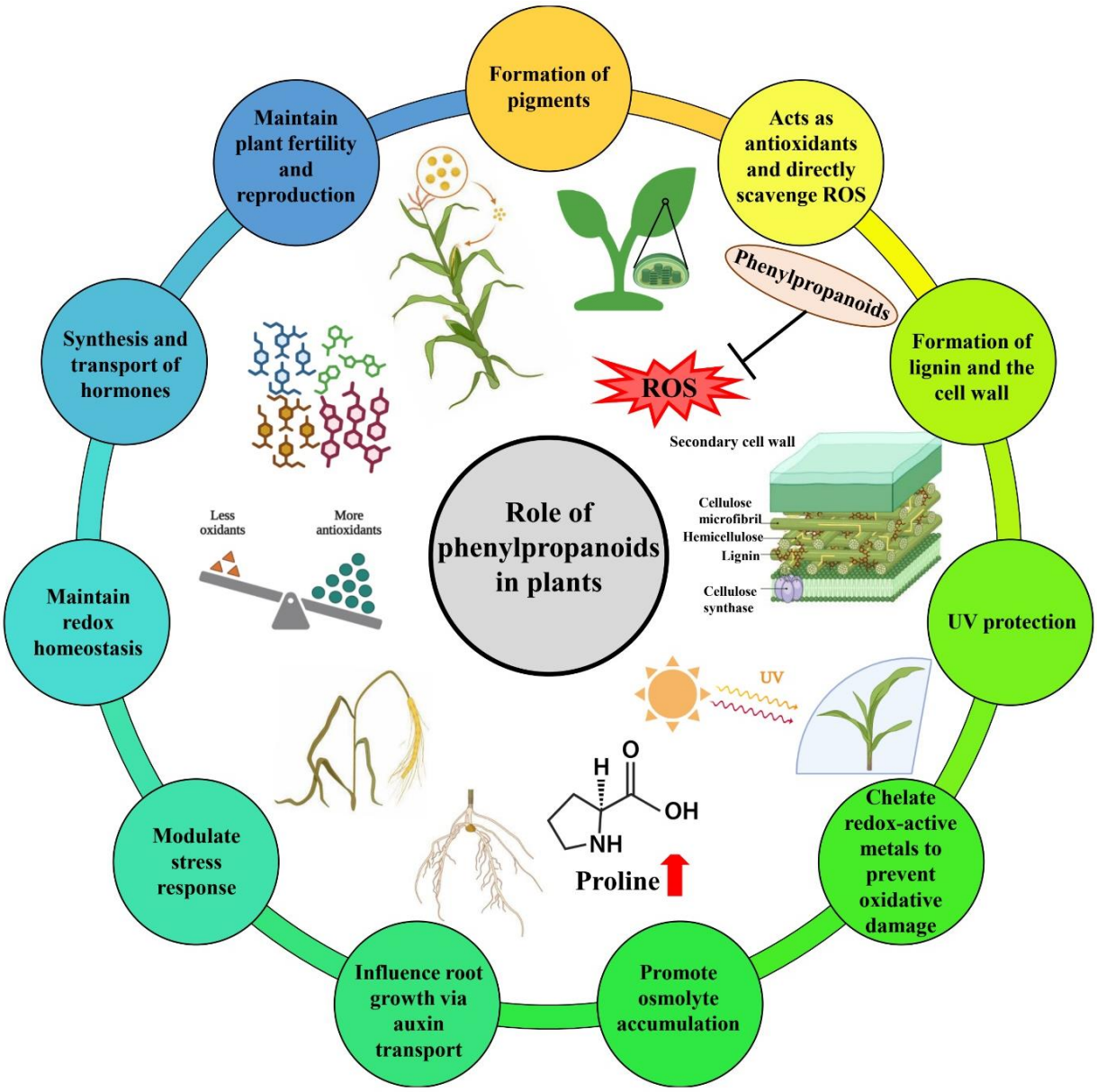

Figure 4: Diverse roles of phenolic compounds in plants. They are involved in pigment, lignin, and cell wall formation, scavenging of ROS, modulating growth and stress response, and are involved in the synthesis of phytohormones and osmolytes such as proline.

Like phenolics, flavonoids also help in maintaining cellular redox homeostasis under stress (**Fig. 4**). Some of the flavonoids, such as naringin, quercetin, luteolin, and rutin, can directly scavenge ROS by neutralising the free radicals. Furthermore, some flavonoids can also chelate metal ions by stabilising their free radicals. Luteolin can also upregulate the antioxidant system and modulate signalling pathways, including nuclear factor erythroid 2-related factor 2 (NRF2), which ultimately helps in maintaining cellular redox homeostasis (**Fig. 4**) (FERNANDO et al., 2024). Likewise, the role of naringin is elucidated in direct ROS scavenging, upregulation of antioxidant enzymes and the Asc-GSH cycle, salt stress tolerance via nitrogen metabolism and ROS signalling (OZFIDAN-KONAKCI et al., 2020).

Thus, with the available literature, it can be concluded that ROS signalling is essential for the synthesis of phenols and flavonoids. These synthesised compounds are not only essential for plant development but are also necessary for maintaining cellular redox balance.

3.4.5. *Sugars and the tricarboxylic acid cycle and their relationship with the redox system*

The process of photosynthesis produces sugars. These sugars are then catabolised in the process of glycolysis. For instance, glucose is broken down to extract the energy for cellular metabolism. Initially in glycolysis, energy is utilised, and glucose is broken down. In the second phase, energy is generated in the form of ATP and NADH, along with two molecules of pyruvate. The cycle is tightly redox-regulated via the enzymes of glycolysis. For instance, pyruvate kinase is sensitive to NAD^+/NADH ratios. It only activates the process when the levels of AMP are high, signalling the need to generate ATP, whereas it slows down the cycle when ATP and NADH levels are high. Thus, it regulates glycolysis and the feeding of substrates for the tricarboxylic acid (TCA) cycle and maintains the cell's overall energy and redox balance (XIONG et al., 2011). The pyruvate is converted to acetyl-CoA by pyruvate dehydrogenase, releasing CO_2 while NAD^+ is reduced to NADH. The produced acetyl-CoA goes to the TCA cycle.

The TCA cycle, or the Krebs cycle, is a sequential chemical conversion of acetyl-CoA to produce energy coins like ATP, NADH, and $FADH_2$. Furthermore, it also provides precursors for the synthesis of essential molecules in a cell. It is a metabolic pathway connecting organic acids, amino acids, and sugars. The cycle is highly redox-regulated via the Cys modifications of the enzymes TRXs. The modifications can either activate or inhibit the enzymes, such as citrate synthase,

succinate dehydrogenase, and fumarase, thereby modulating the carbon flux through the cycle (ZHENG et al., 2025).

The post-translational modifications (PTMs) of the various enzymes of the metabolic pathway are elucidated by ZHENG et al. (2025). For instance, phosphofructokinase is redox sensitive and is inactivated by reduction. Likewise, aldolase and triosephosphate isomerase are S-glutathionylated to partially and reversibly inactivate and inhibit their activity. Other enzymes, such as cytosolic malate dehydrogenase, citrate synthase, aconitase, NAD^+ dependent isocitrate dehydrogenase, succinate dehydrogenase, fumarase, and NAD^+-malic enzyme, exhibit redox switch PTMs to either inhibit or activate the enzyme activity by oxidation or reduction.

3.4.6. *Amino acids and their connection to the redox system*

Amino acids are the building blocks of proteins and thus are indispensable for growth, development, and stress response. They play an integral role in regulating cellular metabolism by serving as the structural components for vital enzymes and precursors for the synthesis of secondary metabolites. It is important to study the modulations of amino acids as they not only confer stress tolerance but also contribute to the nutritional quality of food crops. In the global scenario, wheat and maize can help us not only to fight hunger but also nutritional hunger. To do so, we need to understand the exact mechanism of their biosynthesis and the factors which affect this process. The research can be utilised to modulate or modify amino acid biosynthesis to enhance stress tolerance and elevate the nutritional quality of the target crops as well.

Amino acid biosynthesis and redox regulation are closely interrelated, as these amino acids serve as the precursors for the formation of antioxidant compounds. Glutamate, Cys, and Gly are responsible for the formation of GSH via γ-ECS in energy-dependent enzymatic reactions. Interestingly, γ-ECS is redox-activated, while Cys availability acts as the limiting factor for GSH biosynthesis (DE BONT et al., 2022). In addition, some amino acids, such as Cys and proline, serve as direct antioxidants. Their biosynthesis and signalling are regulated via the redox-dependent modifications of the related enzyme activities. Furthermore, the levels of ROS, Asc, and GSH directly influence the amino acid profile. Redox-based modifications are often observed in the case of Cys and Met. These modifications in the critical residues of the enzymes, in turn, directly regulate the amino acid availability, biosynthesis, signalling, associated metabolic pathways, and ultimately the stress response (GUILLÉN et al., 2022). LIU et al. (2020) observed

nitrogen and sulfur-mediated redox changes in maize. The exogenous application of nitrogen and sulfur increased the levels of GSH, photosynthetic rate, and grain protein concentration. They promoted the amino acid balance by elevating Cys levels in grains along with the levels of lysine, tryptophan, and Met. Therefore, the study concluded the synergistic effects of nitrogen and sulfur on improving maize grain quality and yield by modulation the redox balance of maize leaves and amino acid levels in grains (LIU et al., 2020).

Proline exhibits multiple functions as an osmoprotectant stabilising macromolecules and cell wall and acts as a radical scavenger. It also plays a vital role in vegetative and sexual development. Multiple studies report morphological and developmental changes, and stress sensitivity in proline-deficient mutant or transgenic plants, as reviewed by ALVAREZl et al. (2022). Overexpression of a feedback-insensitive *δ-pyrroline-5-carboxylate synthetase* (*P5CS*) in transgenic *Sorghum* plants positively affected photosynthesis and carbon assimilation rates under salt stress. Similarly, 100 mM proline application to salt-stressed wheat plants improved the stability of photosynthetic pigments. A boost in the activity of photosystems II and I, lowered ROS levels, and enhanced activity of the antioxidant enzymes such as peroxidase, SOD, and CAT were also noted after the treatment. This, in turn, maintained membrane stability and redox balance and reduced salt-stress-induced oxidative damage (KHALID et al., 2025). Likewise, other amino acids, such as GABA, act not only as building blocks but also as signalling molecules. Its crosstalk with other amino acids regulates growth, development, cellular redox homeostasis, and stress response (ZARBAKHSH et al., 2025). In summary, the existing interdependent regulation of amino acids and redox homeostasis regulates plant development and stress adaptation.

3.4.7. *Polyamines*

Amino acids serve as the precursor for the synthesis of polyamines. Major polyamines include putrescine (PUT), spermidine (SPD), and spermine (SPM). They can either be formed from ornithine or arginine. Ornithine decarboxylase directly converts ornithine to PUT with pyridoxal phosphate as the cofactor. In the case of synthesis from arginine, the enzyme arginine decarboxylase utilises arginine as the substrate and converts it to agmatine. This, in turn, is acted upon by agmatine iminohydrolase, which yields N-carbamoylputrescine. Ultimately, N-carbamoylputrescine amidohydrolase yields PUT. The synthesised PUT is converted to SPD and then to SPM via the action of the enzymes spermidine synthase (SPDS) and spermine synthase

(SPMS), respectively (PÁL et al., 2018). The degradation of these polyamines is catalysed by the enzymes diamine oxidase (DAO) and polyamine oxidase (PAO), where DAO shows a preference for PUT, whereas PAO catabolises SPD and SPM. The products of DAO catabolism include 4-aminobutanal (can be converted to GABA), NH_3, and H_2O_2. PAO yields 3-aminopropanal (can be converted to beta-alanine) and H_2O_2. Thus, the oxidation of polyamines yields H_2O_2, which is utilised for stress signalling and contributes to the cellular redox balance directly. On one hand, polyamines act as ROS scavengers, but on the other, contribute to the ROS pool and exhibit pro-oxidant nature. The exogenous application of polyamines induces tolerance in plants against various abiotic and biotic stresses. For example, a dose-dependent and the type of polyamine used (either PUT or SPD or SPM) effects were observed in apricot fruits against *Alternaria alternata*. The application of polyamines modulates redox homeostasis and increases H_2O_2 production, along with the activities and gene expression of antioxidant enzymes. Furthermore, endogenous Asc and GSH levels were also elevated in the fruits after their application (LI et al., 2019). Likewise, SPM and nitric oxide (NO) induced selenium stress tolerance in wheat by improving Asc and GSH levels, activating the antioxidant enzyme activity and lowering the MDA levels (HASAN et al., 2021). In addition, salt-induced osmotic stress was relieved in wheat plants by PUT application by regulating the redox components, including Asc/DHA, GSH/GSSG, APX, GR, DHAR, and MDHAR, with ion homeostasis and MDA levels (ZHAO et al., 2023). Therefore, the available literature hints at the interaction between the redox system and polyamine levels. At the molecular level, studies in Arabidopsis have shown that acetylated PUT catalysed by N-Acetyltransferase Activity1 (NATA1) under pathogen attack competes with SPDS for substrate. Consequently, it lowers H_2O_2 levels and favours the growth of *P. syringae* strain. The lack of H_2O_2 availability hinders stress signalling and represses antimicrobial defence (LOU et al., 2016). Similarly, via H_2O_2-mediated signalling, PUT (8 mM) lowered ABA levels and eventually the stomatal opening. In addition, it also promoted the accumulation of GSH and boosted photosynthesis and growth under salt stress (75 mM) in cucumber plants (MA et al., 2022). In barley, PUT-triggered H_2O_2 accumulation was mediated by H_2S. As the application of hydroxylamine (HA; H_2S scavenger) diminished the effect of PUT-triggered H_2O_2, whereas NaHS application with PUT and H_2O_2 promoted the biosynthesis of UV-absorbing compounds and maintained redox balance (LI et al., 2016). Despite the available literature, most studies focus on the individual pathways and the modulation of specific target genes, but lack the holistic overview of the simultaneous changes

occurring in response to one modification. The present study focuses on the simultaneous changes in the metabolic pathways in response to redox imbalance.

3.5. *Redox modulation of growth and metabolism by Asc, H_2O_2 and NaHS*

The three redox compounds are an integral part of redox sensing and signalling. They interact with other signalling molecules and affect growth, cell division, physiology and biochemistry of plants. Asc is not only an antioxidant, but it also acts as a cofactor for various enzymes (TÓTH, 2023). It reduces Fe^{3+} and makes electrons available for reactions like the synthesis of hormones, alkaloids, and flavonoids. It also serves as a precursor for the synthesis of oxalic acid, L-tartaric acid, and L-threonic acid. In addition, studies elucidate the role of Asc in seed germination and cell division (SINGH et al., 2024). One of the factors that led us to study the effect of Asc on redox-mediated metabolism in maize is its ability to exist in reduced and oxidised forms. Cells maintain a reduced environment by the accumulation of these antioxidant compounds and replenish their pool via energy-investing processes. Under normal conditions, Asc is dominantly present in reduced form; however, under stressful conditions, it is utilised to scavenge H_2O_2 and is converted to its oxidised form (DHA). Plants have dedicated enzymes to convert this oxidised form to the reduced form via DHAR. This process not only scavenges H_2O_2 but also acts as a signal to initiate downstream signalling. The ratios of Asc/DHA and GSH/GSSG are closely related and aid in redox signalling. Studies elucidate the beneficial role of exogenously applying Asc to modulate growth under stressful conditions. For example, the Asc application to marigold flowers under salt stress could mitigate the negative effects of stress on biomass, carotenoids, total phenolics, flavonoids, antioxidant activity, proline accumulation, and membrane injury (AZIZI et al., 2021). Notably, these beneficial effects are concentration-dependent. Higher levels of Asc can cause redox imbalance and even increase the sensitivity to stress. For example, genetically increasing Asc levels in tomatoes caused defects in anther/pollen development, leading to a reduction in fruit yield (DESLOUS et al., 2021). Moreover, in the presence of certain transition metals and an altered redox pool, Asc can exert pro-oxidant effects and generate free radicals (BIELEN et al., 2013). Therefore, we need to understand the beneficial concentration window of Asc and the effects it exerts on redox signalling at a holistic level.

H_2O_2 serves as an excellent signalling molecule due to its ability to cross membranes and its comparatively longer half-life than others. It is used as a signalling molecule to initiate downstream

signalling and induce stress tolerance, along with regulating plant physiology and biochemistry. In contrast, it can cause oxidative damage, membrane injury and electrolyte leakage. It is a double-edged sword that cannot be weighed in the balance of good or bad. It is the necessary evil that nature has artfully invested in. Lower concentrations of H_2O_2 induce stress tolerance, whereas higher levels than the threshold cause oxidative damage. For instance, 1 mM H_2O_2 spraying on the leaves of drought-stressed soybean plants improved relative water content, photosynthetic parameters, lowered membrane injury and stress-induced H_2O_2, along with activating the antioxidant system (SOD, CAT, APX, and POD) and promoting proline accumulation. Thus, H_2O_2 induces stress tolerance via activating the antioxidant system and modulating osmotic balance (RAHMAN et al., 2021). In contrast, LU et al. (2013) noted negative effects of H_2O_2 application on 2 wheat cultivars. The study revealed a significant decrease in root and shoot length and modulations in antioxidant enzyme activity. The underlying reason was the inhibition of cell growth and elongation in roots after H_2O_2 application, which resulted in lower growth parameters. Likewise, inhibition of root elongation and cell expansion was noted in rice (XIONG et al., 2015). In rice, knockout mutants of *NOE1* (encodes for catalase-C) accumulate excessive H_2O_2 and thus, exhibit programmed cell death phenotypes (YOU et al., 2022). Based on the available literature and the reviews (ANJUM et al., 2022; ASAEDA et al., 2022; QURESHI et al., 2022), it is necessary to understand the crop-specific role exerted by H_2O_2 in a concentration-dependent manner. Moreover, utilising the knowledge obtained from model plants needs to be translated to crop plants and field trials for ensuring food security. H_2O_2 is a prime molecule which is an integral part of the signalling cascade and modulates redox balance to regulate growth and development.

H_2S is a gaseous molecule that regulates plant metabolism mainly via protein persulfidation. It is identified to influence seed germination, organ development, stomatal conductance, fruit ripening, photosynthesis, redox balance, and environmental stress response (LI et al., 2024). Like H_2O_2, it is necessary to maintain H_2S homeostasis as it is also toxic at elevated levels. The process of its biosynthesis is tightly regulated by the enzymes. It is synthesised from Cys, mainly via the enzymes L/D-cysteine desulfahydrase (in cytosol), whereas SiR converts SO_3^{2-} to H_2S in the chloroplast. In mitochondria, hydrogen cyanide and L-Cys are utilised to release H_2S along with cyanoalanine. Non-enzymatic H_2S biosynthesis includes the release of H_2S from protein persulfides (P-SSH) by their reactions with oxidants. In addition, mercaptopyruvate sulphurtransferase (MST) forms a sulphur-containing compound MST-SSH. This formed MST-

SSH can react with GSH to produce MST-SH and glutathione persulfide (GSSH). This GSSH can be further converted to H_2S and GSSG. In short, H_2S can be synthesised through both enzymatic and non-enzymatic chemical reactions with sulfur-containing compounds (LI et al., 2024).

Like Asc and H_2O_2, H_2S also exhibits a close relatedness with cellular redox balance as it is known to boost the activity of APX, DHAR, and GR (DE BONT et al., 2022). In addition, it is known to directly interact with ROS metabolism in a redox-dependent manner, modulating the process and enzymes by modifying the Cys residue in PTMs. Conversely, redox homeostasis influences H_2S biosynthesis. The modifications by H_2S at the target Cys residue can alter the protein's structure, location, and activity. In Chinese cabbage, such persulfidation reduces or disrupts the ability of the MADS-box protein encoded by *Flowering Locus C* (*FLC*) to bind its downstream promoters, thereby promoting flowering (MA et al., 2021).

It is imperative to comprehend the interconnected nature of various reactive compounds and redox components (H_2O_2, H_2S, NO), with plant metabolism (glycolysis, TCA cycle, amino acid metabolism, polyamines, and phytohormones), as they function as regulatory agents for growth, in addition to modulating stress and adaptive response. Furthermore, the crosstalk of these pathways influences the biosynthesis of several other compounds, such as flavonoids, thereby contributing to the nutritional quality of the target crops used for food and fodder. However, there is a gap in the exact understanding of the signalling cascade, crosstalk, and fine-tuning of these interrelated molecules under altered redox balance. Therefore, this study focuses on the possible coordination of the changes in redox homeostasis, metabolites, and phytohormones under an altered redox environment induced by the exogenous application of reductants (Asc and NaHS as H_2S donor) and an oxidant (H_2O_2).

4. MATERIALS AND METHODS

4.1. *Plant material and treatments*

Seeds of *Zea mays* L. cultivar 'Ivanka' (Hungarian maize hybrid) were obtained from the Maize Breeding Department of HUN-REN ATK, Martonvásár, Hungary. The seeds were first rinsed with Tween 20, then surface sterilised with 10% sodium hypochlorite, and finally treated with 70% ethanol. Finally, the chemicals were washed off by rinsing the seeds three times with distilled water. Subsequently, the seeds were germinated in rolled moist filter papers for 4 days in the dark at 25 °C. After the emergence of the root and coleoptile, the seeds were transferred to a half-strength Hoagland solution (Hoagland and Arnon, 1938) for cultivation for 7 days at 25 °C with a 12/12 hours light and dark cycle in a growth chamber (Poleco). The seedlings were then treated with 5 mM Asc, 5 mM H_2O_2, and 1 mM NaHS by adding them to the nutrient media in three parallel sets for each treatment, along with the controls. The sampling was done after 3 and 7 days. The concentrations and duration of the treatments were finalised based on the results obtained in pilot experiments. A concentration gradient was set up based on the available literature in other crop plants. Growth parameters were measured to determine the final concentrations that negatively affected plant growth after 3 days of treatment **(Supp. Fig. 1-3)**.

In the final experiments, growth parameters, photosynthetic pigments, electrolyte leakage, lipid peroxidation, endogenous H_2O_2, Asc, GSH, thiols, hormones, flavonoids, and phenylpropanoids, free amino acids, polyamines, metabolites, and NO levels, along with the antioxidant enzymes (APX, MDHAR, DHAR, GR, and CAT) and polyamine catabolism-related enzyme (PAO and DAO) activity, were measured in the shoot samples. To get the insights at the transcriptomic level, the related gene expressions were also analysed.

4.2. *Measurement of photosynthetic pigments*

50 mg of plant tissue was used for the measurement of the photosynthetic pigments. 1 mL of 80% acetone (v/v; 6.65:1 - acetone: milli-q water (MQ)) was added to the sample and centrifuged for 5 minutes at 12,000 g. The supernatant was collected in a sterile tube, and the pellet was washed again with 2 mL of 80% acetone, vortexed and centrifuged. This step was repeated, and the supernatant was pooled until the pellet was white and devoid of pigment. The collected supernatant was diluted to make a final volume of 8 mL, and the absorbance was measured using the spectrophotometer (Varian, Middelburg, The Netherlands) at the wavelengths of 470, 646, 664,

and 750 nm. The calculations of the photosynthetic pigments (chlorophyll a, chlorophyll b, and carotenoids) were performed using the equations outlined by Arnon (1949) (LICHTENTHALER AND BUSCHMANN, 2001).

$$c_a\ (\mu g / mL) = 12.25\ A_{663.2} - 2.79\ A_{646.8}$$

$$c_b\ (\mu g / mL) = 21.50\ A_{646.8} - 5.10\ A_{663.2}$$

$$c_{(x+c)}\ (\mu g / mL) = (1000 A_{470} - 1.82 c_a - 85.02 c_b) / 198$$

4.3. *Measurements of stress markers- electrolyte leakage and lipid peroxidation*

4.3.1. *Electrolyte leakage*

One cm long leaf segments were put into centrifuge tubes containing 10 mL MQ water. They were then incubated for 2 hours on an automatic rotator. The conductance of the 4 mL liquid was measured using a conductometer, and the recordings were noted (termed ECactual- before membrane disruption. After the measurement, the liquid was poured back into the Falcon tubes, and the samples were boiled at 100 °C for 30 minutes to break the cell wall and release all the remaining electrolytes. The conductivity of the liquid was measured again, and the readings were noted again (termed as ECtotal- after membrane disruption). For the calculations, a ratio of ECactual/ECtotal was used, and the results were presented as percentage electrolyte leakage (GULYÁS et al., 2014).

4.3.2. *Lipid peroxidation*

Lipid peroxidation was determined by the endogenous levels of MDA in the shoot samples. 200 mg of the samples were first ground in liquid nitrogen and then homogenised with 600 µL 0.1% (w/v) trichloroacetic acid (TCA; Sigma-Aldrich, St. Louis, MO, USA) with pestle and mortar. The homogenate was centrifuged at 12,000 g for 10 minutes at 4 °C. 2 mL 0.5% (w/v) thiobarbituric acid (TBA; Sigma-Aldrich, St. Louis, MO, USA) dissolved in 20% (w/v) TCA was mixed with the supernatant in a new tube and incubated at 90 °C for 30 minutes. The samples were cooled and then vortexed. Absorbance was measured at 532 and 600 nm using the spectrophotometer (Varian, Middelburg, The Netherlands). The absorbance was corrected by subtracting non-specific absorption obtained at 600 nm from 532 nm. The concentration of MDA was calculated using the extinction coefficient of 155 $mM^{-1}cm^{-1}$ (DE PAULA et al., 1996).

4.4. *Measurement of signalling molecules H_2O_2 and NO*

4.4.1. *Hydrogen peroxide (H_2O_2)*

Endogenous H_2O_2 content was measured using the Ferrous Oxidation-Xylenol Orange assay (FOX1) solution containing 0.1 mM xylenol orange, 100 mM D-sorbitol, and 0.127 mM ammonium Fe sulfate prepared in 2.5 M H_2SO_4. 200 mg of the samples were first homogenised in 1 mL 10% H_3PO_4 and then centrifuged for 15 minutes at 15,000 g and 4 ℃. 50 µL supernatant was mixed with 950 µL of FOX1 solution and incubated in the dark for 30 minutes. Afterwards, the absorbance was measured at 560 nm using the spectrophotometer (Varian, Middelburg, The Netherlands). The reaction was based on the H_2O_2-dependent oxidation of the ferrous ion to the ferric ions, which were detected by xylenol orange as the absorbance at 560 nm (KELLŐS et al., 2008).

4.4.2. *Nitric Oxide (NO)*

Nitric oxide was measured using the Griess diazotisation reaction using the Invitrogen Griess reagent kit (#G7921) and a spectrophotometer. Component A ((1-naphthyl)ethylenediamine) and Component B (sulfanilic acid) were mixed in equal volumes to prepare the working Griess reagent. 200 mg of finely ground samples in liquid nitrogen were homogenised in 600 µL of 0.1 M phosphate buffer (pH 7.4). After centrifugation at 15,000 g, 4 ℃ for 10 minutes, 450 µL supernatant was mixed with 100 µL Griess reagent and 2450 µL MQ water to make a final volume of 3 mL in the tubes. Nitrite standards were prepared by diluting the kit standard to generate a calibration curve. The absorbance was measured at 548 nm using the spectrophotometer (Varian, Middelburg, The Netherlands), and the values were determined using the calibration curve and were expressed on a fresh weight basis.

4.5. *Measurements of Asc and thiols*

4.5.1. *Total Asc*

Total Asc was quantified following the protocol of SZALAI et al. (2014) with modifications. 500 mg of samples ground in liquid nitrogen were homogenised with ice-cold 3 mL 5% (w/v) metaphosphoric acid. The extract was transferred to dark brown centrifuge tubes to protect ascorbate from photodegradation and then centrifuged at 10,000 g for 10 minutes at 4 ℃. To reduce DHA to Asc and allow the measurement of total Asc, 950 µL of the supernatant was mixed with 50 µL freshly prepared dithiothreitol (DTT) solution (40 mg mL^{-1} in MQ water). The mixture

was incubated for 25 minutes in the dark at room temperature. Afterwards, the samples were measured immediately by HPLC using an Alliance 2690 system equipped with a W996 photodiode-array detector (Waters, Milford, MA, USA).

4.5.2. *Total and oxidised thiols*

The measurement of total, reduced, and oxidised thiols was done following the protocol of TARI et al. (2002) with modifications. 200 mg of the samples were homogenised in 0.1 M HCl to stabilise thiols and prevent their oxidation. The homogenate was centrifuged at 15,000 g for 10 minutes at 4 ℃. The supernatant obtained was divided into 2 parts and used subsequently for derivatisation.

For oxidised thiols, 200 µL of the supernatant was mixed with 300 µL 0.2 M 2-[cyclohexylamino]ethane-sulphonic acid (CHES, pH 8.5) and 15 µL of 50 mM N-ethylmaleimide (NEM) to block reduced thiols. The mixture was vortexed and incubated at room temperature for 15 minutes. Excess NEM was removed by washing the solution three times with 500 µL toluene; after each washing, the aqueous phase was recovered and centrifuged at 15,000 g for 5 minutes. The aqueous phase was then transferred to new tubes containing 20 µL of distilled water. To reduce the oxidised thiols, 10 µL of 9 mM DTT was added, and the mixture was incubated for 1 hour at room temperature. Subsequently, 20 µL of 15 mM monobromobimane (mBBr) was added, and the samples were incubated in darkness for 15 minutes. The reaction was stopped by adding 250 µL of 0.25% (v/v) methanesulphonic acid (MSA), and the samples were measured by HPLC using an Alliance 2690 system equipped with a W996 photodiode-array detector (Waters, Milford, MA, USA).

For the determination of total thiols, 200 µL of the acid extract was mixed with 200 µL of 0.2 M CHES and 10 µL of 9 mM DTT and incubated at room temperature for 1 hour to reduce all thiols. The samples were then derivatised with monobromobimane, and the reaction was stopped with 250 µL MSA, following the same steps as for reduced thiols before loading the samples into HPLC.

4.6. *Antioxidant and polyamine catabolism enzymes*

4.6.1. *Antioxidant enzymes - APX, MDHAR, DHAR, GR, and CAT*

The enzyme activity was determined using the MES/KOH extraction buffer, consisting of 50 mM MES, 40 mM KCl, and 2 mM $CaCl_2$ at pH 6.0 (MURSHED et al., 2008). 200 mg plant samples were first pulverised in liquid nitrogen, and then 1 mL of extraction buffer and 100 µL of 1 mM Asc (freshly prepared) were added to each sample. After centrifugation at 14,000 g for 10 minutes

at 4 °C, the plant extract was divided into aliquots for the subsequent measurement of the enzyme activities of GR, APX, DHAR, MDHAR, and CAT. Each reaction mixture contained the following components in the given concentrations in a 1 mL volume. The enzyme activity was calculated on a protein basis, measured according to BRADFORD (1976).

APX: 50 mM Potassium Phosphate buffer (pH 5.7; 0.05% BSA); 0.25 mM Asc; 5 mM H_2O_2; 50 µL plant extract. The activity was measured by the decrease in the H_2O_2 content (decomposition of the H_2O_2) at 290 nm for 2 minutes.

MDHAR: 50 mM Hepes buffer (pH 7.6), 2.5 mM Asc, 0.25 mM NADH, 1 U Ascorbate oxidase, and 50 µL plant extract. The activity was determined by measuring the decrease in the substrate at 340 nm over 2 minutes.

DHAR: 50 mM Hepes buffer (pH 7.0), 0.1 mM EDTA, 2.5 mM GSH, 0.2 mM DHA, 50 µL plant extraction. The activity was measured by the increase in the degradation product at 265 nm for 2 minutes.

GR: 50 mM Hepes (pH 8.0), 0.5 mM EDTA, 0.25 mM NADPH, 0.5 mM GSSG (freshly prepared), 50 µL plant extract. The activity was determined by measuring the decrease in the substrate at 340 nm for 2 minutes.

CAT: 0.5 M Phosphate buffer (pH 7.5), 15 mM 30 % H_2O_2, and 40 µL plant extract. The activity was determined by measuring the decrease in the substrate at 240 nm for 3 minutes (Beers and Sizer, 1952).

4.6.2. *Polyamine catabolism enzymes -DAO and PAO*

DAO (EC 1.4.3.6) and PAO (EC 1.5.3.11) enzyme activities were measured using 200 mg of shoot tissues. The sample was first ground in liquid nitrogen, then homogenised with 600 µL of cold extraction buffer containing 1 M Tris (pH 8), 50% glycerol, 20% Triton X-100, 1 mM peptin, and 100 mM PMSF. After incubation on ice for 20 minutes, the mixture was centrifuged at 12,000 g for 10 minutes at 4 °C. The resulting supernatant was divided into two parts for separate DAO and PAO assays. For each reaction, 150 µL of the supernatant was mixed with potassium phosphate buffer (100 mM, pH 6.6) and 7.5 µL 1 M PUT (for DAO) or SPM (for PAO). The mixture was vortexed and incubated at 37 °C for 90 minutes. The reaction was stopped by adding 48.8 µL of 20% TCA. Then, 22.5 µL of 0.1% 2-aminobenzaldehyde in ethanol was added to develop the Δ-

pyrroline derivative. After 30 minutes of incubation on ice, absorbance was recorded at 430 nm to quantify enzyme activity (TAKÁCS et al., 2016).

4.7. *Gene expression analysis*

100 mg of the sample was pulverised in liquid nitrogen and mixed with TRIzol reagent (Directzol^{TM} RNA miniprep kit, Zymo Research). Total RNA was extracted as per the instructions of the RNA extraction kit (Directzol^{TM} RNA miniprep kit, Zymo Research) with the DNase I treatment. After measuring the RNA concentration using a NanoDrop2000 (Thermo Fisher Scientific, Wilmington, USA), the volume of RNA (which contains 1 µg) was calculated for each sample by the formula: $V_{RNA}(\mu L) = 1000/y$, where y stands for the measured RNA concentration in ng/µL. V_{RNA} was diluted with MQ water to reach a total volume of 10 µL. To each sample, 1 µL of 100 µM oligo-dT primer was added, then it was vortexed, centrifuged and incubated at 70 °C for 5 minutes and then at 4 °C for an additional 5 minutes in MJ Research PTC-200 Thermal Cycler (Bio-Rad Laboratories Inc., CA, USA). The mastermix was prepared with the template solution, 5 µL M-MLV RT 5x buffer, 1.25 µL dNTP mix (10 mM), 0.5 µL M-MLV RT (200 U μL^{-1}; Product number: M1701, Promega Corporation, Madison, WI, USA), and 7.25 µL MQ water. The samples were vortexed, centrifuged and put in the thermocycler (MJ Research PTC-200 Thermal Cycler; Bio-Rad Laboratories Inc., CA, USA) with the conditions as - 25 °C for 5 minutes, then 42 °C for 60 minutes, followed by 70 °C for 15 minutes, and finally at 4 °C for 5 minutes. Following the completion of the programme, 75 µL MQ water was added to each sample, and they were stored at -20 °C for later use.

The qPCR was performed by qPCRBIO SyGreen Blue Mix (PCR Biosystem, London, UK) on a CFX96 Touch Real-Time PCR Detection System (Bio-Rad Laboratories Inc., CA, USA). Each sample had 2.5 µL SyGreen Blue mix, 0.2 µL of 10 mM forward and reverse gene-specific primers (**Supp. table 1**), 1.1 µL MQ water, and 1 µL cDNA template. *Actin1* and *GLYCERALDEHYDE-3-PHOSPHATE DEHYDROGENASE* (*GAPDH*) were used as the reference genes. Primers were designed by Primer-BLAST and manual work, following the proper principles of primer designing (YE et al., 2012). For the calculation of primer efficiencies, LinRegPCR was used (RAMAKERS et al., 2003). The calculation of relative gene expressions was done by the Pfaffl method (PFAFFL, 2001).

4.8. *HPLC measurements of hormones, flavonoids, and phenylpropanoid pathway compounds*

Extraction of the samples was performed following VRHOVSEK et al. (2012) and PÁL et al. (2019) with slight modifications. 200 mg frozen samples were homogenised in 2 mL safety centrifuge tubes and immediately spiked with 40 ng of $^{2}H_{6}$-cis, trans-abscisic acid (OlChemlm s.r.o., Olomouc, Czech Republic) as an internal standard. All solvents and reagents used for sample preparation and analysis were UPLC-gradient or GC-pestinorm supratrace grade (VWR, Randor, PA, USA). Extraction was performed twice with 1 mL methanol: water (2:1, v/v) by vigorous vortexing by shaking in a cryo-cooled Spex MiniG 1600 homogeniser (Metuchen, NJ, USA) at 1250 rpm for 3 minutes. The extracts were centrifuged at 16,500 g for 10 minutes at 4 °C, and the resulting supernatants were pooled together.

To remove carotenoids and lipids, 1 mL of the pooled methanol-water extract was liquid-liquid partitioned with 0.5 mL n-hexane. After centrifugation at 10,000 g (10 minutes, 4 °C), the methanol-water phase was recovered and filtered through 0.22 µm PTFE syringe filters prior to analysis.

Quantification of hormones, flavonoids, and phenylpropanoid intermediates was performed on a Waters Acquity I-class UPLC system equipped with a PDA detector and coupled to a Xevo TQ-XS triple-quadrupole mass spectrometer fitted with a UniSpray^{TM} (US) ion source (Waters Corp., Milford, MA, USA). Separation of phenolic compounds was achieved on an HSS T3 column (1.8 µm, 100 x 2.1 mm) as described by (VRHOVSEK et al., 2012). The Xevo TQ-XS operated in multiple-reaction monitoring (MRM) mode following the method of PÁL et al. (2019). Full UPLC–MS conditions and MRM transitions are provided in **Supp. Table 2**.

For the measurement of SA and *ortho*-hydroxycinnamic acid (*o*HCA), 700 mg of the plant sample was ground in liquid nitrogen with 0.25-0.5 g of quartz sand. The homogenate was extracted with 2 mL of 70% methanol and centrifuged at 10,000 g for 10 minutes at 5 °C. SA and *o*HCA were quantified following PÁL et al. (2005) and Meuwly and Metraux (1993). HPLC analyses were conducted on a Waters W2690 separation module equipped with a W2475 multiwavelength scanning fluorescence detector and a W996 photodiode-array detector, controlled by the Empower software package (Waters, Milford, MA, USA).

4.9. *Measurements of N-containing compounds- free amino acids and polyamines*

4.9.1. *Free amino acids*

For the measurement of free amino acids, 300 mg of samples were extracted using 2 mL cold 10% TCA with constant shaking for 1 hour at room temperature (GULYÁS et al., 2017). Following filtration through a 0.2 μm pore membrane filter, sample detection was conducted using an automatic amino acid analyser (Ingos Ltd., Czech Republic) fitted with an Ionex Ostion LCP5020 cation exchange column. The separation of free amino acids was achieved through a Li^+-citric buffer system (Ingos Ltd., Czech Republic).

4.9.2. *Polyamines*

Extraction of tissues-200 mg tissue was homogenised in chilled mortars with pestles in 2 mL 0.2 N $HClO_4$ (100 mg tissue/ mL acid) and was left on ice for half an hour. The homogenates were centrifuged at 4 °C in a centrifuge for 10 minutes at 10,000 g. The supernatant was analysed for polyamines.

Dansylation- The polyamines were derivatised according to the methods of SMITH AND DAVIES (1985). 100 μL aliquots of the supernatant were added to 200 μL of saturated sodium carbonate, and the reaction was started with 400 μL of dansyl chloride in acetone (5 mg/mL) in Eppendorf tubes, vortexed. The mixture was incubated in a thermal reaction block at 60 °C for 1 hour in the dark. 100 μL of proline (100 mg/mL) was added to the mixture to remove the excess dansyl chloride, and the mixture was vortexed. After 30 minutes, the polyamines were extracted with 500 μL of toluene with vigorous vortexing for 30 seconds. The mixture is separated into two phases, aqueous and organic. The organic (upper phase), containing the polyamines, was completely dried under nitrogen. The polyamine residue was dissolved in 1 mL of methanol, ultrafiltered through nylon membranes, and assayed immediately or stored (no more than 1 week) at -20 °C.

HPLC analyses- Polyamine analysis was carried out as described by NÉMETH et al. (2002). The polyamines were analysed as dansylated derivatives via HPLC using a W2690 separation module and a W474 scanning fluorescence detector with excitation at 340 nm and emission at 515 nm (Waters, Milford, MA, USA).

4.10. *Metabolite profiling*

Metabolite extraction and derivatisation for GC-MS were carried out as outlined by GONDOR et al. (2021) with minor modifications. 100 mg of homogenised plant sample were spiked with 30 µL of an internal standard solution of adonitol (1 mg mL^{-1}). Metabolites were initially extracted using 250 µL 60% methanol. The samples were vortexed for 30 seconds, placed in an ultrasonic bath for 5 minutes, and mixed again for 15 seconds. After centrifugation at 10,000 g for 5 minutes at 4 °C, the supernatant was collected. Subsequent extractions were done sequentially with 500 µL 60% and then 500 µL 90% methanol using the same vortex/ultrasonic steps, collecting the supernatant each time. The pooled supernatant was used for further steps. An aliquot of 200 µL of the combined extract was dried under vacuum. For derivatisation, methoxyamine hydrochloride in pyridine (20 mg mL^{-1}; Merck-Sigma, Darmstadt, Germany) was added to the dried extract and incubated at 37 °C for 90 minutes. This was followed by the addition of N-trimethylsilyl-N-methyltrifluoroacetamide (Merck-Sigma, Darmstadt, Germany) and a further incubation at 37 °C for 30 minutes. Derivatised samples were injected into a 30 m HP-5MS UI column (30 m x 0.25 mm, 0.25 µm film thickness) using helium as the carrier gas at a constant flow of 1 mL $minute^{-1}$. The injector was operated in split mode at 230 °C. The oven temperature programme began at 70 °C (held for 1 minute), increased at 7 $minutes^{-1}$ to 320 °C, and was then held at 320 °C for 10 minutes. Data acquisition and evaluation were performed using LabSolutions GC-MS software (version 4.53SP1). Metabolite identification was based on analytic standards, Kovats retention indices, and mass spectral matching against the Wiley 229 and NIST 2.3 libraries.

4.11. *Statistical analysis*

Statistical differences were calculated by one-way analysis of variance (ANOVA) using GraphPad Prism 10. Fisher's Least Significant Difference (LSD) test was performed as a post hoc test, with the expressed means considered significantly different at $p \leq 0.05$. For the statistical analysis, three biological replicates were utilised per treatment, with each replicate consisting of a mixture of 5 individual plants. The heatmaps in the result section were created using the software MultiExperiment viewer (MeV).

5. RESULTS AND THEIR DISCUSSION

5.1. *Growth parameters, photosynthetic pigments, and stress parameters*

Morphological differences were noted after the three redox treatments (5 mM Asc, 5 mM H_2O_2, and 1 mM NaHS) **(Supp. Fig. 4)**. No significant differences were noted after 3 days in the measured growth parameters; however, after 7 days, all treatments reduced root and shoot fresh weight, except for NaHS, which did not result in a significant difference in shoot fresh weight **(Fig. 5a-d)**.

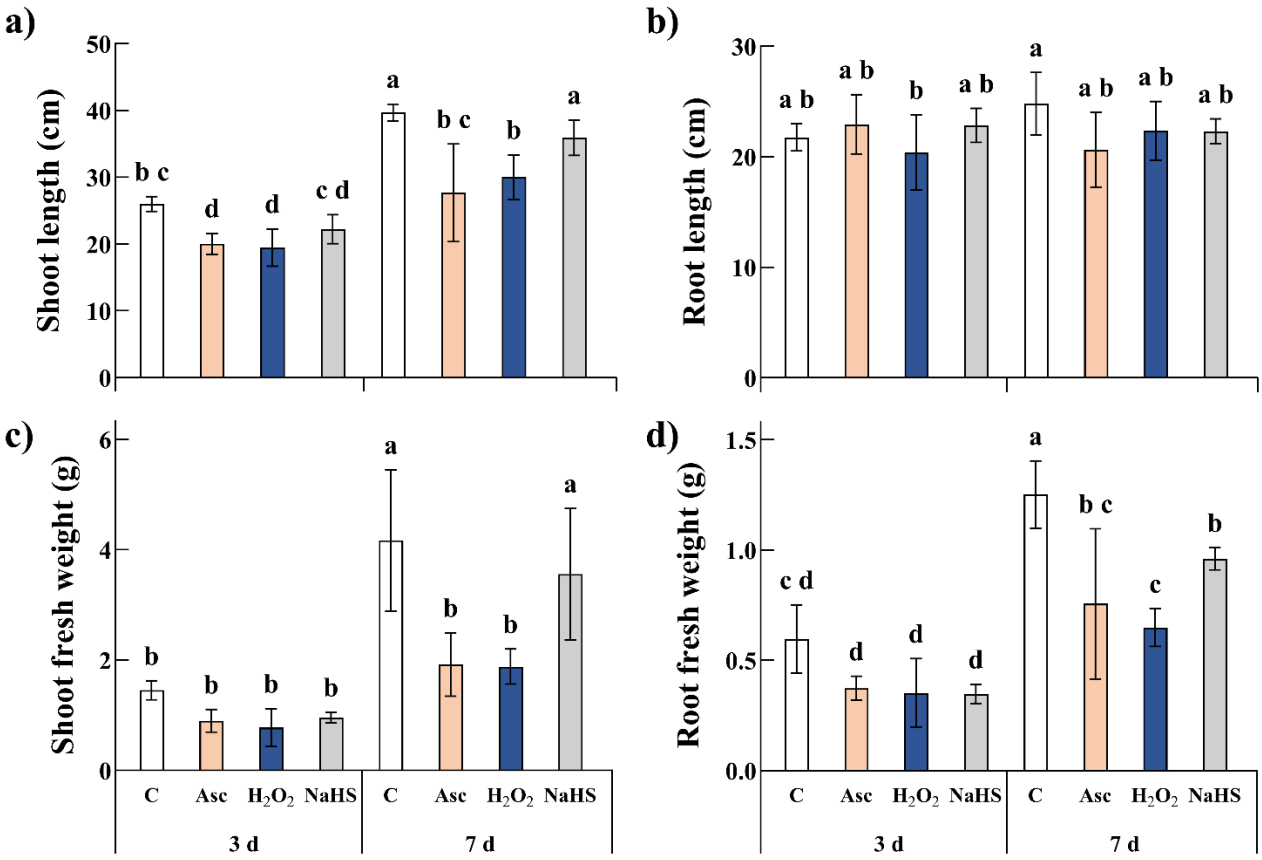

Figure 5: The effect of 5 mM ascorbate (Asc), 5 mM hydrogen peroxide (H_2O_2), and 1 mM sodium hydrosulfide (NaHS) on the growth parameters of maize seedlings along with the controls (C) after 3 and 7 days of the treatments. (a) shoot length, (b) root length, (c) shoot fresh weight, (d) root fresh weight. Values marked with different letters are significantly different from each other at $p < 0.05$ levels (One-way ANOVA followed by Fisher's Least Significant Difference (LSD) Test for the data obtained with three biological replicates each).

The concentration of photosynthetic pigments, including chlorophyll a, chlorophyll b, and carotenoids, was also measured. Interestingly, only the H_2O_2- and Asc-treated plants exhibited a significant decrease after 3 and 7 days, respectively, in chlorophyll a **(Fig. 6a)**. In the case of chlorophyll b, NaHS treatment resulted in higher levels after 3 days, and the plants maintained levels similar to the control after 7 days as well. A significant reduction in of chlorophyll b content was noted after 7-day Asc treatment **(Fig. 6b)**. No notable changes were observed in carotenoid levels across treatments on both sampling days **(Fig. 6c)**.

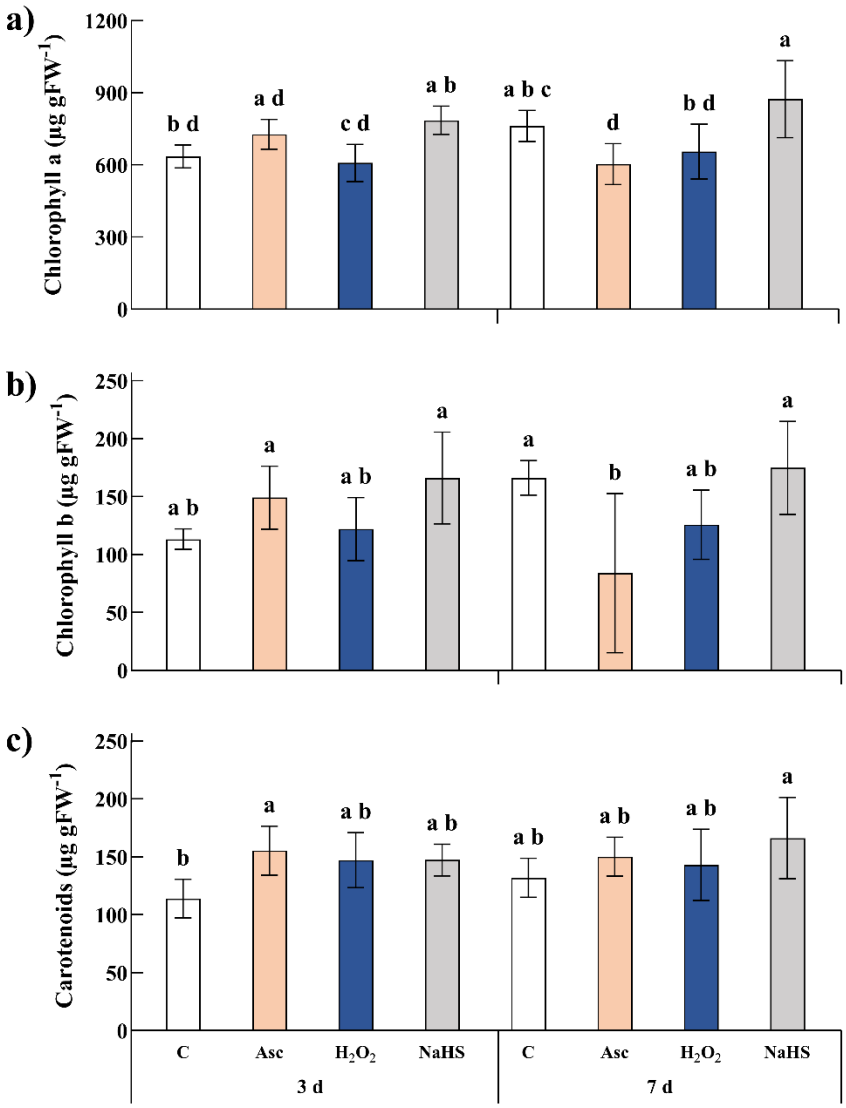

Figure 6: The effect of 5 mM ascorbate (Asc), 5 mM hydrogen peroxide (H_2O_2), and 1 mM sodium hydrosulfide (NaHS) on (a) chlorophyll a, (b) chlorophyll b, (c) carotenoids, after 3 and 7 days of the treatment along with the respective controls (C). Values marked with different letters are significantly different from each other at $p \leq 0.05$

levels (One-way ANOVA followed by Fisher's Least Significant Difference (LSD) Test for the data obtained with three biological replicates each).

All the treatments significantly increased electrolyte leakage in the order Asc>H_2O_2>NaHS after 3 days. In contrast, electrolyte leakage decreased after 7 days in H_2O_2 and NaHS-treated plants, showing levels similar to the control, but Asc-treated plants had significantly higher levels **(Fig. 7a).**

Lipid peroxidation (indicated in terms of MDA) showed a similar trend to that of electrolyte leakage. MDA levels increased significantly after 3 days in all the treated plants in comparison to the control. Asc caused the highest lipid peroxidation after both sampling days, while NaHS resulted in the lowest **(Fig. 7b)**.

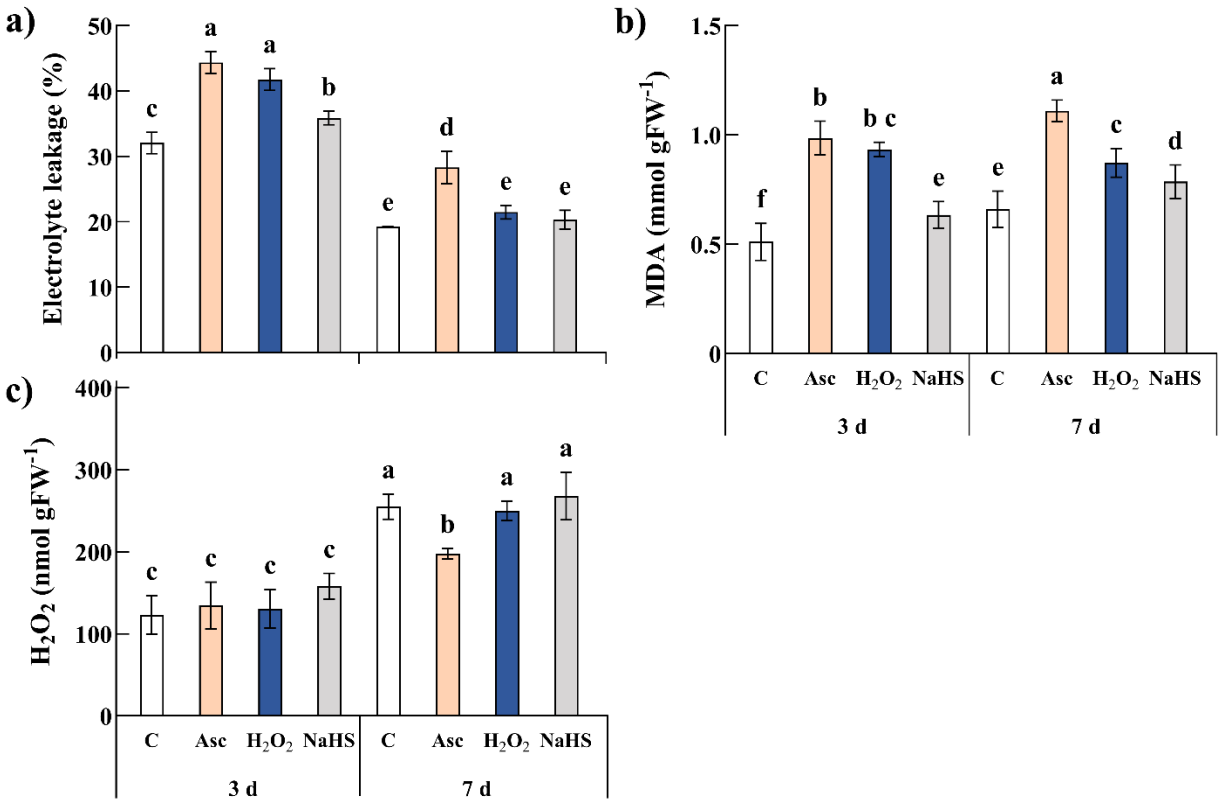

Figure 7: The effect of 5 mM ascorbate (Asc), 5 mM hydrogen peroxide (H_2O_2), and 1 mM sodium hydrosulfide (NaHS) on stress markers in maize seedlings along with the controls (C) after 3 and 7 days of the treatments. (a) electrolyte leakage, (b) lipid peroxidation, and (c) endogenous hydrogen peroxide (H_2O_2) levels. Values marked with different letters are significantly different from each other at $p \leq 0.05$ levels (One-way ANOVA followed by Fisher's Least Significant Difference (LSD) Test for the data obtained with three biological replicates each).

The three treatments caused only slight but non-significant changes in endogenous H_2O_2 levels after 3 days. However, Asc and NaHS applications resulted in the lowest and highest levels of endogenous H_2O_2, respectively **(Fig. 7c)**.

Plant morphology is the cumulative result of all the internal metabolic processes, including photosynthesis. A reduction in growth parameters after Asc and H_2O_2 could be attributed to disrupted photosynthesis, redox imbalance, and modulations in stress markers caused by these chemicals. These results are in accordance with the previous findings of (ASGHAR et al., 2023b), who observed a significant reduction in plant biomass after the application of 5 mM Asc and H_2O_2 in wheat plants after 3 and 7 days. In addition, lower levels of chlorophyll a and b after prolonged Asc application could be due to redox imbalance-induced damage to chloroplasts and related enzymes. This damage reduces the plant's ability to assimilate carbon. This observation, combined with the results of lipid peroxidation and electrolyte leakage, consequently affects biomass accumulation. Likewise, results were obtained in wheat seedlings as well (ASGHAR et al., 2022). Unlike Asc and H_2O_2, NaHS exhibited different results in growth parameters and photosynthetic pigments. Literature supports these findings, as no notable changes were observed in non-stressed maize plants after 0.6 mM NaHS application (SHAN et al., 2014). Other studies in wheat and Arabidopsis are consistent with the present findings of plant height, chlorophyll, and MDA levels (DING et al., 2019; QIAN et al., 2014; ZHANG et al., 2010).

5.2. *Ascorbate and thiols*

Asc and GSH are the primary components of the Asc-GSH cycle to effectively scavenge ROS and maintain redox homeostasis. To evaluate the redox buffering capacity of the plants, total Asc and GSH/GSSG ratios were measured. Total Asc accumulation increased from 3 to 7 days following Asc and H_2O_2 application, while no changes were observed in the case of NaHS **(Supp. Fig. 5)**.
The amount of Cys, an intermediate product, γ-glutamylcysteine (γ-EC), and a degradation product, Cysteinylglycine (CG) of GSH were also measured. Total Cys levels were maintained at the highest levels by H_2O_2 after both treatment durations in comparison to the other two treatments. No significant differences were noted after NaHS treatment from 3 to 7 days, though a significant reduction in comparison to control was recorded for total Cys **(Fig. 8a)**. The amount of oxidised

Cys was the highest and lowest after 7 day Asc and NaHS treatment, respectively **(Fig. 8b)**. This indicates a shift in the redox balance towards a more oxidised state after Asc, while a reduced cellular environment is maintained after 7 days of NaHS. These results are further supported by the ratio of reduced Cys/ oxidised Cys (**Fig. 8d**). Interestingly, H_2O_2-treated plants exhibited the highest reduced Cys/oxidised Cys ratio amongst the three treatments after 3 days, while after 7 days, it was similar after H_2O_2 and NaHS addition **(Fig. 8d)**.

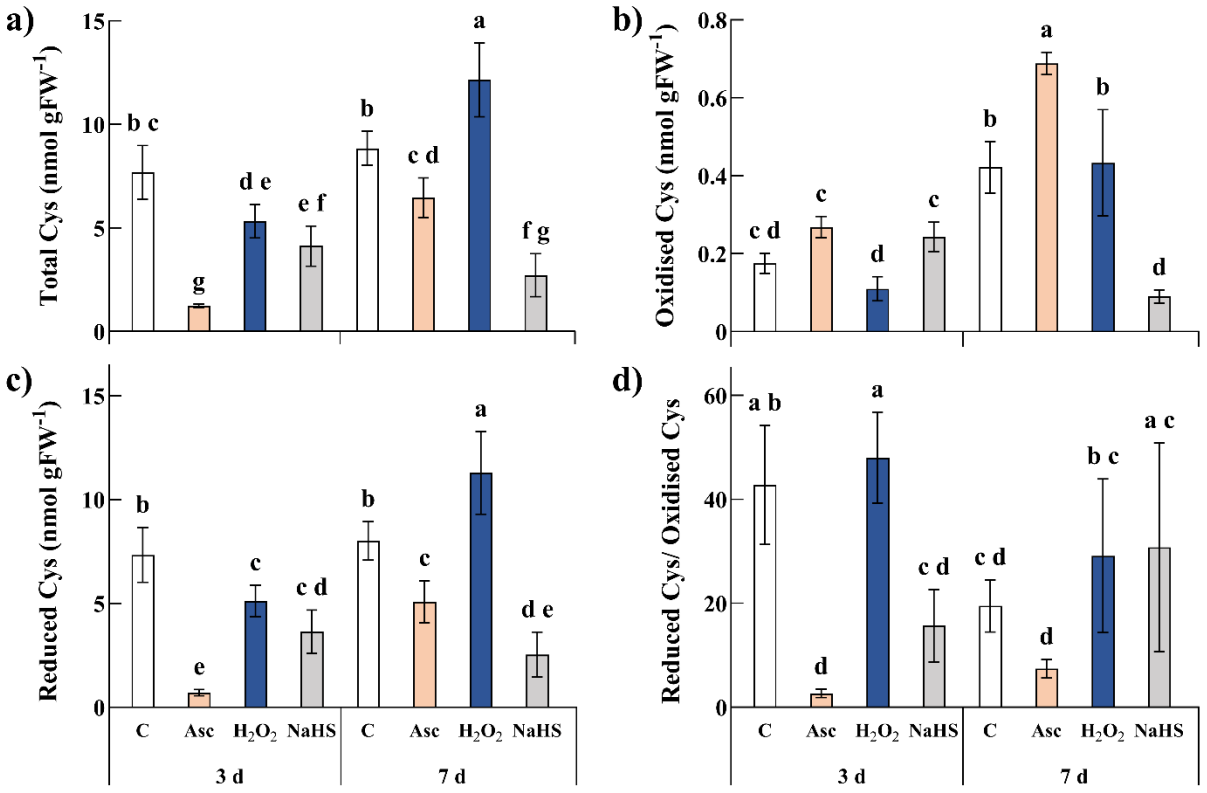

Figure 8: The effect of 5 mM ascorbate (Asc), 5 mM hydrogen peroxide (H_2O_2), and 1 mM sodium hydrogensulfide (NaHS) on cysteine levels in maize seedlings along with the controls (C) after 3 and 7 days of the treatments. (a) Total cysteine (Cys), (b) oxidised Cys, (c) reduced Cys, (d) the ratio of reduced to oxidised Cys. Values marked with different letters are significantly different from each other at $p \leq 0.05$ levels (One-way ANOVA followed by Fisher's Least Significant Difference (LSD) test for the data obtained with three biological replicates each).

γ-EC is formed during GSH biosynthesis and was observed to be the lowest after 3 days of Asc treatment, with similar levels recorded after 7 days in all the treated groups compared to the control **(Fig. 9).**

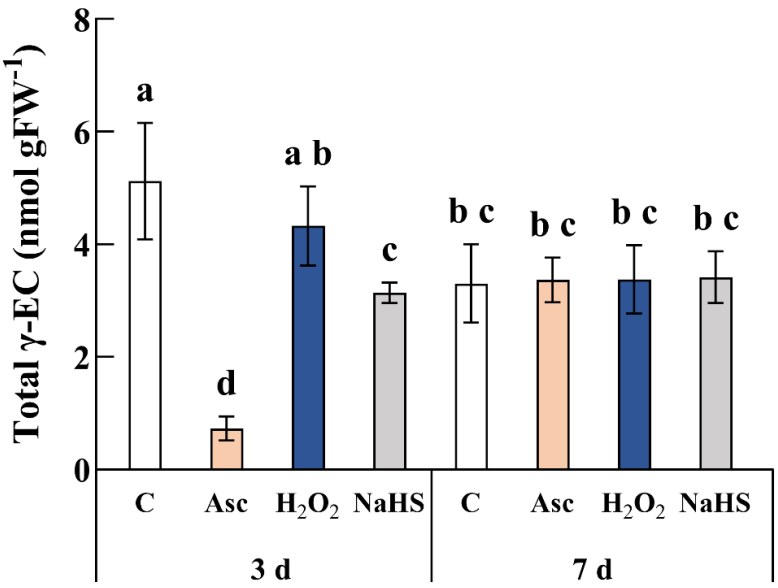

Figure 9: The effect of 5 mM ascorbate (Asc), 5 mM hydrogen peroxide (H_2O_2), and 1 mM sodium hydrogensulfide (NaHS) on γ-glutamylcysteine (γ-EC) levels in maize seedlings along with the controls (C) after 3 and 7 days of the treatments. Values marked with different letters are significantly different from each other at $p \leq 0.05$ levels (One-way ANOVA followed by Fisher's Least Significant Difference (LSD) test for the data obtained with three biological replicates each).

Total GSH (reduced + oxidised) was significantly lower after both days of Asc and NaHS application **(Fig. 10a)**. However, H_2O_2 application caused either a similar (after 3 days) or significantly higher accumulation (after 7 days) of total GSH and reduced GSH **(Fig. 10a-b)**. The oxidised glutathione (GSSG) content peaked after 3 days of H_2O_2 treatment but became comparable to the control after 7 days. Interestingly, NaHS application caused a significant reduction in GSSG levels after 7 days compared to the respective control **(Fig. 10c)**. As a consequence, similar to reduced Cys/oxidised Cys, NaHS-treated plants showed the highest GSH/GSSG ratio after 7 days, whereas Asc showed the lowest ratio after 3 and 7 days of treatment **(Fig. 10d)**.

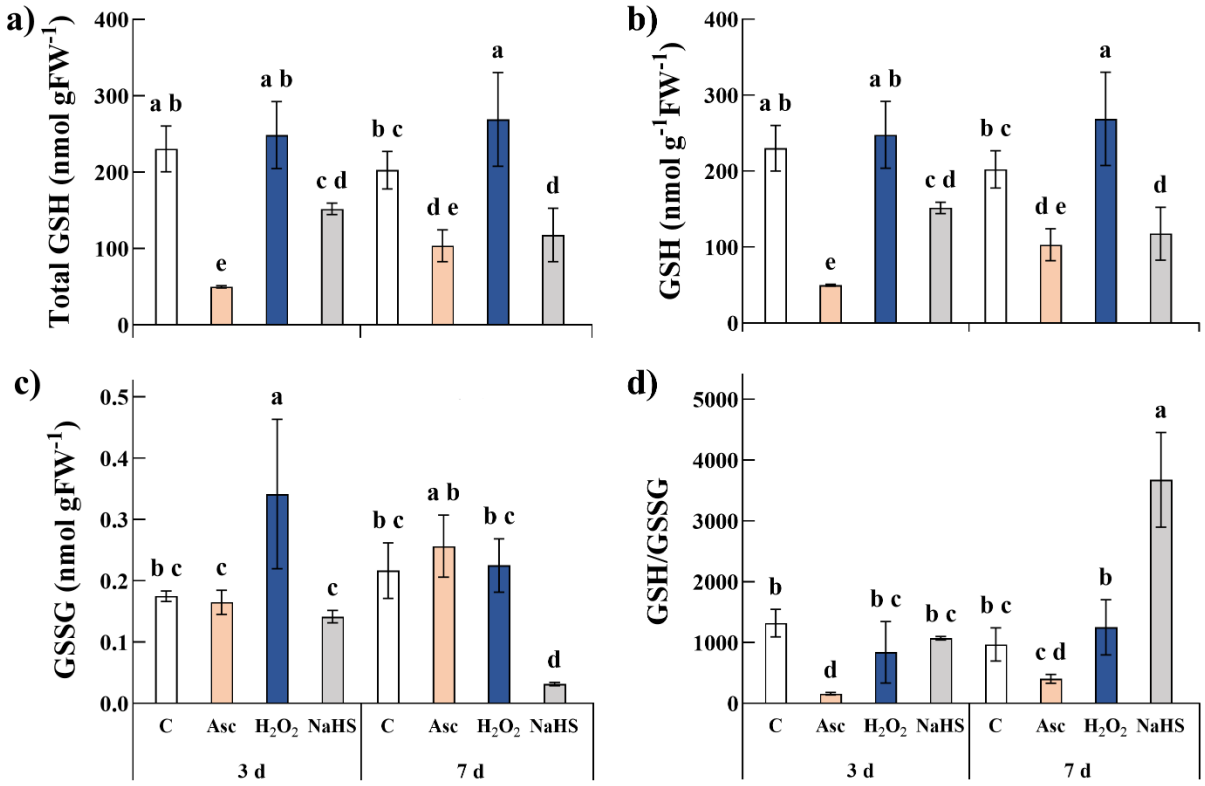

Figure 10: The effect of 5 mM ascorbate (Asc), 5 mM hydrogen peroxide (H_2O_2), and 1 mM sodium hydrogensulfide (NaHS) on glutathione levels in maize seedlings along with the controls (C) after 3 and 7 days of the treatments. (a) Total glutathione (reduced + oxidised, GSH + 2 GSH for GSSG), (b) reduced glutathione, (c) glutathione disulfide (GSSG; oxidised form), (d) the ratio of reduced to oxidised glutathione (GSH/GSSG). Values marked with different letters are significantly different from each other at $p \leq 0.05$ levels (One-way ANOVA followed by Fisher's Least Significant Difference (LSD) test for the data obtained with three biological replicates each).

H_2O_2 treatment resulted in the least amount of degraded product-CG after 3 days amongst the treatments, followed by Asc and NaHS. However, the trend changed after 7 days for the order H_2O_2>NaHS>Asc, though non-significant amongst each other, still showed a significant increase with respect to the control **(Fig. 11)**.

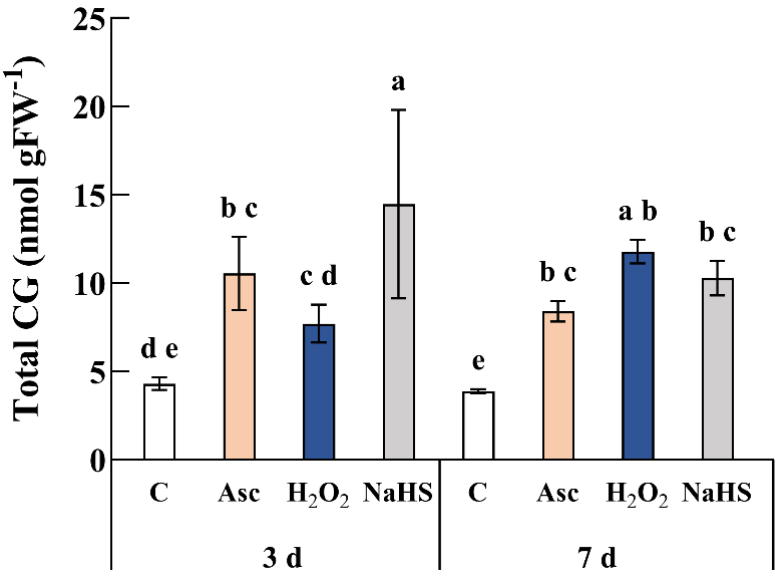

Figure 11: The effect of 5 mM ascorbate (Asc), 5 mM hydrogen peroxide (H_2O_2), and 1 mM sodium hydrogensulfide (NaHS) on total cysteinylglycine (CG) levels in maize seedlings along with the controls (C) after 3 and 7 days of the treatments. Values marked with different letters are significantly different from each other at $p \leq 0.05$ levels (One-way ANOVA followed by Fisher's Least Significant Difference (LSD) test for the data obtained with three biological replicates each).

The application of Asc, H_2O_2 and NaHS differently affected the redox environment. Asc shifted the GSH/GSSG-dependent redox environment towards a more oxidised side; H_2O_2 did not affect it, while NaHS shifted it towards a more reducing environment. Our results are in accordance with those of (ASGHAR et al., 2023a), who observed similar changes in the GSH/GSSG ratio after Asc and H_2O_2 application in wheat seedlings. In addition, SHI et al. (2013) reported an increase in the GSH/GSSG ratio in bermudagrass after NaHS application. On the contrary, the negative effects of 3 and 7 mM NaHS were described in cellular redox homeostasis in *Schrophularia striata* (KHODAMORADI et al., 2022). It is therefore evident that NaHS exhibits dose-dependent effects, with higher concentrations being lethal.

5.3. *Asc-GSH cycle enzymes and related gene expression*

In addition to Asc and GSH levels, the enzyme activity of the Asc-GSH cycle and expression of the related genes were also analysed. APX showed the highest activity following H_2O_2 application. Asc and NaHS treatment did not result in any significant changes in comparison to the control **(Fig. 12a)**. A varied trend was seen in gene expression after the treatments. For instance, H_2O_2

lowered *peroxisomal APX* (*pAPX3)* expression but transiently increased *cytosolic APXs* (*cAPXs*: *cAPX1.1*, *cAPX1.2*, *cAPX2*, and *cAPX4*) expression after 3 days, returning to control levels by 7 days **(Fig. 12f)**. In contrast to the unchanged enzyme activity, Asc upregulated *cAPXs* and *gECS*, and lowered *mitochondrial APX* (*mAPX*) and *chloroplastic APX* (*chAPX)* expression. NaHS caused a significant decline in APX activity from 3 to 7 days **(Fig. 12a)**, and the expression of genes exhibited a similar trend. *cAPXs*, *mAPX*, *pAPX*, and *chAPX* expression was reduced from 3 to 7 days of NaHS application **(Fig. 12f)**.

DHAR enzyme activity peaked after prolonged Asc application **(Fig. 12b)**. In contrast, a greater reduction in *chloroplastic DHAR* (*chDHAR1*) and *mitochondrial DHAR* (*mDHAR3*) expression was observed in Asc-treated plants between 3 and 7 days, and an increase in *cytosolic DHAR* (*cDHAR2*) in comparison to the control **(Fig. 12f)**.

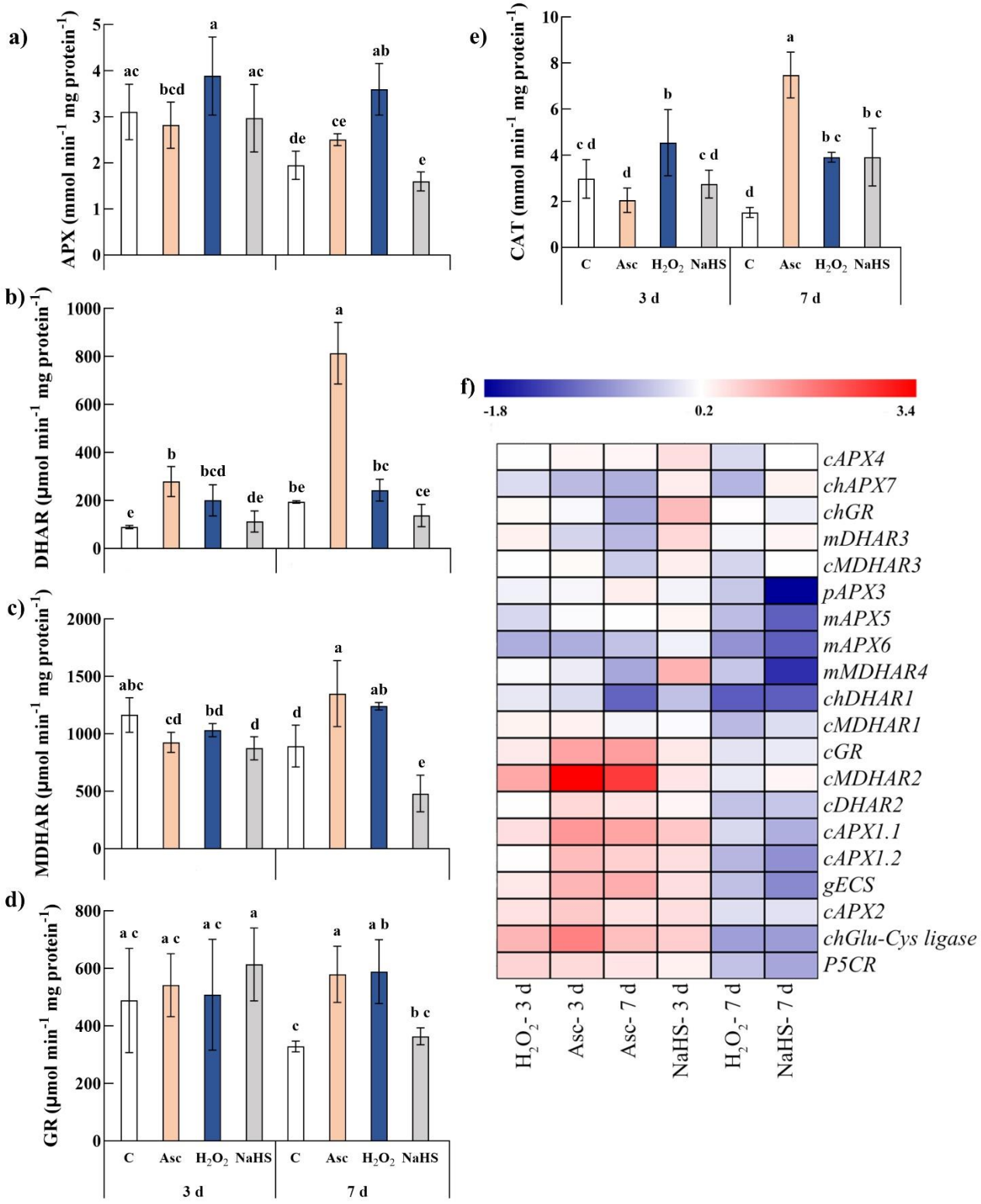

Figure 12: The effect of 5 mM ascorbate (Asc), 5 mM hydrogen peroxide (H_2O_2), and 1 mM sodium hydrosulfide (NaHS) on the antioxidant enzyme activities and related gene expression in maize seedlings along with the respective controls (C) after 3 and 7 days of treatment. (a) ascorbate peroxidase (APX), (b) dehydroascorbate

reductase (DHAR), (c) monodehydroascorbate reductase (MDHAR), (d) glutathione reductase (GR), (e) catalase (CAT), (f) the expression of the genes related to antioxidants. For the graphs, values marked with different letters are significantly different from each other at $p \leq 0.05$ levels (One-way ANOVA followed by Duncan's multiple range test for the data obtained by three biological replicates each). For the heatmap, the alphabet at the beginning of the gene name -*c, ch, m, p* refers to cytosolic, chloroplastic, mitochondrial and peroxisomal, respectively. The heatmap was created using the software MultiExperiment Viewer (MeV). *MDHAR: monodehydroascorbate reductase, GR: glutathione reductase, APX: ascorbate peroxidase, gECS: gamma-glutamylcysteine synthetase, Glu-Cys ligase: glutamine-cysteine ligase, DHAR: dehydroascorbate reductase, P5CR: δ1-pyrroline-5-carboxylate reductase*. The colours represent the log2 values of the relative gene expression in treated plants with respect to the control.

MDHAR activity increased following prolonged Asc and H_2O_2 application, while significantly lowered after 7 days of NaHS addition **(Fig. 12c)**. The gene expression of *cytosolic MDHARs* (*cMDHAR1*, *cMDHAR2*, and *cMDHAR3*) was higher than control after 3 days of Asc and H_2O_2 treatment. Interestingly, *cMDHAR2* expression in 3-day Asc-treated plants increased 10-fold relative to control, which lowered to 6-fold after 7 days. On the contrary, *mitochondrial MDHAR - mMDHAR4* showed a 2-fold increase in relative gene expression but declined significantly from 3 to 7 days following NaHS treatment **(Fig. 12f)**. A similar trend in *δ1-pyrroline-5-carboxylate reductase* (*P5CR*) expression was noted.

GR activity dropped in NaHS-treated plants from 3 to 7 days. Asc and H_2O_2 maintained a significantly higher GR activity in comparison to the control after 7 days **(Fig. 12d)**. Likewise, the expression of *chloroplastic GR* (*chGR*) decreased from 3 to 7 days after NaHS treatment, while *cytosolic GR* (*cGR*) expression increased after 7 days of Asc treatment **(Fig. 12f)**.

The H_2O_2-degrading enzyme CAT showed significantly increased activity only after 7 days of all the treatments, though it increased slightly after 3 days of H_2O_2 application **(Fig. 12e)**.

To compensate for the strong shift in the redox balance after Asc treatment, the activity of the antioxidant enzymes (DHAR and CAT) was elevated after 7 days. In contrast, the reducing cellular redox environment of NaHS-treated plants could explain the lower activities of APX and MDHAR. Likewise, the enzyme activity can be explained at the transcriptional level. After 3 days, Asc treatment caused the highest expression of *cGR*, *MDHAR2*, *cAPX1.1*, *gECS*, and *chGlu-Cys ligase*. By 7 days, Asc resulted in increased expression levels, whereas H_2O_2 and NaHS decreased them, reflecting the GSH/GSSG ratio trend (Asc<H_2O_2<NaHS). These higher enzyme activities

are in accordance with the results obtained in wheat (ASGHAR et al., 2023b) and maize roots (ANJUM et al., 2015). The compartment-specific changes in gene expression by the three treatments reveal the changes that are made to maintain redox balance. These results are also similar to those obtained in wheat (ASGHAR et al., 2023b) and rice (TSAI et al., 2005).

5.4. *Carbohydrates and components of the TCA cycle*

Sugars are essential for energy production and are the backbone for plant growth and development. During glycolysis, glucose is broken down to generate energy coins- ATP and NADH, along with the precursors for amino acid, hormones and other metabolite synthesis. H_2O_2-mediated disturbance in redox homeostasis caused a significant reduction in sucrose, whereas Asc and NaHS exhibited higher levels than the control after 3 days; however, it came to the control levels after 7 days **(Fig. 13)**. In the case of ribose, the highest accumulation was noted after Asc application, followed by NaHS and H_2O_2 and this trend diminished by 7 days. D-arabinose accumulated to the highest levels after 7 days of H_2O_2 and Asc treatment, maintaining relatively high levels after both durations of treatment. Prolonged NaHS treatment alone caused higher glucose levels, whereas other treatments did not affect it **(Fig. 13)**.

µg gFW^{-1}	C-3	Asc-3	H_2O_2-3	NaHS-3	C-7	Asc-7	H_2O_2-7	NaHS-7
Succinate	a 25.95± 7.19	b 17.24± 3.22	bc 14.95± 4.11	b 17.72± 3.89	bd 13.69± 3.88	d 7.3± 2.23	cd 8.81± 1.01	b 16.37± 4.96
Malic Acid	ac 289.45± 37.24	ac 286.6± 13.12	c 231.88± 70.83	ac 298.44± 11.43	bc 278.83± 23.88	bc 266.41± 39.27	ab 315.86± 46.92	a 362.32± 71.59
Oxo-proline	a 220.59± 35.20	de 29.11± 5.67	bcd 71.89± 27.36	bc 80.93± 23.94	ce 55.79± 15.43	e 8.31± 1.80	bc 83.65± 4.12	b 112.85± 58.83
α-ketoglutaric acid	ab 60.41± 15.35	bd 40.17± 9.36	d 24.3± 5.84	bd 44.3± 13.63	a 69.27± 16.38	cd 33.6± 11.21	d 22.61± 6.33	abc 51.19± 17.77
D-arabinose	c 5.58± 1.24	b 9.63± 1.68	bc 7.11± 1.78	bc 6.26± 0.62	c 5.37± 1.65	b 9.46± 2.36	a 14.38± 3.67	bc 6.21± 1.77
D-ribose	ab 89.75± 19.63	a 109.12± 24.52	bc 70.33± 2.47	ab 85.71± 18.03	c 56.79± 10.15	c 57.85± 9.73	bc 68.47± 6.47	c 54.47± 7.91
Citric acid	bc 116.78± 2.85	bc 105.74± 17.79	ab 139.5± 16.06	cd 98.11± 14.28	bc 118.7± 9.44	d 69.79± 23.11	a 156.18± 28.34	ab 140.26± 35.12
D-glucose	b 204.9± 17.36	b 242.9± 22.61	b 237.21± 17.14	b 246.57± 10.32	b 237.85± 15.91	b 257.17± 21.65	b 240.35± 24.59	a 339.75± 120.15
Myo-inositol	d 57.32± 11.59	b 114.4± 12.8	ab 117.9± 23.13	bc 96.17± 11.09	cd 74.4± 13.41	ab 122.37± 15.57	a 151.19± 35.56	cd 68.79± 23.57
Sucrose	b 10.53± 2.97	a 16.74± 4.21	c 5.66± 1.82	a 15.38± 2.8	bc 8.78± 3.43	bc 9.54± 1.48	bc 10.02± 2.88	bc 8.63± 0.81

Minimum Maximum

Figure 13: The effect of 5 mM ascorbate (Asc), 5 mM hydrogen peroxide (H_2O_2), and 1 mM sodium hydrosulfide (NaHS) on the metabolite profile after 3 and 7 days of the treatments along with the respective controls (C). The

numbers 3 and 7 refer to the sampling day after treatment. Colouring is done individually for each row, with blue representing the lowest level and red representing the highest level. Values marked with different letters are significantly different from each other at $p \leq 0.05$ levels (One-way ANOVA followed by Fisher's Least Significant Difference (LSD) Test for the data obtained with three biological replicates each).

The end product of glycolysis is pyruvate, serving as the precursor for acetyl-CoA in the TCA cycle**.** Its several components (succinate, α-ketoglutaric acid, and malic acid) exhibited a lower accumulation trend after 3 days of H_2O_2 treatment, while citric acid showed significant accumulation after 7 days. In the case of Asc addition, succinate was significantly higher after 3 days but was significantly lower after 7 days. Malic acid did not exhibit any change, as opposed to α-ketoglutaric acid and citric acid, which were strongly lowered after 7 days. NaHS application only triggered malic acid accumulation after 7 days.

Other metabolites, such as oxo-proline, were lowered following Asc, contrary to NaHS treatment, which indicated an upward accumulation trend. Myo-inositol serves as one of the precursors for Asc synthesis, and its levels were significantly higher in Asc- and H_2O_2-treated plants compared to the controls. NaHS only transiently increased myo-inositol levels, and they were in a comparable range after 7 days.

The redox changes caused a metabolic reprogramming of glycolysis and the TCA cycle, which could be due to disturbed photosynthesis, limited availability of components for energy production and ultimately affected amino acid synthesis and other metabolites. The Asc and H_2O_2-mediated redox shift was accompanied by depressed intermediates of the TCA cycle. Similar results of lower accumulation of α-ketoglutaric acid and aconitic acid were noted in wheat (ASGHAR et al., 2023a). In the case of NaHS application, ZHANG et al. (2023) and YANG et al. (2024) reported accumulation/alterations of the TCA cycle components in tomato fruit and tobacco, respectively. Furthermore, an accumulation of soluble sugars was observed following pre-soaking of seeds in 0.5 mM NaHS, followed by lead stress for 9 days (ZANGANEH et al., 2021). Thus, it can be concluded that there exists a specific modulatory effect of the redox balance on sugars and organic acids.

5.5. *N-containing compounds- amino acids, polyamines and NO and related gene expression*

5.5.1. *Free amino acids*

Altered redox balance affected photosynthesis and sugar metabolism. As a consequence, the amino acid profile was severely modified. H_2O_2 and Asc sustained an opposite effect on total amino acid levels after 3 days, with H_2O_2 increasing it and Asc lowering it. However, after 7 days, Asc continued to decrease it significantly, while H_2O_2 exhibited levels similar to those of the control. No changes were noted after NaHS treatment on both days of sampling **(Fig. 14b)**. Interestingly, following the Asc application, a decrease in the amino acids of the glutamate family was observed (Glu, GABA, Orn, and Arg). Our analysis also revealed a lowering trend of Glu and Gln content in H_2O_2-treated plants, while GABA and Arg were significantly higher after 3 days **(Fig. 14a; Supp. Fig. 6)**. On the contrary, Pro and Gln were at the highest levels after 3 days of NaHS treatment and were in a comparable range with the control after 7 days. From the serine (Ser) family, H_2O_2 triggered the accumulation of Ser and Gly, whereas Asc application caused a significant decrease in their levels from 3 to 7 days. Notably, NaHS-treated plants exhibited a significant accumulation of Cys after 3 days, whereas no changes were observed for Gly in comparison to the respective controls **(Fig. 14a; Supp. Fig. 6)**. Among the aromatic amino acids, Tyr showed the lowest levels after 7 days of Asc. Phe reached its highest levels following H_2O_2 exposure for 3 days. In contrast, NaHS treatment did not cause any notable differences compared to the control **(Fig. 14a; Supp. Fig. 6)**. Additionally, Ile, β-aminoisobutyric acid, Lys, His, Thr, Asp, and Asn all increased after 3 days of H_2O_2 exposure but declined after 7 days of Asc treatment **(Fig. 14a; Supp. Fig. 6)**.

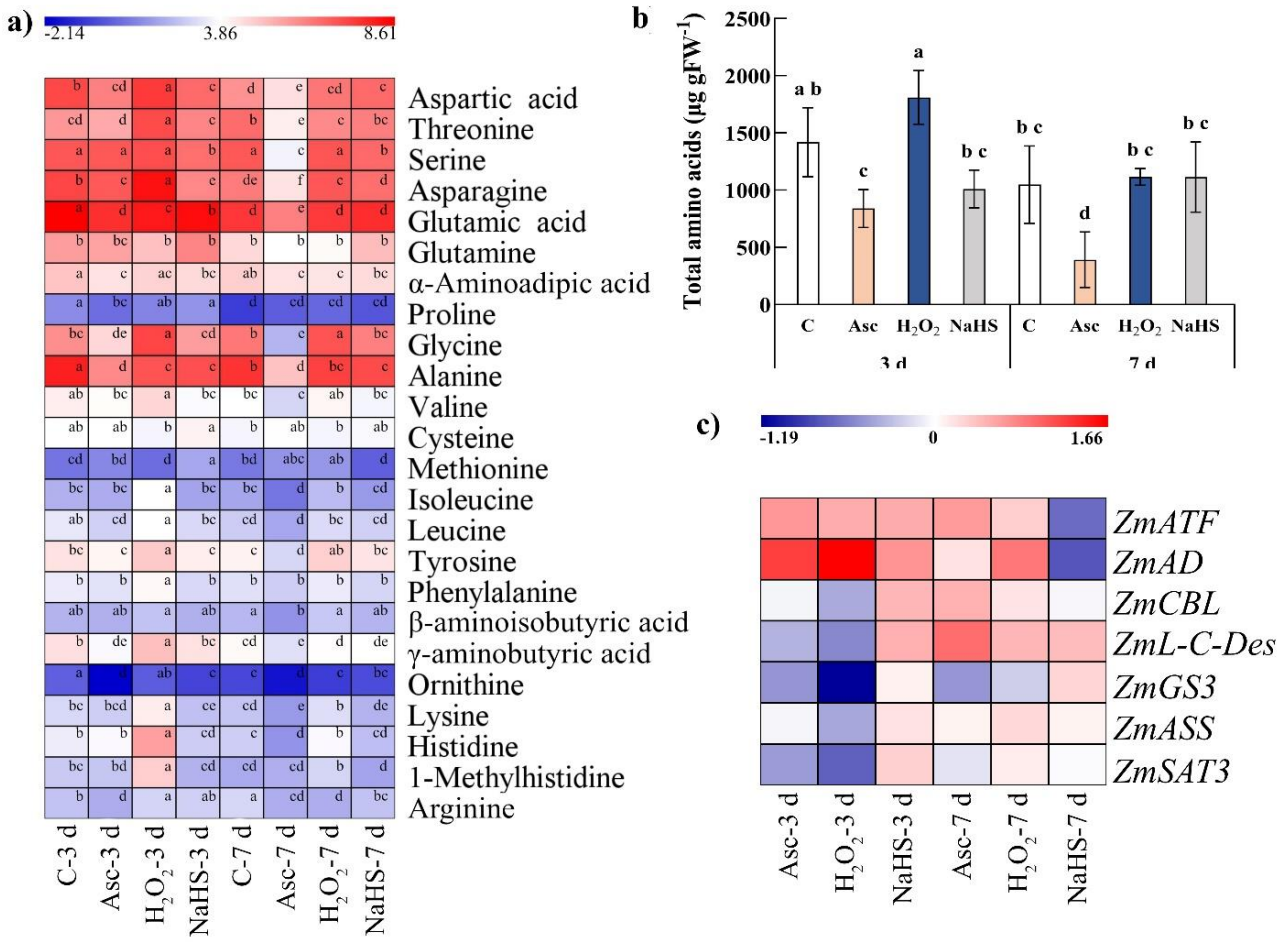

Figure 14: The effect of 5 mM ascorbate (Asc), 5 mM hydrogen peroxide (H_2O_2), and 1 mM sodium hydrosulfide (NaHS) on a) the free amino acids, b) total amino acids, and c) the relative gene expression after 3 and 7 days of the treatments along with the respective controls (C). The numbers 3 and 7 refer to the sampling day after treatment. For the heatmaps, the colours represent the log2 values of the average of three biological replicates used to measure the endogenous levels of the amino acids and the relative gene expression, with blue indicating lower levels and red indicating higher levels. Boxes marked with different letters are significantly different from each other at $p \leq 0.05$ levels (One-way ANOVA followed by Fisher's Least Significant Difference (LSD) test for the actual data obtained with three biological replicates each). Please refer to **Supp. Fig. 6** for the individual graphs of each amino acid with their actual detected values. The heatmap was created using the software MultiExperiment Viewer (MeV). *ZmATF- Zea mays aminotransferase y4uB; ZmAD- Zea mays arogenate dehydrogenase; ZmCBL- Zea mays cystathionine beta-lyase chloroplastic; ZmL-C-Des- Zea mays L-cysteine desulfhydrase chloroplastic; ZmGS3- Zea mays Glutamine synthetase3; ZmASS- Zea mays argininosuccinate synthase; ZmSAT3- Zea mays serine acetyltransferase3*

From the measured amino acids, those exhibiting varied levels across the treatments were further studied at the transcriptional level as well. Thus, we could obtain insights into the redox-mediated transcriptional regulation of amino acids. Glutamine synthetase 3 is responsible for nitrogen assimilation by converting ammonia to glutamine (Gln). Its gene in maize - *ZmGS3* was upregulated after NaHS application, whilst being downregulated in Asc- and H_2O_2-treated plants **(Fig. 14c)**. A likewise pattern in gene expression was noted for *argininosuccinate synthase* enzyme (*ZmASS*), responsible for Arg biosynthesis. After 3 days, all the treatments exhibited an increase in the expression of *aminotransferase y4uB* (*ZmATF*), which is involved in GABA metabolism. However, this increase was not sustained in prolonged NaHS-treated plants **(Fig. 14c)**. Ser, along with acetyl-CoA, forms O-acetylserine via the action of the enzyme serine acetyltransferase. The formed O-acetylserine serves as the precursor for Cys biosynthesis. In the present experiment, the gene *serine acetyltransferase 3* (*ZmSAT3*) displayed lower expression levels after 3 days but revealed a similar expression pattern to the control after 7 days in H_2O_2-treated plants **(Fig. 14c)**. Simultaneously, the initial Asc application downregulated *L-cysteine desulfhydrase chloroplastic* (*ZmL-C-Des*), but prolonged application resulted in a relatively higher expression than the two treatments. In contrast, NaHS-treated plants maintained higher expression of *ZmL-C-Des* after both days of sampling **(Fig. 14c)**. Similar to *ZmL-C-Des*, the expression of *cystathionine beta-lyase chloroplastic* (*ZmCBL*) transiently lowered and then elevated after 7 days of Asc. The literature documents a dual role for the enzyme cystathionine beta-lyase. It plays a vital role in Met biosynthesis by cleaving cystathionine to produce homocysteine, which then produces Met. In addition, the enzyme can produce H_2S by utilising Cys as the substrate under stressful conditions and governs plant stress response (WANG et al., 2022). Furthermore, all the treatments triggered the expression of *arogenate dehydrogenase* (forms Tyr by catalysing arogenate; *ZmAD*) after 3 days to a varying degree in the order H_2O_2>Asc>NaHS, while after 7 days, the most pronounced decrease in the expression was after NaHS, followed by Asc and H_2O_2 **(Fig. 14c)**. The enzyme encoded by the gene *myo-inositol-1-P-synthase* (*ZmMIPS*) catalyses the rate-limiting step in the biosynthesis of myo-inositol. Its expression was solely upregulated by Asc after both days. On the contrary, NaHS and H_2O_2 exhibited its strong suppression **(Fig. 14c)**.

The balance of the Asc-GSH cycle-based redox exerts a delicate yet precise regulation over the levels of free amino acids (GULYÁS et al., 2017). In light of the present results, it can be concluded that there exists a specific modulatory effect exerted by the various redox compounds

that control amino acid levels in plants. The literature also documents the effect of GSH application as a redox treatment to GSH-deficient *Arabidopsis*. The exogenous feeding led to a higher accumulation of total amino acids in the mutants than in the wild type (GULYÁS et al., 2017). Treatments with H_2O_2 resulted in a greater accumulation of Ser and Gly after 7 days. Conversely, Asc led to a significant decrease in these amino acids. Ser serves as a precursor in Cys biosynthesis, thereby playing a vital role in the maintenance of cellular redox homeostasis. This observation is in accordance with a higher ratio for the reduced Cys to oxidised Cys after H_2O_2, contrasting with Asc. Furthermore, the application of 4 mM Asc and 10 mM H_2O_2 to *Arabidopsis* resulted in a significantly higher ratio of Ser family than observed in the controls (GULYÁS et al., 2017). Moreover, the Ser family is essential for sulfur assimilation as well. The possible explanation for a higher expression of *ZmSAT* after NaHS, compared to Asc and H_2O_2, could be attributed to the reprogramming of sulfur metabolism in the presence of higher H_2S availability. As proposed by WANG et al. (2021), there exists NaHS-dependent modulation of the sulfur assimilation pathway via the promotion of the activity of OASTL. Additionally, the reprogramming of Ser-Cys flux by NaHS could be a contributing factor to a more reduced cellular environment. The integrated analyses of transcriptomic and metabolomic results demonstrated alterations in Arg biosynthesis, Ser and Thr metabolism-related genes in NaHS-treated plants. Therefore, it is evident that the process of amino acid biosynthesis is modulated by H_2S. For instance, the root development in tobacco is modified by H_2S (YANG et al., 2024).

Tyr was the most significantly accumulated aromatic compound following H_2O_2, as evidenced by both metabolic and transcriptomic analysis. It is possible that the plants may initiate the accumulation of Tyr as a response mechanism to withstand H_2O_2-induced oxidative stress. Likewise, the beneficial effects of Tyr application on organic osmolyte accumulation, biomass, photosynthesis, H_2O_2 scavenging, MDA and electrolyte leakage on drought-stressed maize plants were noted by EL-MOGY et al. (2024). Therefore, the effective accumulation of Tyr, along with the other free amino acids, may be one of the underlying causes of the reduced oxidative stress observed in H_2O_2-fed plants as compared to those treated with Asc.

Following NaHS application, Glu levels showed a notable accumulation compared with Asc treatment, and similar trends were observed for GABA, Gln, Arg, and PUT-all derived from Glu. Thus, making Glu a central hub in nitrogen metabolism and regulation (FORDE AND LEA, 2007). Elevated Gln after NaHS exposure appears linked to enhanced transcription of the Gln synthase

gene (*ZmGS3*), suggesting a control mechanism at the transcriptional level. Interestingly, the strongest expression of the GABA-specific *aminotransferase y4uB* gene occurred after 7 days of Asc treatment, coinciding with the lowest GABA accumulation.

Apart from its role in nitrogen metabolism, Glu also contributes to osmotic adjustments and redox balance through its conversion into Pro and GSH (FORDE AND LEA, 2007). Nevertheless, NaHS-treated maize seedlings exhibited higher Pro and GSH than those treated with Asc. Redox modulation of Pro levels has been demonstrated in Arabidopsis (GULYÁS et al., 2017). Similarly, GABA plays a part in shaping the redox state, with exogenous application increasing H_2O_2, Asc, and GSH, and antioxidant enzyme activity in apple (CHENG et al., 2023) and boosting Asc synthesis gene expression in kiwifruit (LIU et al., 2023).

Moreover, Gly and Ser contributors of GSH biosynthesis also accumulated more strongly after prolonged NaHS exposure than after Asc treatments. Together, these changes help explain the enhancement of GSH levels in NaHS-treated plants.

5.5.2. *Polyamines*

The role of polyamines in oxidative stress signalling and tolerance is pivotal. The process of conversion of PUT to SPD and SPM is successive. The formation of 1,3-diaminopropane (DAP) is a consequence of the oxidative deamination of SPD and SPM by PAO, while PUT is catalysed by DAO. In the present experiment, Asc and H_2O_2 significantly increased PUT levels after 3 days, though this discrepancy was diminished after 7 days **(Fig. 15a)**. SPD and SPM did not show any significant changes after 3 days. However, prolonged treatments significantly lowered them with respect to the control **(Fig. 15b-c)**. DAP content presented varied trends, with the lowest levels after Asc and the highest levels after H_2O_2 treatments. Nevertheless, no significant changes were noted after NaHS application **(Fig. 15d)**. The enzyme activity of DAO and PAO was also analysed to give a clearer picture of the polyamine metabolism. DAO activity was only significantly increased after 7 days of the treatments, with the trend Asc>H_2O_2>NaHS **(Fig. 15e)**. In the case of PAO, H_2O_2-treated plants maintained continuously significantly higher activity. No significant changes were observed for the other two treatments except for the 7 days NaHS-treated plants in comparison to the controls **(Fig. 15f)**.

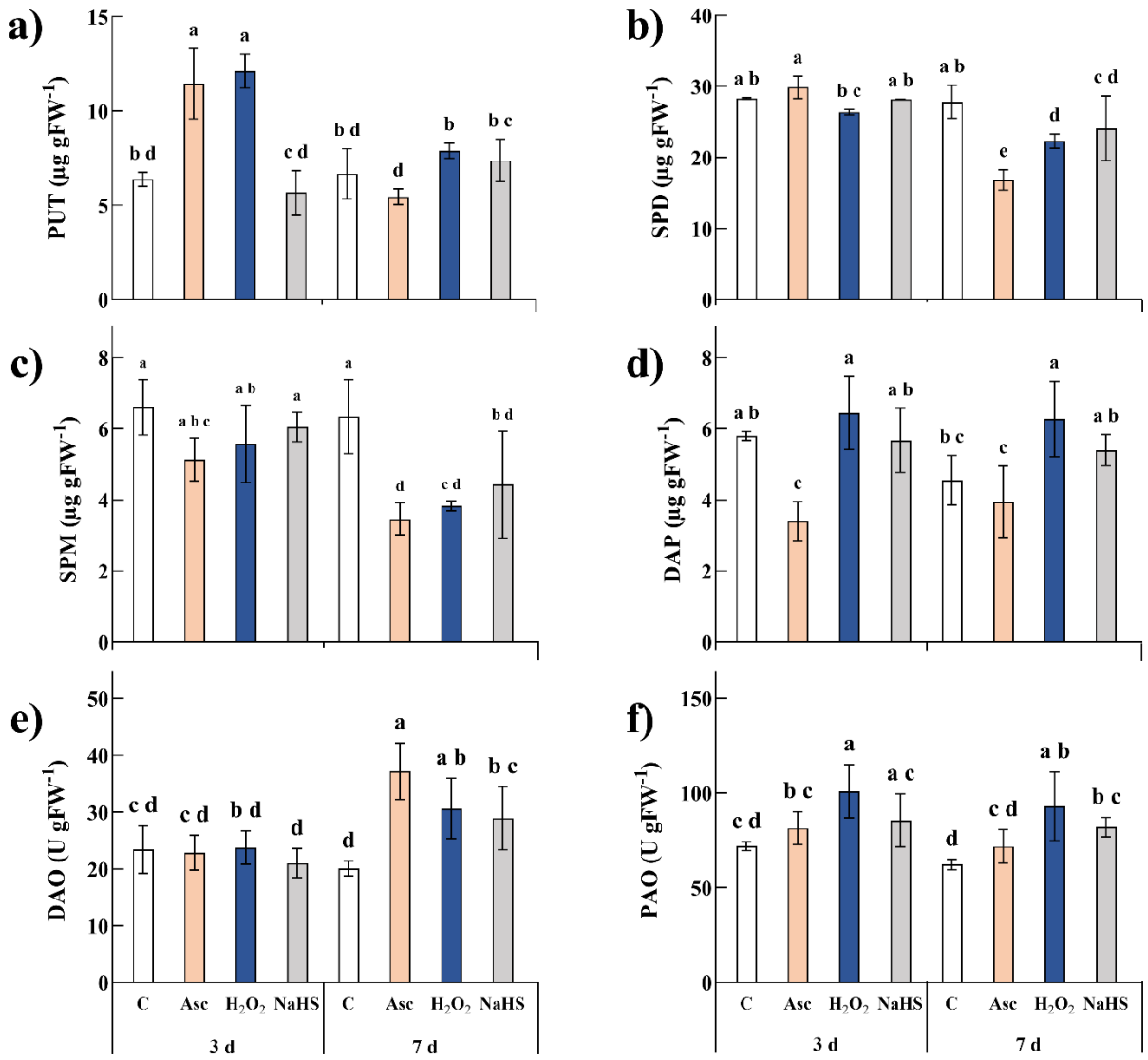

Figure 15: The effect of 5 mM ascorbate (Asc), 5 mM hydrogen peroxide (H_2O_2), and 1 mM sodium hydrosulfide (NaHS) treatment on PAs, (a) Putrescine (PUT), (b) Spermidine (SPD), (c) Spermine (SPM), (d) 1,3-diaminopropane (DAP), (e) Diamine oxidase (DAO), and (f) Polyamine oxidase (PAO) in maize seedlings after 3 and 7 days of the treatment along with the respective controls (C). Values marked with different letters are significantly different from each other at $p \leq 0.05$ levels (One-way ANOVA followed by Fisher's Least Significant Difference (LSD) Test for the data obtained with three biological replicates each).

Redox-mediated transcriptional regulation of the polyamine metabolism was analysed as well. The gene encoding the enzyme arginine decarboxylase (responsible for PUT synthesis; *ZmADC*) was transiently elevated after 3 days of all the treatments, with the most pronounced expression after

Asc application **(Fig. 16)**. However, this discrepancy was no longer observed after 7 days, as all the treatments caused a lower expression of the gene. In contrast, after 3 days, Asc and H_2O_2 exhibited a decline in the gene expression associated with SPD and SPM enzymes (*ZmSPDS* and *ZmSPMS*) **(Fig. 16)**. On the contrary, the expression was higher following 7 days. A comparable trend was also recorded for *ZmSAMDC2*. Furthermore, the expression of *ZmPAO1* was significantly reduced after 3 days of Asc and H_2O_2 treatment **(Fig. 16)**.

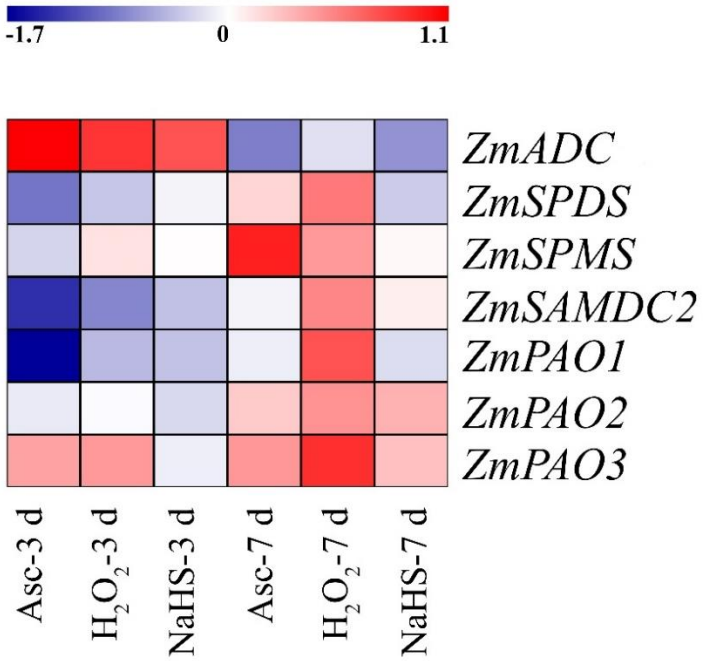

Figure 16: The effect of 5 mM ascorbate (Asc), 5 mM hydrogen peroxide (H_2O_2), and 1 mM sodium hydrosulfide (NaHS) on the relative gene expression of the polyamine-related genes in maize seedlings relative to the respective controls after 3 and 7 days of treatments. The colouring represents the log2 values of the relative gene expression, with blue as the downregulated and red as the upregulated values. The heatmap was created using the software MultiExperiment Viewer (MeV). *ZmADC- Zea mays arginine decarboxylase 1; ZmSPDS- Zea mays spermidine synthase; ZmSPMS- Zea mays spermine synthase; ZmSAMDC2- Zea mays S-adenosylmethionine decarboxylase 2; ZmPAO1,2,3- Zea mays polyamine oxidase1,2,3*

Orn and Arg serve as the polyamine precursor. Their lowest levels were detected after Asc treatment. This trend was reflected in reduced SPD, SPM, and DAP levels. These observations are also supported by the available literature that tightly links polyamine metabolism and nitrogen assimilation. For instance, exogenous SPD has been shown to enhance ammonia assimilation by

stimulating related enzymes, thereby influencing amino acid precursor levels (DONG et al., 2022). Additionally, H_2O_2 generated during polyamine catabolism can further modulate this pathway.

Met is one of the precursors of polyamines via S-adenosyl-L-methionine (SAM). SAM acts as a point of divergence between ethylene and polyamine biosynthesis pathways. SAM can either be converted to ACC and commit to ethylene synthesis. Or, it can be decarboxylated to form decarboxylated S-adenosylmethionine (dcSAM), which promotes SPD and SPM formation (PÁL et al., 2021). However, it is to be noted that the availability of SAM *in vivo* does not represent the rate-limiting step in the biosynthesis of either ethylene or polyamines, and both pathways can be operational simultaneously (MEHTA et al., 2002). In the present study, after Asc application, there was a significant elevation in *ZmACCO* expression (discussed in section 5.6; **Fig. 18b**). Concurrently, PUT, SPD, and SPM decreased from 3 to 7 days along with a higher activity of DAP. These observations further support the coordinated control of polyamines and ethylene formation as polyamines are considered to be anti-senescence growth regulators and act antagonistically to ethylene (ANWAR et al., 2015). A similar reduction in polyamine biosynthesis and increased catabolism was observed in detached maize leaves treated with 0.1 mM Asc by TERZI et al. (2015). In the case of H_2O_2, a significant accumulation of DAP can be attributed to the higher PAO activity and expression of the *ZmPAO1* gene. This is also reflected in the levels of SPD and SPM. Comparable results were obtained by ZHAO et al. (2024) in *Chenopodium quinoa* Wild as well. The low-temperature-induced oxidative stress promoted polyamine catabolism, even at the transcriptional level of certain genes, including *CqPAO* genes.

5.5.3. *NO*

Endogenous NO level varied among the treatments. After 3 days, though all the treatments caused higher NO levels, only Asc caused a significant increase. However, after 7 days, the levels of NO in Asc-treated plants were similar to the control **(Fig. 17a)**. On the contrary, its level increased markedly in H_2O_2 and NaHS-treated plants after 7 days. Thus, all the treatments exhibited an upward trend, but only H_2O_2 and NaHS could sustain this after 7 days as well. At the transcriptional level, all the chemicals resulted in a lower expression of the *ZmNNR1 (Zea mays nitrate reductase 1)* gene after both days of sampling, with the greatest downregulation recorded after 7 days of Asc application **(Fig. 17b)**.

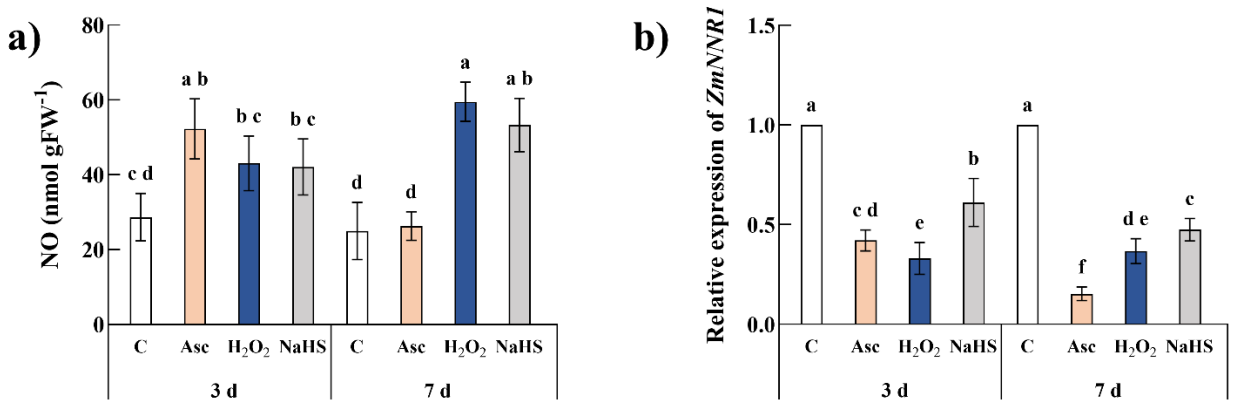

Figure 17: The effect of 5 mM ascorbate (Asc), 5 mM hydrogen peroxide (H_2O_2), and 1 mM sodium hydrosulfide (NaHS) treatment on a) endogenous nitric oxide (NO) levels and b) relative expression of *Zea mays nitrate reductase 1* (*ZmNNR1*) after 3 and 7 days of the treatment along with the respective controls (C). Values marked with different letters are significantly different from each other at $p \leq 0.05$ levels (One-way ANOVA followed by Fisher's Least Significant Difference (LSD) test for the data obtained with three biological replicates each).

NO is one of the most important signalling molecules regulating plant physiology and biochemistry. The transient elevations in its levels by Asc after 3 days and lowering to control levels could be attributed to a feedback inhibition mechanism, as is noted with *ZmNNR1* expression after 7 days. The higher levels of NO can cause toxic effects and inhibit growth. Therefore, optimal levels are maintained in plants (KHAN et al., 2023). A close interdependency between Asc and NO is elucidated by KUMAR et al. (2016), where lower levels of Asc coincided with lower NO levels, and exogenous application of 5 mM Asc resulted in higher NO levels along with a higher nitrate reductase activity. Furthermore, an interaction between polyamines, NO and H_2O_2 under chilling stress was elucidated in tomato seedlings, where H_2O_2 acted upstream of NO (DIAO et al., 2017). In addition, NO promoted H_2O_2 production, the promotion of the activity of RuBisCo, and the elevation of Asc, glucose, fructose, sucrose, and glutathione in low-temperature stressed cucumber seedlings. The application of the ROS inhibitor, however, diminished all these NO-induced beneficial effects. Thus, depicting the dependencies of NO and H_2O_2 in modulating the Asc-GSH cycle under cold stress (WU et al., 2021).

An increasing tendency was noted in the case of NaHS as well. These results are in accordance with the available literature, where the interactive effects of H_2S and NO are studied. For instance, NO triggers the L-C-Des/H_2S signalling pathway to induce thermotolerance in maize seedlings

(SUN et al., 2022). Likewise, NaHS-NO interaction induced salt stress tolerance in barley (CHEN et al., 2015), Arabidopsis (SCUFFI et al., 2014), and Capsicum (LISJAK et al., 2011). Thus, these studies provide further evidence in support of the crosstalk between NO and cellular redox balance. There exists a redox compound concentration- and treatment duration-dependent effect on NO production.

5.6. *Hormones and their gene expression*

A varied trend was noted for hormones after the treatments. *o*HCA, a precursor for SA, was accumulated the most after H_2O_2 treatment. It showed reduced levels after 7 days of Asc and NaHS addition **(Fig. 18a)**. Consequently, Asc and H_2O_2 resulted in significantly higher levels of the two forms of SA on both sampling days. Likewise, higher levels were observed for JA and its bioactive form, JA-LE/ILE, in Asc and H_2O_2-treated plants. ABA and its catabolic products (phaseic acid and dihydrophaseic acid) were all higher after Asc and H_2O_2 application, with multifold accumulation after 3 days of H_2O_2 treatment (26-, 8.6- and 21- fold increase in ABA, PA and DPA, respectively) **(Fig. 18a)**. To get insight into the transcriptional control of ABA level, the expression of biosynthesis (*ZmVP14-1*, *ZmVP14-2*, and *ZmNCED*) and catabolism-related genes (*ZmABAox1a*, *ZmABAox3a*) were investigated. The results were in accordance with the ABA levels, as *ZmVP14-1* and *ZmVP14-2* (*Zea mays viviparous 14*) were all upregulated in response to Asc and H_2O_2 after both days (except *ZmVP14-2* in 7 day H_2O_2); conversely, NaHS treatment displayed downregulation in the expression, exhibiting levels similar to the control **(Fig. 18b)**. Opposite to NaHS, *ZmNCED* (*Zea mays nine-cis epoxycarotenoid dioxygenase*) was continuously upregulated in response to Asc, while it only showed higher expression after 7 days of H_2O_2 application **(Fig. 18b)**. The catabolism-related genes *ZmABAox1a* and *ZmABAox3a* (*Zea mays abscisic acid oxidase 1a/3a*) were downregulated in all the treatments after 3 days. *ZmABAox3a* showed slight upregulation after 7 days of NaHS, while *ZmABAox1a* was strongly downregulated in all the treated plants **(Fig. 18b)**. In addition, ethylene biosynthesis-related genes *1-Aminocyclopropane-1-carboxylate synthase* (*ZmACS*) and *1-aminocyclopropane-1-carboxylic acid oxidase* (*ZmACCO*) were also investigated. *ZmACS* expression was downregulated by H_2O_2 after both treatment durations. Conversely, the Asc application maintained its relatively higher expression levels, whereas NaHS caused their transient increase after 3 days. However, after 7 days, the *ZmACS* expression was downregulated by NaHS. In the case of *ZmACCO*, Asc strongly

upregulated the expression (6 times) relative to the control after 7 days. However, NaHS and H_2O_2 lowered it after 7 days **(Fig. 18b)**.

a)

ng g^{-1} FW^{-1}	3 d				7 d			
	C	Asc	H_2O_2	NaHS	C	Asc	H_2O_2	NaHS
Bound *o*HCA	b 9488.00	b 10775.00	a 12362.33	b 9575.00	b 9519.00	c 6054.00	a 12497.00	c 5718.00
Free SA	c 22.00	b 38.00	bc 31.33	bc 25.33	c 23.67	a 62.67	bc 30.00	c 24.33
Bound SA	de 284.33	b 460.67	bc 383.67	cd 359.00	e 251.00	a 567.33	bc 403.67	bc 373.67
Auxin	a 2.15	ab 1.86	ab 2.04	ab 1.90	ab 2.02	b 1.34	ab 1.65	ab 1.82
ABA	d 4.38	b 65.90	a 117.50	d 9.57	d 5.47	c 32.23	b 53.93	d 3.74
PA	d 2.42	bc 8.71	a 20.73	d 3.82	d 3.49	cd 5.94	b 10.75	d 2.20
DPA	d 7.37	cd 25.57	a 155.50	cd 21.50	cd 13.16	c 33.23	b 92.77	d 12.00
JA	ab 160.33	ab 202.00	a 236.00	ab 182.33	b 90.10	ab 199.67	ab 160.00	b 103.35
JA-LE/ILE	a 6.41	a 7.58	a 8.29	a 5.58	a 3.01	a 6.43	a 6.03	a 5.16

Minimum — Maximum

b)

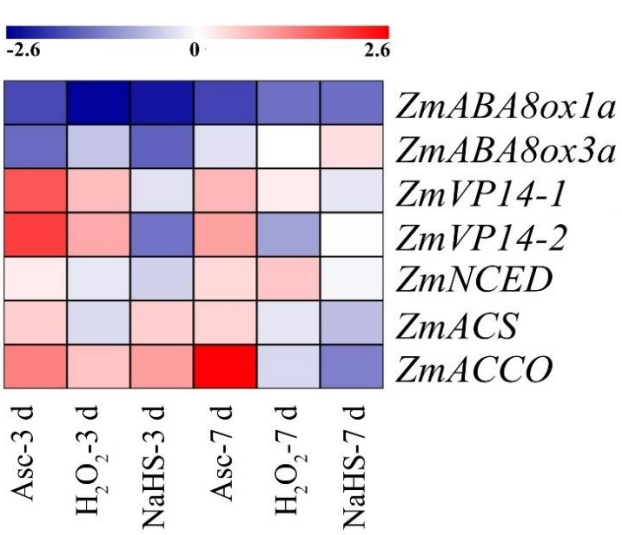

Figure 18: The effect of 5 mM ascorbate (Asc), 5 mM hydrogen peroxide (H2O2), and 1 mM sodium hydrosulfide (NaHS) on a) the hormonal profile, b) the relative gene expression of the hormones related genes of maize seedlings along with the respective controls (C) after 3 and 7 days of the treatments. For a) the colouring is applied individually to each row, while for b) the overall heat map is coloured (created using MultiExperiment Viewer

MeV), representing log2 values with blue representing the lowest level and red representing the highest level. Values marked with different letters are significantly different from each other at $p \leq 0.05$ level (One-way ANOVA followed by Fisher's Least Significant Difference (LSD) Test for the data obtained with three biological replicates each). *o*HCA: *ortho*-hydroxycinnamic acid, SA: salicylic acid, ABA: abscisic acid, PA: phaseic acid, DPA: dihydrophaseic acid, JA: jasmonic acid, JA-LE/ILE: JA-isoleucine/ leucine, *ZmVP14*: *Zea mays viviparous 14*, *ZmACCO: 1-aminocyclopropane-1-carboxylic acid oxidase*, *ZmACS: 1-aminocyclopropane-1-carboxylate synthase*, *ZmABAox1a/3a: abscisic acid oxidase 1a/3a*, *ZmNCED: nine-cis epoxycarotenoid dioxygenase*.

Redox-dependent changes in hormones were observed at the metabolite and transcriptional levels, with a more oxidising environment promoting the accumulation of SA, ABA, and JA, while a reduced environment coincided with their lowest levels. Results similar to ours of hormone accumulation were obtained in rice (ZHOU et al., 2020), wheat (ASGHAR et al., 2023a), and Arabidopsis (BULLEY et al., 2021). Interestingly, literature suggests ABA-associated JA signalling via the interaction of the PYL6 ABA receptor with the MYC2 transcription factor in Arabidopsis (ALEMAN et al., 2016). This could be a possible factor in their simultaneous accumulation. In addition, ABA accumulation is affected by Asc redox state and promotes the antioxidant activity (LÓPEZ-CARBONELL et al., 2006; LU et al., 2009). Likewise, Asc metabolism can be modulated by exogenous application of JA (Alharbi and Alaklabi, 2022), with H_2O_2 build-up and promoting antioxidant activity (SOARES et al., 2010). Taken together, different redox compounds exerted different effects on the redox state, which in turn affected hormone accumulation, metabolism and plant physiology.

5.7. *Phenols (phenylpropanoids and flavonoids)*

Plant metabolism is tightly regulated by redox processes, and vice versa. Thus, to understand the redox-mediated changes in the amounts of flavonoids and the components of phenylpropanoid pathways was investigated. Cinnamic acid (involved in the synthesis of various alkaloids, secondary metabolites, and hormones) was strongly lowered after 3 days of H_2O_2 treatment **(Fig. 19a)**. Vanillin isomer and vanillic acid showed a similar trend of being accumulated after application of Asc and H_2O_2 but showed similar levels to the control after NaHS treatment. Asc and H_2O_2 after 3 days reduced *p*-coumaric acid content, while it was not affected by NaHS. After 7 days of NaHS and H_2O_2 treatment, its level was similar to that in treated and control plants **(Fig. 19a)**. Ferulic acid is the most abundant hydroxycinnamic acid that influences cell wall extensibility

and the strength of the cell wall. Ferulic acid 2 and 3 showed alike patterns of being accumulated in H_2O_2-treated plants after both treatment durations and increasing from 3 to 7 days after Asc application **(Fig. 19a)**.

Flavonoids, including kaempferol, naringenin, chlorogenic acid, and luteolin, showed treatment- and time-dependent changes. Naringenin levels were lowest after 3 days of H_2O_2 treatment, while NaHS treatment resulted in the highest levels of naringenin and related compounds (dihydrokaempferol, quercetin) **(Fig. 19b)**. Though they declined after 7 days. Luteolin-7-O-glucoside peaked after 7 days in Asc-treated plants but was lowest after H_2O_2 addition. Luteolin increased as a response to Asc and NaHS treatment. It remained high under Asc, but declined with NaHS after 7 days **(Fig. 19b)**.

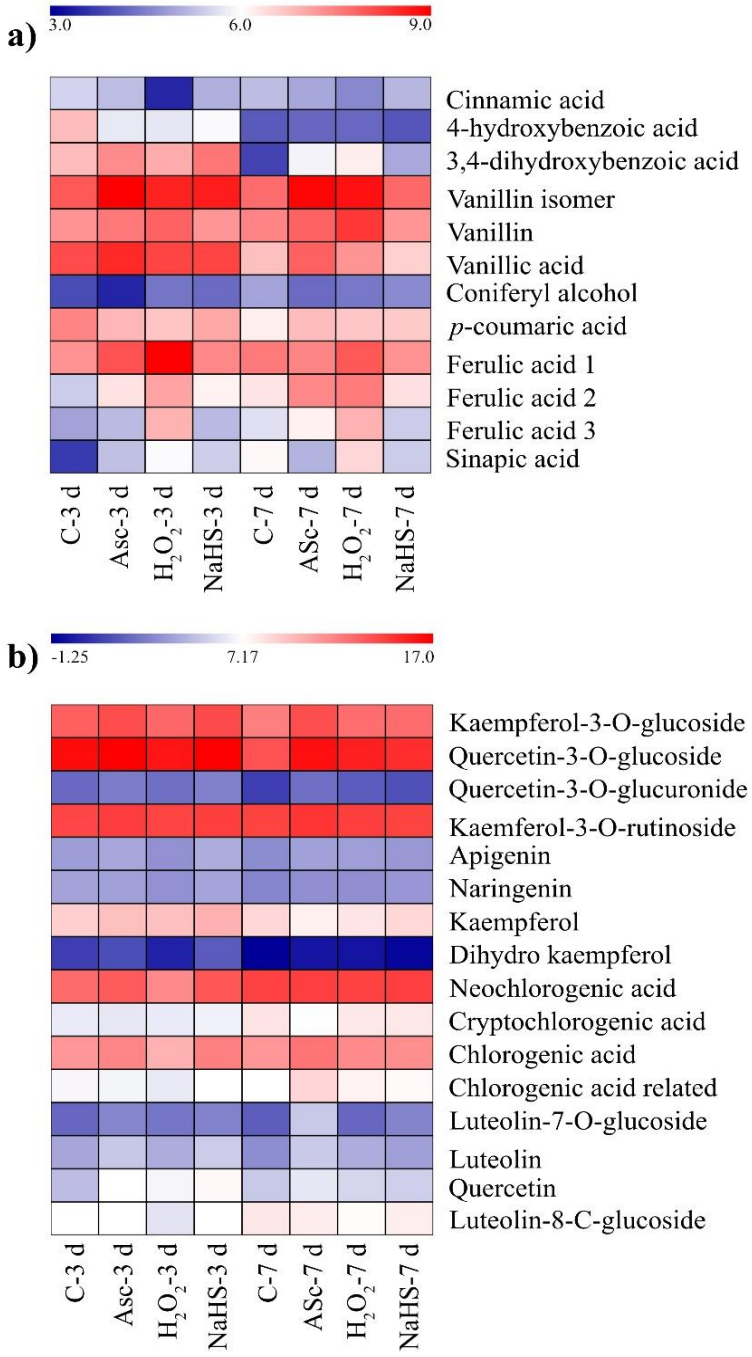

Figure 19: The effect of 5 mM ascorbate (Asc), 5 mM hydrogen peroxide (H_2O_2), and 1 mM sodium hydrosulfide (NaHS) on phenylpropanoids in maize seedlings along with the controls (C) after 3 and 7 days of the treatments. (a) phenylpropanoid compounds, (b) flavonoids. The numbers 3 and 7 refer to the sampling day after treatment. The colours represent the log2 values of the average of three biological replicates used to measure the endogenous levels of the various compounds. The heatmap was created using the software MultiExperiment Viewer (MeV).

The redox state and phytohormones are key regulators in phenol and flavonoid metabolism, which in turn also modulate cellular redox homeostasis (BERGONCI et al., 2023). For instance, JA is reported to promote the production of these compounds (FAROOQ et al., 2016). In the present experiment, Asc treatment led to higher JA levels **(Fig. 19a)**, which were accompanied by an increase in kaempferol, quercetin, apigenin, chlorogenic acid, luteolin, vanillic acid, and ferulic acid. Similarly, H_2O_2 treatment raised ABA, JA, and SA levels, resulting in higher accumulation of coniferyl alcohol, 3,4-dihydroxybenzoic acid, vanillin and its isomers, sinapic acid, ferulic acid, kaempferol, quercetin, and luteolin. Comparable patterns were reported in Chinese cabbage, where 100 μM SA increased trans-ferulic acid, kaempferol, and quercetin levels under salt stress (LINIĆ et al., 2021). NaHS treatment did not show much variation in measured phytohormones and related phenolic compounds, whereas Asc and H_2O_2 treatments significantly boosted them. Thus, exhibiting different redox compound-dependent influences in phenolic metabolism in maize.

5.8. *Interconnectedness of the studied parameters*

The application of Asc, H_2O_2, and NaHS caused a shift in the redox balance. The ratio of GSH/GSSG was shifted towards a more oxidised state by Asc and H_2O_2, while NaHS created a more reducing environment. Likewise, the total ascorbate pool also changed. As a consequence of this redox imbalance, changes in H_2O_2 levels were observed along with the varied degrees of electrolyte leakage and lipid peroxidation. Simultaneously, modulations in the antioxidant enzyme activities were noted to compensate for the redox shift. The redox imbalance also affected carbon assimilation, as was evident in the changes in the amounts of carbohydrates and organic acids. These further affected the dependent downstream cycles, such as the TCA cycle, amino acid metabolism, phenylpropanoid and flavonoid synthesis, polyamine metabolism, and hormonal profiles as well. With the available literature, it can be concluded that there exists a tight interdependence of the redox system and metabolism (GEIGENBERGER AND FERNIE, 2014).

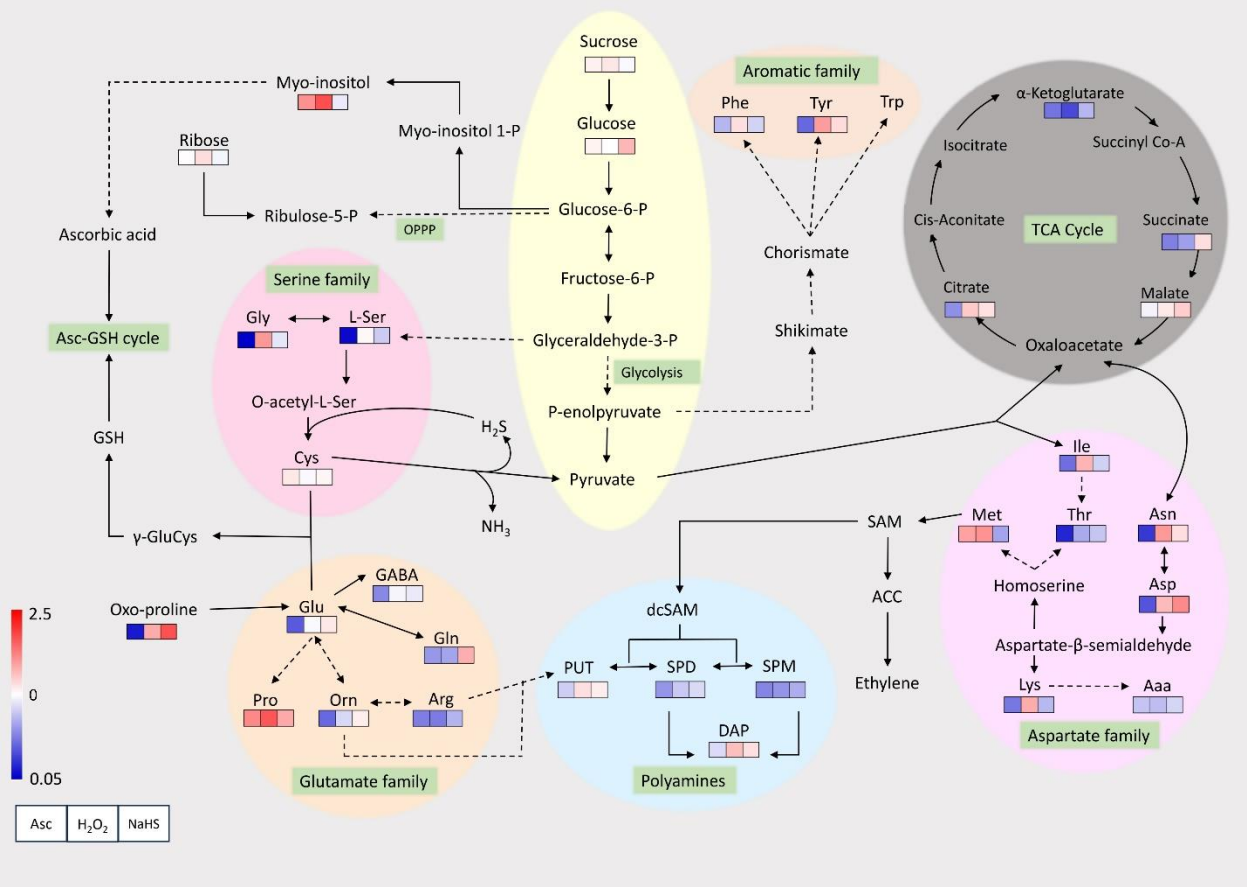

Figure 20: An overview of metabolic changes involved in primary pathways of maize seedlings after 7 days of 5 mM Asc, 5 mM H_2O_2, and 1 mM NaHS treatment. The horizontal boxes follow the order of Asc, H_2O_2, and NaHS from left to right. The colour coding represents the relative fold change value with respect to the control. The control value is zero here as the relative fold change is measured. Values above 0 (in red) represent a higher value, and values below 0 (in blue) indicate a lower value. The continuous lines indicate a direct metabolic connection, and the dotted lines show several intermediate products between them. With the three-letter abbreviations of the amino acids, the following other ones are used: Aaa- α-Aminoadipic acid; PUT- Putrescine; SPD- Spermidine; SPM- Spermine; DAP- 1,3-diaminopropane; γ-GluCys- gamma-glutamylcysteine; GABA- gamma-aminobutyric acid; OPPP- Oxidative pentose phosphate pathway; TCA- Tricarboxylic acid cycle; Asc-GSH cycle- Ascorbate-Glutathione cycle.

The three chemicals modified every studied aspect differently and exhibited varied changes **(Fig. 20)**. The applied chemicals exhibit beneficial changes at lower concentrations. Whereas negative effects are recorded at higher concentrations (ASGHAR et al., 2023b; SINGH et al., 2024).

In the case of Asc treatment, the oxidising environment caused higher electrolyte leakage, lipid peroxidation, and H_2O_2 accumulation after 7 days. Simultaneously, it resulted in higher CAT, GR,

DHAR and MDHAR activity. As a consequence of redox imbalance, carbon assimilation was negatively affected. The various components of the TCA cycle (succinic acid and citric acid) were reduced, whereas in the case of H_2O_2 addition, α-ketoglutaric acid was lowered. On the contrary, malic acid, arabinose, citric acid, and myoinositol were accumulated, and subsequently, the amino acid profile was modified **(Fig. 20)**. ABA, SA, and JA were accumulated. Hormonal crosstalk with the other measured components (such as phenylpropanoids, organic acids, and amino acids) further affected polyamine metabolism at the transcriptional level and at the metabolic level. These simultaneous molecular changes were reflected in plant morphology and anatomy as the growth was compromised. The plants had visibly less sturdiness **(Supp. Fig. 4)**. Disturbed redox balance mediated changes, and the lack of essential building block amino acids was evident in growth parameters as reduced shoot length and fresh weight.

Considering the effects of Asc on polyamines and ABA synthesis, it can be concluded that Asc probably led to ABA accumulation and triggered *ZmADC1*-mediated PUT burst after 3 days. This is further supported by the findings of WAHEED et al. (2024) and JIANG et al. (2025), who elucidated the process of salt stress-induced ABA promotion. This, in turn, triggered polyamine biosynthesis in maize under salt stress. However, the strategy changes in the prolonged redox imbalance. The effect of Asc and H_2O_2 on polyamine metabolism may be ABA-mediated, as is evidenced by ABA accumulation at the metabolic and transcriptional level. Likewise, H_2O_2-mediated ABA accumulation was noted in the leaves of *Brassica napus* under drought stress (LEE et al., 2022). These results indicate a tightly regulated redox metabolism of polyamines with phytohormones.

6. CONCLUSIONS AND RECOMMENDATIONS

Plants being fixed in the soil can't evade the harsh environment. These unavoidable conditions, including abiotic and biotic stresses, induce oxidative stress in plants. The redox imbalance negatively affects plant growth and development, ultimately leading to yield loss. From the perspective of the current global climate scenario, the increasing temperature, along with frequent flooding or drought, is projected to further increase yield losses. Thus, imposing the need to develop climate-resilient crops by understanding oxidative stress-mediated changes in the plant metabolism. In the current study, we could simulate the disturbing effects of environmental stresses on the redox environment using oxidants and reductants. The three compounds- Asc, H_2O_2, and NaHS- have different effects on plant physiological, biochemical and molecular processes.

The three chemicals altered the redox homeostasis to a varying degree, as was evident by the measurement of membrane damage, electrolyte leakage and endogenous H_2O_2 levels. Asc application caused the maximum membrane damage, followed by H_2O_2 and NaHS. Furthermore, as expected, the GSH/GSSG ratio exhibited the trend as Asc<H_2O_2<NaHS. Reduced to the oxidised Cys ratio was also the lowest for Asc after both days. Prolonged Asc-mediated oxidative stress also negatively affected photosynthetic pigments (Chlorophyll a and b) significantly. In contrast, NaHS application did not show any damage to the photosynthetic machinery, which could be the result of a more reduced cellular environment. Furthermore, due to redox imbalance, the antioxidant system is activated in plants. In the current study, Asc and H_2O_2 triggered the activity of the antioxidant enzymes (APX, MDHAR, DHAR, GR, and CAT). Such changes were manifested at the transcriptional level as well after these two treatments. However, NaHS mostly exhibited the antioxidant enzyme activities similar to those of the control plants, with the lower expression of the related genes as well. In the case of non-enzymatic antioxidants, Asc and H_2O_2 showed a general accumulation of oxidised Cys and GSSG, while NaHS-treated plants had an opposite trend.

These chemical-mediated redox changes and antioxidant activation affected redox-dependent metabolic processes such as glycolysis and the TCA cycle. Asc and H_2O_2-treated plants had a lower accumulation of most of the measured metabolites except for sucrose after 3 days of Asc,

while prolonged application of the two chemicals affected metabolite biosynthesis differently. In contrast, NaHS again had levels comparable to the control group. The changes in the metabolites of glycolysis and the TCA cycle affected the downstream processing of amino acids and subsequently polyamines and phenolic compounds. As a result, total amino acids were significantly lower in Asc, and H_2O_2 exhibited a significant decrease from 3 to 7 days of the treatment. NaHS-treated plants had levels similar to the control. Consequently, corresponding changes in the accumulation of polyamines, phenylpropanoids, and flavonoids were noted.

The synthesis and metabolism of phenolic compounds are also redox sensitive. Due to disturbed redox homeostasis, the modified phenylpropanoid and flavonoid profile was observed. Some of these phenolic compounds act as antioxidants, and their accumulation could be attributed to the same. In addition, these phenolic compounds serve as the precursor for the biosynthesis of phytohormones. Therefore, a modified hormonal profile was expected. Moreover, these phytohormones are redox responsive. They accumulate under stressful conditions to help induce tolerance and survival. The accumulation of ABA, SA, and JA could be a stress response to further stabilise the cellular redox balance, as phytohormones are known to trigger the antioxidant machinery as well. In summary, the reduced growth parameters in Asc and H_2O_2-treated plants could be a cumulative result of the above-mentioned parameters. Non-significant changes in growth are not surprising in the case of NaHS because the majority of the factors had levels similar to the control.

In light of the present results, future studies can be focused on the specific redox sensors, such as Quiescin sulfhydryl oxidase 1 (boosts plant immunity), the subcellular distribution of these antioxidant compounds, and their interaction with other signalling molecules. Studies with mutants and transgenic plants could be conducted to analyse the direct functional involvement at the molecular level of the identified compounds. Practical use of modulating the redox environment to induce stress protection, regulating growth and development can be conducted. Furthermore, gene editing, seed coating or spraying with certain redox compounds could be investigated under varied or combined stresses, imitating field conditions. The redox-modulating effect by modifying GSH metabolism to ultimately influence plant physiology and stress response is of benefit to increase amino acid accumulation resulting in improved nutritional quality as well.

7. NEW SCIENTIFIC RESULTS

1. Asc, H_2O_2, and NaHS have specific physiological effects, since only Asc and H_2O_2 decreased the growth, chlorophyll content and increased lipid peroxidation.
2. Asc shifts the GSH-dependent redox environment in a more oxidising and NaHS in a more reducing direction, while its intermediate state occurs after H_2O_2 addition.
3. The more oxidising redox environment after Asc -treatment activates some antioxidant enzymes (CAT, DHAR) at the gene expression and activity level.
4. The redox compounds control the metabolism in a specific way, since lower level of several compounds of glycolysis, tricarboxylate cycle and nitrogen metabolism (amino acids, polyamines, NO) was detected after Asc and H_2O_2 application compared to NaHS treatment.
5. Different redox regulation of some phenolics and flavonoids occurs by the three studied compounds since they exhibited a greater increase after Asc and H_2O_2 addition compared to the effect of NaHS.
6. The specific interaction between the hormonal and redox system is indicated by greater SA, JA and ABA levels after Asc and H_2O_2 treatments compared to NaHS addition.

8. SUMMARY

Environmental conditions pose an unavoidable stress to plants. The harsh abiotic stressors include drought, salt, flood, extreme temperatures (hot and cold), and light (intensity and spectrum variations). Biotic factors include viruses, bacteria, fungi, insects, and nematodes (MITTAL et al., 2023). All these factors cause oxidative stress in plants, disrupting the normal plant physiology and ultimately affecting the yields of crop plants. The redox imbalance for a prolonged period severely reduces yield by damaging cellular components such as membranes, pigments, DNA and proteins as well. Furthermore, it negatively affects photosynthesis, energy metabolism, cellular organelles development, vital metabolic processes, grain filling, and overall plant growth and development (TAVU AND REDILLAS, 2025). Based on the data from 1985-2023, the maize yield failure exhibited an increasing trend in Hungary (HUZSVAI et al., 2024). Furthermore, the news article published on the Agroberichten Buitenland (an online platform for Dutch agricultural cooperation and news) in July 2024, clearly stated that a sudden heatwave could be the reason for a 30 to 40% harvest loss of maize in 2024 in Hungary alone (AGROBERICHTEN BUITENLAND, 2024). Therefore, the need of the hour is not only to understand the stress-mediated molecular changes, but also to develop climate-resilient crops. The understanding of the redox-mediated changes in plant metabolism could provide helpful insights to solve the problem at hand.

The current study focuses on the simultaneous changes caused by the disruption of the redox balance via the application of the 3 redox chemicals – Asc, H_2O_2, and NaHS. The study aimed to understand the altered redox homeostasis and its crosstalk with other components, including hormones, amino acids, thiols, organic acids, polyamines, and phenols. Thus, giving a holistic view of redox chemistry mediating maize growth and stress response. To achieve the objectives, maize seeds were first germinated and then cultivated for a week in a growth chamber. After 7 days of cultivation, the Hoagland solution was supplemented with either 5 mM Asc, 5 mM H_2O_2, or 1 mM NaHS. Sampling was done after 3 and 7 days of the chemical treatments. The shoot samples were collected and used for biochemical and transcriptional analysis.

The chemical treatments applied altered the cellular redox balance. As a result, they differently affected plant growth. For instance, Asc-treated plants exhibited significantly higher electrolyte

leakage, lipid peroxidation, oxidised Cys, and total CG (GSH degradation product). In addition, a lower GSH/GSSG and reduced Cys/oxidised Cys ratios were noted. As a consequence of oxidative stress, lower photosynthetic pigment accumulation and compromised shoot - root FW and shoot length were observed. In the case of H_2O_2, despite similar reduced Cys/oxidised Cys and GSH/GSSG ratios, GSH levels, photosynthetic pigments, and H_2O_2 levels to the control plants, higher electrolyte leakage and lipid peroxidation were noted. Thus, after 7 days of continuous treatment, compromised shoot FW and length with lower root FW were observed. Interestingly, for NaHS, the plants maintained a reduced cellular environment as shown by reduced Cys/oxidised Cys and GSH/GSSG ratios. Furthermore, comparable levels to control plants were detected of electrolyte leakage, H_2O_2, and chlorophyll a and b after 7 days. Ultimately leading to non-significant changes in shoot growth and root length.

To get the insights into the modulation of antioxidant machinery due to redox imbalance, the enzymes of the Asc-GSH cycle were analysed. Interestingly, Asc caused a significant increase in the enzyme activity of DHAR, MDHAR, GR, and CAT after 7 days. These changes were noted at the transcriptional level as well, with the *cMDHAR2* gene exhibiting a 10-fold increase. These relatively higher activities of the antioxidant enzymes could be a possible explanation for the lower H_2O_2 levels detected after 7 days in Asc-treated plants amid oxidative stress. In the case of H_2O_2, APX, MDHAR, GR, and CAT maintained a higher activity than the control plants after prolonged treatment. In contrast to Asc, H_2O_2 plants showed a relatively lower gene expression of the antioxidant enzyme-related genes after 7 days. The comparable activities of the antioxidant enzymes do not come as a surprise, as NaHS did not disturb the redox homeostasis.

To understand the simultaneous changes in the plant metabolic process as a result of redox imbalance, carbon and nitrogen metabolism were studied. A general lower accumulation of metabolites, including succinate, malic acid, α-ketoglutarate, and oxo-proline, was observed after Asc and H_2O_2. Conversely, NaHS caused the accumulation of malic acid, α-ketoglutarate, succinate, oxo-proline, and D-glucose after 7 days. The underlying reason for these different changes could be attributed to the efficient or disturbed photosynthesis and the limited availability of the components for energy production. Consequently, nitrogen metabolism was also modified. Total amino acid accumulation was significantly lowered by Asc, while H_2O_2 and NaHS had similar levels to the control. NaHS promoted Pro, Gln, and Cys accumulation, and the levels of

other amino acids were similar to the control plants. Likewise, NaHS triggered a higher expression of the *ZmGS3* gene responsible for glutamate synthase3 (involved in nitrogen assimilation by converting ammonia to glutamine). On the other hand, Asc and H_2O_2 downregulated *ZmGS3* expression. Moreover, the expression trend for the *ZmNNR1* gene was NaHS>H2O2>Asc after 7 days. Therefore, pointing to an altered nitrogen metabolism after the three treatments. The polyamine profile, its related enzymes' activities and transcriptional regulation were also modified differently after the application of the redox chemicals. Asc and H_2O_2-mediated PUT accumulation was noted after 3 days, which was lowered after prolonged treatment. SPD and SPM were significantly decreased after 7 days. In addition, H_2O_2-treated plants exhibited elevated levels of polyamine degradation product- DAP after both days of sampling. Interestingly, NaHS application-mediated depletion in the levels of SPD and SPM, along with a higher activity of DAO and PAO, was detected after 7 days. Therefore, providing evidence of differently redox-regulated metabolism by the three treatments.

Carbon metabolism supplies both energy and carbon skeletons for phenol biosynthesis. In addition, nitrogen assimilation facilitates aromatic amino acid biosynthesis. Thus, limited carbon availability, altered nitrogen metabolism, and oxidative stress conditions affected phenolic compound accumulation. As a result, in Asc and H_2O_2-treated plants, vanillin isomer, vanillic acid, vanillin, and ferulic acid were accumulated after 7 days. Likewise, NaHS promoted the accumulation of flavonoids, including naringenin, its related compounds and luteolin-7-O-glucoside after 3 days. Thus, Asc and H_2O_2 promoted the accumulation of phenylpropanoids, while NaHS favoured flavonoid biosynthesis via the H_2S signalling pathway. The available literature supports NaHS-mediated flavonoid accumulation under stress conditions in rice (TIAN et al., 2024) and ginkgo (LU et al., 2024).

The chemical-induced oxidative stress also affected the hormonal profile. Unlike NaHS, a greater alteration in redox balance after Asc and H_2O_2 treatments was accompanied by a higher accumulation of SA, ABA, and JA, especially after 3 days. The gene expression analysis exhibited a similar trend, as ABA synthesis-related genes were upregulated while catabolism-related genes were downregulated in Asc and H_2O_2-treated plants. Therefore, it can be concluded that altered redox homeostasis promoted the hormone production as an adaptive strategy.

Combining the studied parameters, it can be concluded that Asc and H_2O_2 caused more oxidative stress than NaHS. As a response, plants activated the antioxidant system and the production of stress hormones to counteract the accumulating ROS. In addition, glycolysis, the TCA cycle, nitrogen metabolism, and the synthesis of secondary metabolites were altered differently by the three treatments. The accumulation of various compounds exhibiting antioxidant activities was promoted. Oxidative stress disrupted the cellular redox environment, damaged photosynthetic pigments, and compromised membrane stability. This ultimately negatively affected plant growth. Thus, further confirming the interdependencies of redox balance on metabolism and vice versa.

The available results provide a holistic view of the simultaneous changes in glycolysis, the TCA cycle, amino acid biosynthesis, thiols, polyamines, NO, phenylpropanoids, flavonoids, hormones, and the antioxidant machinery under altered redox homeostasis. Thus, integrating primary metabolism, signalling pathways, and secondary metabolism under redox imbalance. The insights can be utilised in the models of redox-controlled metabolic reprogramming, identification of redox-sensitive metabolic nodes and regulatory checkpoints. Furthermore, the study supports the role of priming and treating the seeds or seedlings to enhance stress adaptation and nutritional quality and flavours in the crops.

9. APPENDICES

A1: Bibliography

Agroberichten Buitenland, 2024. Hungary: Heat wave hits, causing huge losses – What crops can farmers pin their hopes on now?

Aleman, F., Yazaki, J., Lee, M., Takahashi, Y., Kim, A.Y., Li, Z., Kinoshita, T., Ecker, J.R., Schroeder, J.I., 2016. An ABA-increased interaction of the PYL6 ABA receptor with MYC2 Transcription Factor: A putative link of ABA and JA signaling. Sci. Rep. 6, 28941. https://doi.org/10.1038/srep28941

Alharbi, K., Alaklabi, A., 2022. Alleviation of salinity induced growth and photosynthetic decline in wheat due to biochar and jasmonic acid application involves up-regulation of ascorbate-glutathione pathway, glyoxylase system and secondary metabolite accumulation. Rhizosphere 24, 100603. https://doi.org/10.1016/j.rhisph.2022.100603

Ali, E., Hussain, S., Jalal, F., Khan, M.A., Imtiaz, M., Said, F., Ismail, M., Khan, S., Ali, H.M., Hatamleh, A.A., Al-Dosary, M.A., Mosa, W.F.A., Shah, F., 2023. Salicylic acid-mitigates abiotic stress tolerance via altering defense mechanisms in *Brassica napus* L. Front. Plant Sci. 14. https://doi.org/10.3389/fpls.2023.1187260

Ali, S., Tyagi, A., Bae, H., 2023. ROS interplay between plant growth and stress biology: Challenges and future perspectives. Plant Physiol. Biochem. 203, 108032. https://doi.org/10.1016/j.plaphy.2023.108032

Alvarez, M.E., Savouré, A., Szabados, L., 2022. Proline metabolism as regulatory hub. Trends Plant Sci. 27, 39–55. https://doi.org/10.1016/j.tplants.2021.07.009

Anjum, N.A., Gill, S.S., Corpas, F.J., Ortega-Villasante, C., Hernandez, L.E., Tuteja, N., Sofo, A., Hasanuzzaman, M., Fujita, M., 2022. Editorial: Recent Insights Into the Double Role of Hydrogen Peroxide in Plants. Front. Plant Sci. 13. https://doi.org/10.3389/fpls.2022.843274

Anjum, S.A., Tanveer, M., Hussain, S., Bao, M., Wang, L., Khan, I., Ullah, E., Tung, S.A., Samad, R.A., Shahzad, B., 2015. Cadmium toxicity in Maize (*Zea mays* L.): consequences on antioxidative systems, reactive oxygen species and cadmium accumulation. Environ. Sci. Pollut. Res. 22, 17022–17030. https://doi.org/10.1007/s11356-015-4882-z

Anwar, R., Mattoo, A.K., Handa, A.K., 2015. Polyamine Interactions with Plant Hormones: Crosstalk at Several Levels, in: Polyamines. Springer Japan, Tokyo, pp. 267–302. https://doi.org/10.1007/978-4-431-55212-3_22

Asaeda, T., Rahman, M., Liping, X., Schoelynck, J., 2022. Hydrogen Peroxide Variation Patterns as Abiotic Stress Responses of Egeria densa. Front. Plant Sci. 13. https://doi.org/10.3389/fpls.2022.855477

Asghar, M.A., Balogh, E., Ahres, M., Szalai, G., Gondor, O.K., Darkó, É., Borbély, P., Kulman, K., Mednyánszky, Z., Simon-Sarkadi, L., Kocsy, G., 2023a. Ascorbate and Hydrogen Peroxide Modify Metabolite Profile of Wheat Differently. J. Plant Growth Regul. 42, 6155–6170. https://doi.org/10.1007/s00344-022-10793-0

Asghar, M.A., Balogh, E., Szalai, G., Galiba, G., Kocsy, G., 2022. Differences in the light-dependent changes of the glutathione metabolism during cold acclimation in wheat varieties with different freezing tolerance. J. Agron. Crop Sci. 208, 65–75. https://doi.org/10.1111/jac.12566

Asghar, M.A., Kulman, K., Szalai, G., Gondor, O.K., Mednyánszky, Z., Simon-Sarkadi, L., Gaudinova, A., Dobrev, P.I., Vanková, R., Kocsy, G., 2023b. Effect of ascorbate and hydrogen peroxide on hormone and metabolite levels during post-germination growth in wheat. Physiol. Plant. 175. https://doi.org/10.1111/ppl.13887

Azizi, F., Farsaraei, S., Moghaddam, M., 2021. Application of Exogenous Ascorbic Acid Modifies Growth and Pigment Content of *Calendula officinalis* L. Flower Heads of Plants Exposed to NaCl Stress. J. Soil Sci. Plant Nutr. 21, 2803–2814. https://doi.org/10.1007/s42729-021-00567-0

Beers, R.F., Sizer, I.W., 1952. A Spectrophotometric Method For Measuring The Breakdown Of Hydrogen Peroxide By Catalase. J. Biol. Chem. 195, 133–140. https://doi.org/10.1016/S0021-9258(19)50881-X

Bergonci, T., Fomsgaard, I.S., Kjaer, K.H., Paponov, I.A., 2023. Hormone–Flavonoid Patterns in Two Genotypes of *Campanula portenschlagiana* with Distinct Adventitious Rooting Competence. Horticulturae 9, 121. https://doi.org/10.3390/horticulturae9010121

Bielen, A., Remans, T., Vangronsveld, J., Cuypers, A., 2013. The Influence of Metal Stress on the Availability and Redox State of Ascorbate, and Possible Interference with Its Cellular Functions. Int. J. Mol. Sci. 14, 6382–6413. https://doi.org/10.3390/ijms14036382

Boutin, C., Clément, C., Rivoal, J., 2024. Post-Translational Modifications to Cysteine Residues in Plant Proteins and Their Impact on the Regulation of Metabolism and Signal Transduction. Int. J. Mol. Sci. 25, 9845. https://doi.org/10.3390/ijms25189845

Bradford, M.M., 1976. A rapid and sensitive method for the quantitation of microgram quantities of protein utilizing the principle of protein-dye binding. Anal. Biochem. 72, 248–254. https://doi.org/10.1016/0003-2697(76)90527-3

Buchanan, B.B., Luan, S., 2005. Redox regulation in the chloroplast thylakoid lumen: a new frontier in photosynthesis research. J. Exp. Bot. 56, 1439–1447. https://doi.org/10.1093/jxb/eri158

Bulley, S.M., Cooney, J.M., Laing, W., 2021. Elevating Ascorbate in Arabidopsis Stimulates the Production of Abscisic Acid, Phaseic Acid, and to a Lesser Extent Auxin (IAA) and Jasmonates, Resulting in Increased Expression of *DHAR1* and Multiple Transcription Factors Associated with Abiotic Stress Tolerance. Int. J. Mol. Sci. 22, 6743. https://doi.org/10.3390/ijms22136743

Cejudo, F.J., González, M.-C., Pérez-Ruiz, J.M., 2021. Redox regulation of chloroplast metabolism. Plant Physiol. 186, 9–21. https://doi.org/10.1093/plphys/kiaa062

CGIAR initiative on foresight, 2024. what do we know about the future of maize chains in changing climate and agri-food system?

Chen, J., Wang, W.-H., Wu, F.-H., He, E.-M., Liu, X., Shangguan, Z.-P., Zheng, H.-L., 2015. Hydrogen sulfide enhances salt tolerance through nitric oxide-mediated maintenance of ion homeostasis in barley seedling roots. Sci. Rep. 5, 12516. https://doi.org/10.1038/srep12516

Chen, Z., Gallie, D.R., 2006. Dehydroascorbate Reductase Affects Leaf Growth, Development, and Function. Plant Physiol. 142, 775–787. https://doi.org/10.1104/pp.106.085506

Cheng, P., Yue, Q., Zhang, Y., Zhao, S., Khan, A., Yang, X., He, J., Wang, S., Shen, W., Qian, Q., Du, W., Ma, F., Zhang, D., Guan, Q., 2023. Application of γ-aminobutyric acid

(GABA) improves fruit quality and rootstock drought tolerance in apple. J. Plant Physiol. 280, 153890. https://doi.org/10.1016/j.jplph.2022.153890

Chin, D.-C., Senthil Kumar, R., Suen, C.-S., Chien, C.-Y., Hwang, M.-J., Hsu, C.-H., Xuhan, X., Lai, Z.X., Yeh, K.-W., 2019. Plant Cytosolic Ascorbate Peroxidase with Dual Catalytic Activity Modulates Abiotic Stress Tolerances. iScience 16, 31–49. https://doi.org/10.1016/j.isci.2019.05.014

Considine, M.J., Foyer, C.H., 2014. Redox Regulation of Plant Development. Antioxid. Redox Signal. 21, 1305–1326. https://doi.org/10.1089/ars.2013.5665

Creissen, G., Firmin, J., Fryer, M., Kular, B., Leyland, N., Reynolds, H., Pastori, G., Wellburn, F., Baker, N., Wellburn, A., Mullineaux, P., 1999. Elevated Glutathione Biosynthetic Capacity in the Chloroplasts of Transgenic Tobacco Plants Paradoxically Causes Increased Oxidative Stress. Plant Cell 11, 1277–1291. https://doi.org/10.1105/tpc.11.7.1277

Cuong, D.M., Kwon, S.-J., Jeon, J., Park, Y.J., Park, J.S., Park, S.U., 2018. Identification and Characterization of Phenylpropanoid Biosynthetic Genes and Their Accumulation in Bitter Melon (*Momordica charantia*). Molecules 23, 469. https://doi.org/10.3390/molecules23020469

Das, A., Pal, S., Chakraborty, N., Hasanuzzaman, M., Adak, M.K., 2024. Regulation of reactive oxygen species metabolism and oxidative stress signaling by abscisic acid pretreatment in rice (*Oryza sativa* L.) seedlings through sub1A QTL under salinity. Plant Stress 11, 100422. https://doi.org/10.1016/j.stress.2024.100422

Das, S., Shil, S., Rime, J., Alice, A.K., Yumkhaibam, T., Mounika, V., Singh, A.P., Kundu, M., Lalhmangaihzuali, H., Hazarika, T.K., Singh, A.K., Singh, S., 2025. Phytohormonal signaling in plant resilience: advances and strategies for enhancing abiotic stress tolerance. Plant Growth Regul. 105, 329–360. https://doi.org/10.1007/s10725-025-01279-6

de Bont, L., Mu, X., Wei, B., Han, Y., 2022. Abiotic stress-triggered oxidative challenges: Where does H_2S act? J. Genet. Genomics 49, 748–755. https://doi.org/10.1016/j.jgg.2022.02.019

De Paula, M., Perez-Otaola, M., Darder, M., Torres, M., Frutos, G., Martinez-Honduvilla, C.J.,

1996. Function of the ascorbate-glutathione cycle in aged sunflower seeds. Physiol. Plant. 96, 543–550. https://doi.org/10.1034/j.1399-3054.1996.960401.x

Deslous, P., Bournonville, C., Decros, G., Okabe, Y., Mauxion, J.-P., Jorly, J., Gadin, S., Brès, C., Mori, K., Ferrand, C., Prigent, S., Ariizumi, T., Ezura, H., Hernould, M., Rothan, C., Pétriacq, P., Gibon, Y., Baldet, P., 2021. Overproduction of ascorbic acid impairs pollen fertility in tomato. J. Exp. Bot. 72, 3091–3107. https://doi.org/10.1093/jxb/erab040

Devireddy, A.R., Tschaplinski, T.J., Tuskan, G.A., Muchero, W., Chen, J.-G., 2021. Role of Reactive Oxygen Species and Hormones in Plant Responses to Temperature Changes. Int. J. Mol. Sci. 22, 8843. https://doi.org/10.3390/ijms22168843

Diao, Q., Song, Y., Shi, D., Qi, H., 2017. Interaction of Polyamines, Abscisic Acid, Nitric Oxide, and Hydrogen Peroxide under Chilling Stress in Tomato (*Lycopersicon esculentum* Mill.) Seedlings. Front. Plant Sci. 8. https://doi.org/10.3389/fpls.2017.00203

Dias, M.C., Pinto, D.C.G.A., Silva, A.M.S., 2021. Plant Flavonoids: Chemical Characteristics and Biological Activity. Molecules 26, 5377. https://doi.org/10.3390/molecules26175377

Ding, H., Ma, D., Huang, X., Hou, J., Wang, C., Xie, Y., Wang, Y., Qin, H., Guo, T., 2019. Exogenous hydrogen sulfide alleviates salt stress by improving antioxidant defenses and the salt overly sensitive pathway in wheat seedlings. Acta Physiol. Plant. 41, 123. https://doi.org/10.1007/s11738-019-2918-6

Dong, L., Li, L., Meng, Y., Liu, H., Li, J., Yu, Y., Qian, C., Wei, S., Gu, W., 2022. Exogenous Spermidine Optimizes Nitrogen Metabolism and Improves Maize Yield under Drought Stress Conditions. Agriculture 12, 1270. https://doi.org/10.3390/agriculture12081270

El-Mogy, M.M., Sattar, A., Ali, Q., Alharbi, B.M., Abbas, Z.K., AL-Balawi, S.M., Althaqafi, M.M., Al-Harb, N.A., Al-Qahtani, S.M., Darwish, D.B.E., 2024. Exogenous Application of Tyrosine Mitigated the Adversities of Drought Stress in Maize Seedlings through Modulation of Photosynthetic Performance and Antioxidants Defense Systems. J. Soil Sci. Plant Nutr. 24, 5067–5080. https://doi.org/10.1007/s42729-024-01892-w

FAOSTAT, 2023. Analytical brief 79; agricultural production statistics 2000-2022 (Food and Agriculture Organization of the United Nations, Statistics Division. 2023. Agricultural

production statistics 2000–2022. FAOSTAT Analytical Brief 79. Rome: FAO.

Farooq, M.A., Gill, R.A., Islam, F., Ali, B., Liu, H., Xu, J., He, S., Zhou, W., 2016. Methyl Jasmonate Regulates Antioxidant Defense and Suppresses Arsenic Uptake in *Brassica napus* L. Front. Plant Sci. 7. https://doi.org/10.3389/fpls.2016.00468

Fernando, P.D.S.M., Ko, D.O., Piao, M.J., Kang, K.A., Herath, H.M.U.L., Hyun, J.W., 2024. Protective effect of luteolin against oxidative stress-mediated cell injury via enhancing antioxidant systems. Mol. Med. Rep. 30, 121. https://doi.org/10.3892/mmr.2024.13244

Fichman, Y., Rowland, L., Oliver, M.J., Mittler, R., 2023. ROS are evolutionary conserved cell-to-cell stress signals. Proc. Natl. Acad. Sci. 120. https://doi.org/10.1073/pnas.2305496120

Forde, B.G., Lea, P.J., 2007. Glutamate in plants: metabolism, regulation, and signalling. J. Exp. Bot. 58, 2339–2358. https://doi.org/10.1093/jxb/erm121

Foyer, C.H., 2018. Reactive oxygen species, oxidative signaling and the regulation of photosynthesis. Environ. Exp. Bot. 154, 134–142. https://doi.org/10.1016/j.envexpbot.2018.05.003

Foyer, C.H., Halliwell, B., 1976. The presence of glutathione and glutathione reductase in chloroplasts: A proposed role in ascorbic acid metabolism. Planta 133, 21–25. https://doi.org/10.1007/BF00386001

Foyer, C.H., Kunert, K., 2024. The ascorbate–glutathione cycle coming of age. J. Exp. Bot. 75, 2682–2699. https://doi.org/10.1093/jxb/erae023

Foyer, C.H., Noctor, G., 2013. Redox Signaling in Plants. Antioxid. Redox Signal. 18, 2087–2090. https://doi.org/10.1089/ars.2013.5278

Geigenberger, P., Fernie, A.R., 2014. Metabolic Control of Redox and Redox Control of Metabolism in Plants. Antioxid. Redox Signal. 21, 1389–1421. https://doi.org/10.1089/ars.2014.6018

Gill, S.S., Anjum, N.A., Hasanuzzaman, M., Gill, R., Trivedi, D.K., Ahmad, I., Pereira, E., Tuteja, N., 2013. Glutathione and glutathione reductase: A boon in disguise for plant abiotic stress defense operations. Plant Physiol. Biochem. 70, 204–212.

https://doi.org/10.1016/j.plaphy.2013.05.032

Gondor, O.K., Tajti, J., Hamow, K.Á., Majláth, I., Szalai, G., Janda, T., Pál, M., 2021. Polyamine Metabolism under Different Light Regimes in Wheat. Int. J. Mol. Sci. 22, 11717. https://doi.org/10.3390/ijms222111717

Gulyás, Z., Boldizsár, Á., Novák, A., Szalai, G., Pál, M., Galiba, G., Kocsy, G., 2014. Central role of the flowering repressor ZCCT2 in the redox control of freezing tolerance and the initial development of flower primordia in wheat. BMC Plant Biol. 14, 91. https://doi.org/10.1186/1471-2229-14-91

Gulyás, Z., Simon-Sarkadi, L., Badics, E., Novák, A., Mednyánszky, Z., Szalai, G., Galiba, G., Kocsy, G., 2017. Redox regulation of free amino acid levels in *Arabidopsis thaliana*. Physiol. Plant. 159, 264–276. https://doi.org/10.1111/ppl.12510

Haque, M.S., Mondal, S., Hossain, K.S., Baroi, A., Hussain, M.T., Mia, M.A., Uddin, M.N., Sarwar, A.K.M.G., Hossain, M.A., Islam, M.A., 2025. Methyl jasmonate counteracts cadmium toxicity in water spinach plant by adjusting growth, physiology and redox regulation. Sci. Rep. 15, 24805. https://doi.org/10.1038/s41598-025-09852-9

Hasan, M.M., Alharbi, B.M., Alhaithloul, H.A.S., Abdulmajeed, A.M., Alghanem, S.M., Al-Mushhin, A.A.M., Jahan, M.S., Corpas, F.J., Fang, X.-W., Soliman, M.H., 2021. Spermine-Mediated Tolerance to Selenium Toxicity in Wheat (*Triticum aestivum* L.) Depends on Endogenous Nitric Oxide Synthesis. Antioxidants 10, 1835. https://doi.org/10.3390/antiox10111835

Herrera-Vásquez, A., Salinas, P., Holuigue, L., 2015. Salicylic acid and reactive oxygen species interplay in the transcriptional control of defense genes expression. Front. Plant Sci. 6. https://doi.org/10.3389/fpls.2015.00171

Hoagland, D.R., Arnon, D.I., 1938. The water-culture method for growing plants without soil. Circ. Calif. Agric. Exp. Stn. https://doi.org/10.1097/00010694-193910000-00022

Huzsvai, L., Juhász, C., Seddik, L., Kovács, G., Zsembeli, J., 2024. The Future Probability of Winter Wheat and Maize Yield Failure in Hungary Based on Long-Term Temporal Patterns. Sustainability 16, 3962. https://doi.org/10.3390/su16103962

Jánossy, A., Komlóssy, G., Mórász, S., Taróczy, H., 1957. Magyar kukoricafajták és termesztésük. (Hungarian maize varieties and their production). Mezőgazdasági Kiadó, Budapest.

Jardim-Messeder, D., de Souza-Vieira, Y., Sachetto-Martins, G., 2025. Dressed Up to the Nines: The Interplay of Phytohormones Signaling and Redox Metabolism During Plant Response to Drought. Plants 14, 208. https://doi.org/10.3390/plants14020208

Jia, X., Xu, S., Wei, J., Wang, F., Qing, Y., Zhang, Z., Gao, T., Mu, X., Liu, C., Mao, K., Gong, X., Ma, F., Li, C., 2025. Cytokinin mediates age-dependent drought response by regulating the removal reactive oxygen species in apple. Plant J. 121. https://doi.org/10.1111/tpj.70023

Jiang, C., Sun, J., Li, R., Yan, S., Chen, W., Guo, L., Qin, G., Wang, P., Luo, C., Huang, W., Zhang, Q., Fernie, A.R., Jackson, D., Li, X., Yan, J., 2022. A reactive oxygen species burst causes haploid induction in maize. Mol. Plant 15, 943–955. https://doi.org/10.1016/j.molp.2022.04.001

Jiang, Y., Jiang, S., Liu, L., 2025. Understanding the multifaceted role of ABA signaling in orchestrating plant developmental transition. Stress Biol. 5, 5. https://doi.org/10.1007/s44154-024-00203-8

Kellős, T., Tímár, I., Szilágyi, V., Szalai, G., Galiba, G., Kocsy, G., 2008. Stress hormones and abiotic stresses have different effects on antioxidants in maize lines with different sensitivity. Plant Biol. 10, 563–572. https://doi.org/10.1111/j.1438-8677.2008.00071.x

Khan, K.A., Saleem, M.H., Afzal, S., Hussain, I., Ameen, F., Fahad, S., 2024. Ferulic acid: therapeutic potential due to its antioxidant properties, role in plant growth, and stress tolerance. Plant Growth Regul. 104, 1329–1353. https://doi.org/10.1007/s10725-024-01243-w

Khan, M., Ali, S., Al Azzawi, T.N.I., Yun, B.-W., 2023. Nitric Oxide Acts as a Key Signaling Molecule in Plant Development under Stressful Conditions. Int. J. Mol. Sci. 24, 4782. https://doi.org/10.3390/ijms24054782

Khodamoradi, S., Sagharyan, M., Samari, E., Sharifi, M., 2022. Changes in phenolic compounds production as a defensive mechanism against hydrogen sulfide pollution in *Scrophularia*

striata. Plant Physiol. Biochem. 177, 23–31. https://doi.org/10.1016/j.plaphy.2022.02.013

Kılıç, M., Gollan, P.J., Aro, E.-M., Rintamäki, E., 2025. Jasmonic acid signaling and glutathione coordinate plant recovery from high light stress. Plant Physiol. 197. https://doi.org/10.1093/plphys/kiaf143

Kocsy, G., Tari, I., Vanková, R., Zechmann, B., Gulyás, Z., Poór, P., Galiba, G., 2013. Redox control of plant growth and development. Plant Sci. 211, 77–91. https://doi.org/10.1016/j.plantsci.2013.07.004

Lamers, J., van der Meer, T., Testerink, C., 2020. How Plants Sense and Respond to Stressful Environments. Plant Physiol. 182, 1624–1635. https://doi.org/10.1104/pp.19.01464

Lee, B.-R., La, V.H., Park, S.-H., Mamun, M. Al, Bae, D.-W., Kim, T.-H., 2022. H_2O_2-Responsive Hormonal Status Involves Oxidative Burst Signaling and Proline Metabolism in Rapeseed Leaves. Antioxidants 11, 566. https://doi.org/10.3390/antiox11030566

Li, Q., Wang, Z., Zhao, Y., Zhang, X., Zhang, S., Bo, L., Wang, Y., Ding, Y., An, L., 2016. Putrescine protects hulless barley from damage due to UV-B stress via H_2S- and H_2O_2-mediated signaling pathways. Plant Cell Rep. 35, 1155–1168. https://doi.org/10.1007/s00299-016-1952-8

Li, Y., Ma, Y., Zhang, T., Bi, Y., Wang, Y., Prusky, D., 2019. Exogenous polyamines enhance resistance to *Alternaria alternata* by modulating redox homeostasis in apricot fruit. Food Chem. 301, 125303. https://doi.org/10.1016/j.foodchem.2019.125303

Li, Z.-G., Fang, J.-R., Bai, S.-J., 2024. Hydrogen sulfide signaling in plant response to temperature stress. Front. Plant Sci. 15. https://doi.org/10.3389/fpls.2024.1337250

Liao, W.-B., Xiao, H.-L., Zhang, M.-L., 2010. Effect of Nitric Oxide and Hydrogen Peroxide on Adventitious Root Development from Cuttings of Ground-Cover Chrysanthemum and Associated Biochemical Changes. J. Plant Growth Regul. 29, 338–348. https://doi.org/10.1007/s00344-010-9140-5

Lichtenthaler, H.K., Buschmann, C., 2001. Chlorophylls and Carotenoids: Measurement and Characterization by UV - VIS Spectroscopy. Curr. Protoc. Food Anal. Chem. 1. https://doi.org/10.1002/0471142913.faf0403s01

Linić, I., Mlinarić, S., Brkljačić, L., Pavlović, I., Smolko, A., Salopek-Sondi, B., 2021. Ferulic Acid and Salicylic Acid Foliar Treatments Reduce Short-Term Salt Stress in Chinese Cabbage by Increasing Phenolic Compounds Accumulation and Photosynthetic Performance. Plants 10, 2346. https://doi.org/10.3390/plants10112346

Lisjak, M., Teklić, T., Wilson, I.D., Wood, M., Whiteman, M., Hancock, J.T., 2011. Hydrogen sulfide effects on stomatal apertures. Plant Signal. Behav. 6, 1444–1446. https://doi.org/10.4161/psb.6.10.17104

Liu, H., Timko, M.P., 2021. Jasmonic Acid Signaling and Molecular Crosstalk with Other Phytohormones. Int. J. Mol. Sci. 22, 2914. https://doi.org/10.3390/ijms22062914

Liu, J., Osbourn, A., Ma, P., 2015. MYB Transcription Factors as Regulators of Phenylpropanoid Metabolism in Plants. Mol. Plant 8, 689–708. https://doi.org/10.1016/j.molp.2015.03.012

Liu, Q., Li, X., Jin, S., Dong, W., Zhang, Y., Chen, W., Shi, L., Cao, S., Yang, Z., 2023. γ-Aminobutyric acid treatment induced chilling tolerance in postharvest kiwifruit (*Actinidia chinensis* cv. Hongyang) via regulating ascorbic acid metabolism. Food Chem. 404, 134661. https://doi.org/10.1016/j.foodchem.2022.134661

Liu, S., Cui, S., Zhang, X., Wang, Y., Mi, G., Gao, Q., 2020. Synergistic Regulation of Nitrogen and Sulfur on Redox Balance of Maize Leaves and Amino Acids Balance of Grains. Front. Plant Sci. 11. https://doi.org/10.3389/fpls.2020.576718

López-Carbonell, M., Munné-Bosch, S., Alegre, L., 2006. The Ascorbate-deficient *vtc-1* Arabidopsis Mutant Shows Altered ABA Accumulation in Leaves and Chloroplasts. J. Plant Growth Regul. 25, 137–144. https://doi.org/10.1007/s00344-005-0119-6

Lou, Y.-R., Bor, M., Yan, J., Preuss, A.S., Jander, G., 2016. Arabidopsis NATA1 acetylates putrescine and decreases defense-related hydrogen peroxide accumulation. Plant Physiol. pp.00446.2016. https://doi.org/10.1104/pp.16.00446

Lu, B., Luo, X., Gong, C., Bai, J., 2021. Overexpression of *γ-glutamylcysteine synthetase* gene from *Caragana korshinskii* decreases stomatal density and enhances drought tolerance. BMC Plant Biol. 21, 444. https://doi.org/10.1186/s12870-021-03226-9

Lu, J., Hu, Y., Chen, Y., Liu, R., Di, J., Feng, T., Cao, F., 2024. Hydrogen sulfide promoted cell differentiation, antioxidant ability, and flavonoids accumulation in *Ginkgo biloba* L. suspension cells. Plant Cell, Tissue Organ Cult. 156, 36. https://doi.org/10.1007/s11240-023-02631-2

Lu, J., Li, X.N., Yang, Y.L., Jia, L.Y., You, J., Wang, W.R., 2013. Effect of hydrogen peroxide on seedling growth and antioxidants in two wheat cultivars. Biol. Plant. 57, 487–494. https://doi.org/10.1007/s10535-013-0312-6

Lu, Q., Bi, S., Dong, S., Wang, X., Guo, F., Wang, W., 2025. ABA orchestrates molecular networks linking antioxidant defense, sugar metabolism and circadian clock for combined stress tolerance in Quinoa (*Chenopodium quinoa* Willd.). Plant Physiol. Biochem. 229, 110536. https://doi.org/10.1016/j.plaphy.2025.110536

Lu, S., Su, W., Li, H., Guo, Z., 2009. Abscisic acid improves drought tolerance of triploid bermudagrass and involves H_2O_2- and NO-induced antioxidant enzyme activities. Plant Physiol. Biochem. 47, 132–138. https://doi.org/10.1016/j.plaphy.2008.10.006

Ma, S., Zhou, X., Jahan, M.S., Guo, S., Tian, M., Zhou, R., Liu, H., Feng, B., Shu, S., 2022. Putrescine regulates stomatal opening of cucumber leaves under salt stress via the H_2O_2-mediated signaling pathway. Plant Physiol. Biochem. 170, 87–97. https://doi.org/10.1016/j.plaphy.2021.11.028

Ma, X., Zhang, Liping, Pei, Z., Zhang, Linlin, Liu, Z., Liu, D., Hao, X., Jin, Z., Pei, Y., 2021. Hydrogen sulfide promotes flowering in heading Chinese cabbage by S-sulfhydration of BraFLCs. Hortic. Res. 8, 19. https://doi.org/10.1038/s41438-020-00453-3

Martí-Guillén, J.M., Pardo-Hernández, M., Martínez-Lorente, S.E., Almagro, L., Rivero, R.M., 2022. Redox post-translational modifications and their interplay in plant abiotic stress tolerance. Front. Plant Sci. 13. https://doi.org/10.3389/fpls.2022.1027730

Marton, L.C., 2013. Hybrid maize in Hungary is 60 years old. In L. C. Marton & T. Spitkó (Eds.), 60 Years of Hungarian Hybrid Maize 1953–2013. Pannonian Plant Biotechnol. Assoc.

Mehla, N., Sindhi, V., Josula, D., Bisht, P., Wani, S.H., 2017. An Introduction to Antioxidants

and Their Roles in Plant Stress Tolerance, in: Reactive Oxygen Species and Antioxidant Systems in Plants: Role and Regulation under Abiotic Stress. Springer Singapore, Singapore, pp. 1–23. https://doi.org/10.1007/978-981-10-5254-5_1

Mehta, R.A., Cassol, T., Li, N., Ali, N., Handa, A.K., Mattoo, A.K., 2002. Engineered polyamine accumulation in tomato enhances phytonutrient content, juice quality, and vine life. Nat. Biotechnol. 20, 613–618. https://doi.org/10.1038/nbt0602-613

Meuwly, P., Metraux, J.P., 1993. Ortho-Anisic Acid as Internal Standard for the Simultaneous Quantitation of Salicylic Acid and Its Putative Biosynthetic Precursors in Cucumber Leaves. Anal. Biochem. 214, 500–505. https://doi.org/10.1006/abio.1993.1529

Mittal, U., Kumar, V., Kukreja, S., Singh, B., Pandey, N.K., Goutam, U., 2023. Role of Beneficial Elements in Developing Resilience to Abiotic and Biotic Stresses in Plants: Present Status and Future Prospects. J. Plant Growth Regul. 42, 3789–3813. https://doi.org/10.1007/s00344-022-10840-w

Mittler, R., Jones, D.P., 2024. The redox code of plants. Plant. Cell Environ. 47, 2821–2829. https://doi.org/10.1111/pce.14787

Mittler, R., Zandalinas, S.I., Fichman, Y., Van Breusegem, F., 2022. Reactive oxygen species signalling in plant stress responses. Nat. Rev. Mol. Cell Biol. 23, 663–679. https://doi.org/10.1038/s41580-022-00499-2

Mondal, S., Haque, M.S., Rabbi, M.F., Tasnim, H., Iffat, A., Baroi, A., Mia, M.A., Uddin, M.N., Hossain, M.A., 2025. Salicylic Acid and Methyl Jasmonate Mitigate Cadmium Toxicity in Spinach (*Spinacea oleracea* L.) by Modulating Metal Translocation, Growth, Photo-Physiology and Redox Regulation. J. Soil Sci. Plant Nutr. 25, 1524–1540. https://doi.org/10.1007/s42729-025-02220-6

Murshed, R., Lopez-Lauri, F., Sallanon, H., 2008. Microplate quantification of enzymes of the plant ascorbate–glutathione cycle. Anal. Biochem. 383, 320–322. https://doi.org/10.1016/j.ab.2008.07.020

Németh, M., Janda, T., Horváth, E., Páldi, E., Szalai, G., 2002. Exogenous salicylic acid increases polyamine content but may decrease drought tolerance in maize. Plant Sci. 162,

569–574. https://doi.org/10.1016/S0168-9452(01)00593-3

Nkomo, M., Gokul, A., Keyster, M., Klein, A., 2019. Exogenous *p*-Coumaric Acid Improves *Salvia hispanica* L. Seedling Shoot Growth. Plants 8, 546. https://doi.org/10.3390/plants8120546

Noctor, G., Mhamdi, A., Chaouch, S., Han, Y., Neukermans, J., Marquez-Garcia, B., Queval, G., Foyer, C.H., 2012. Glutathione in plants: an integrated overview. Plant. Cell Environ. 35, 454–484. https://doi.org/10.1111/j.1365-3040.2011.02400.x

Noctor, G., Queval, G., Mhamdi, A., Chaouch, S., Foyer, C.H., 2011. Glutathione. Arab. B. 9, 1–32. https://doi.org/10.1199/tab.0142

Noshi, M., Hatanaka, R., Tanabe, N., Terai, Y., Maruta, T., Shigeoka, S., 2016. Redox regulation of ascorbate and glutathione by a chloroplastic dehydroascorbate reductase is required for high-light stress tolerance in *Arabidopsis*. Biosci. Biotechnol. Biochem. 80, 870–877. https://doi.org/10.1080/09168451.2015.1135042

Noshi, M., Yamada, H., Hatanaka, R., Tanabe, N., Tamoi, M., Shigeoka, S., 2017. *Arabidopsis* dehydroascorbate reductase 1 and 2 modulate redox states of ascorbate-glutathione cycle in the cytosol in response to photooxidative stress. Biosci. Biotechnol. Biochem. 81, 523–533. https://doi.org/10.1080/09168451.2016.1256759

Ozfidan-Konakci, C., Yildiztugay, E., Alp, F.N., Kucukoduk, M., Turkan, I., 2020. Naringenin induces tolerance to salt/osmotic stress through the regulation of nitrogen metabolism, cellular redox and ROS scavenging capacity in bean plants. Plant Physiol. Biochem. 157, 264–275. https://doi.org/10.1016/j.plaphy.2020.10.032

Pál, M., Horváth, E., Janda, T., Páldi, E., Szalai, G., 2005. Cadmium stimulates the accumulation of salicylic acid and its putative precursors in maize (*Zea mays*) plants. Physiol. Plant. 125, 356–364. https://doi.org/10.1111/j.1399-3054.2005.00545.x

Pál, M., Ivanovska, B., Oláh, T., Tajti, J., Hamow, K.Á., Szalai, G., Khalil, R., Vanková, R., Dobrev, P., Misheva, S.P., Janda, T., 2019. Role of polyamines in plant growth regulation of *Rht* wheat mutants. Plant Physiol. Biochem. 137, 189–202. https://doi.org/10.1016/j.plaphy.2019.02.013

Pál, M., Szalai, G., Gondor, O.K., Janda, T., 2021. Unfinished story of polyamines: Role of conjugation, transport and light-related regulation in the polyamine metabolism in plants. Plant Sci. 308, 110923. https://doi.org/10.1016/j.plantsci.2021.110923

Pál, M., Tajti, J., Szalai, G., Peeva, V., Végh, B., Janda, T., 2018. Interaction of polyamines, abscisic acid and proline under osmotic stress in the leaves of wheat plants. Sci. Rep. 8, 12839. https://doi.org/10.1038/s41598-018-31297-6

Parveen, N., Kandhol, N., Sharma, S., Singh, V.P., Chauhan, D.K., Ludwig-Müller, J., Corpas, F.J., Tripathi, D.K., 2023. Auxin Crosstalk with Reactive Oxygen and Nitrogen Species in Plant Development and Abiotic Stress. Plant Cell Physiol. 63, 1814–1825. https://doi.org/10.1093/pcp/pcac138

Pasternak, T., 2025. Ascorbate Regulates Root Development Through Auxin Response in *Arabidopsis thaliana*. Int. J. Plant Biol. 16, 74. https://doi.org/10.3390/ijpb16030074

Pasternak, T., Palme, K., Paponov, I.A., 2020. Glutathione Enhances Auxin Sensitivity in Arabidopsis Roots. Biomolecules 10, 1550. https://doi.org/10.3390/biom10111550

Pfaffl, M.W., 2001. A new mathematical model for relative quantification in real-time RT-PCR. Nucleic Acids Res. 29, 45e – 45. https://doi.org/10.1093/nar/29.9.e45

Pivato, M., Fabrega-Prats, M., Masi, A., 2014. Low-molecular-weight thiols in plants: Functional and analytical implications. Arch. Biochem. Biophys. 560, 83–99. https://doi.org/10.1016/j.abb.2014.07.018

Qian, H.F., Peng, X.F., Han, X., Ren, J., Zhan, K.Y., Zhu, M., 2014. The stress factor, exogenous ascorbic acid, affects plant growth and the antioxidant system in *Arabidopsis thaliana*. Russ. J. Plant Physiol. 61, 467–475. https://doi.org/10.1134/S1021443714040141

Qureshi, M.K., Gawroński, P., Munir, S., Jindal, S., Kerchev, P., 2022. Hydrogen peroxide-induced stress acclimation in plants. Cell. Mol. Life Sci. 79, 129. https://doi.org/10.1007/s00018-022-04156-x

Rahantaniaina, M.-S., Li, S., Chatel-Innocenti, G., Tuzet, A., Issakidis-Bourguet, E., Mhamdi, A., Noctor, G., 2017. Cytosolic and Chloroplastic DHARs Cooperate in Oxidative Stress-Driven Activation of the Salicylic Acid Pathway. Plant Physiol. 174, 956–971.

https://doi.org/10.1104/pp.17.00317

Rahman, M.A., Alam, I., Sharmin, S.A., Kabir, A.H., Kim, Y.-G., Liu, G., Lee, B.-H., 2021. Physiological and proteomic analyses reveal the protective roles of exogenous hydrogen peroxide in alleviating drought stress in soybean plants. Plant Biotechnol. Rep. 15, 805–818. https://doi.org/10.1007/s11816-021-00719-9

Rai, G.K., Kumar, P., Choudhary, S.M., Singh, H., Adab, K., Kosser, R., Magotra, I., Kumar, R.R., Singh, M., Sharma, R., Corrado, G., Rouphael, Y., 2023. Antioxidant Potential of Glutathione and Crosstalk with Phytohormones in Enhancing Abiotic Stress Tolerance in Crop Plants. Plants 12, 1133. https://doi.org/10.3390/plants12051133

Ramakers, C., Ruijter, J.M., Deprez, R.H.L., Moorman, A.F.., 2003. Assumption-free analysis of quantitative real-time polymerase chain reaction (PCR) data. Neurosci. Lett. 339, 62–66. https://doi.org/10.1016/S0304-3940(02)01423-4

Riaz, A., Deng, F., Chen, G., Jiang, W., Zheng, Q., Riaz, B., Mak, M., Zeng, F., Chen, Z.-H., 2022. Molecular Regulation and Evolution of Redox Homeostasis in Photosynthetic Machinery. Antioxidants 11, 2085. https://doi.org/10.3390/antiox11112085

Romero, L.C., Aroca, M.Á., Laureano-Marín, A.M., Moreno, I., García, I., Gotor, C., 2014. Cysteine and Cysteine-Related Signaling Pathways in *Arabidopsis thaliana*. Mol. Plant 7, 264–276. https://doi.org/10.1093/mp/sst168

Scuffi, D., Álvarez, C., Laspina, N., Gotor, C., Lamattina, L., García-Mata, C., 2014. Hydrogen Sulfide Generated by L-Cysteine Desulfhydrase Acts Upstream of Nitric Oxide to Modulate Abscisic Acid-Dependent Stomatal Closure. Plant Physiol. 166, 2065–2076. https://doi.org/10.1104/pp.114.245373

Senthil Kumar, R., Shen, C.-H., Wu, P.-Y., Suresh Kumar, S., Hua, M.S., Yeh, K.-W., 2016. Nitric oxide participates in plant flowering repression by ascorbate. Sci. Rep. 6, 35246. https://doi.org/10.1038/srep35246

Shan, C., Liu, H., Zhao, L., Wang, X., 2014. Effects of exogenous hydrogen sulfide on the redox states of ascorbate and glutathione in maize leaves under salt stress. Biol. Plant. 58, 169–173. https://doi.org/10.1007/s10535-013-0366-5

Shi, H., Ye, T., Chan, Z., 2013. Exogenous application of hydrogen sulfide donor sodium hydrosulfide enhanced multiple abiotic stress tolerance in bermudagrass (*Cynodon dactylon* (L). Pers.). Plant Physiol. Biochem. 71, 226–234. https://doi.org/10.1016/j.plaphy.2013.07.021

Singh, K., Asghar, M.A., Jobbágy, K., Kulman, K., Szalai, G., Hamow, K.Á., Soltész, A., Polgári, D., Gulyás, Z., Kocsy, G., 2025. Different modulation of the redox homeostasis and hormone levels by ascorbate, hydrogen peroxide and hydrogen sulfide in maize. Physiol. Plant. 177. https://doi.org/10.1111/ppl.70215

Singh, K., Gupta, R., Shokat, S., Iqbal, N., Kocsy, G., Pérez-Pérez, J.M., Riyazuddin, R., 2024. Ascorbate, plant hormones and their interactions during plant responses to biotic stress. Physiol. Plant. 176. https://doi.org/10.1111/ppl.14388

Singh, P.K., Singh, R., Singh, S., 2013. Cinnamic acid induced changes in reactive oxygen species scavenging enzymes and protein profile in maize (*Zea mays* L.) plants grown under salt stress. Physiol. Mol. Biol. Plants 19, 53–59. https://doi.org/10.1007/s12298-012-0126-6

Smith, M.A., Davies, P.J., 1985. Separation and Quantitation of Polyamines in Plant Tissue by High Performance Liquid Chromatography of Their Dansyl Derivatives. Plant Physiol. 78, 89–91. https://doi.org/10.1104/pp.78.1.89

Soares, A.M. dos S., Souza, T.F. de, Jacinto, T., Machado, O.L.T., 2010. Effect of Methyl Jasmonate on antioxidative enzyme activities and on the contents of ROS and H_2O_2 in Ricinus communis leaves. Brazilian J. Plant Physiol. 22, 151–158. https://doi.org/10.1590/S1677-04202010000300001

Sun, Y.-Y., Wang, J.-Q., Xiang, R.-H., Li, Z.-G., 2022. Key role of reactive oxygen species-scavenging system in nitric oxide and hydrogen sulfide crosstalk-evoked thermotolerance in maize seedlings. Front. Plant Sci. 13. https://doi.org/10.3389/fpls.2022.967968

Szalai, G., Janda, T., Pál, M., 2014. Routine sample preparation and HPLC analysis for ascorbic acid (vitamin C) determination in wheat plants and *Arabidopsis* leaf tissues. Acta Biol. Hung. 65, 205–217. https://doi.org/10.1556/ABiol.65.2014.2.8

Szalai, G., Kellős, T., Galiba, G., Kocsy, G., 2009. Glutathione as an Antioxidant and Regulatory

Molecule in Plants Under Abiotic Stress Conditions. J. Plant Growth Regul. 28, 66–80. https://doi.org/10.1007/s00344-008-9075-2

Takács, Z., Poór, P., Tari, I., 2016. Comparison of polyamine metabolism in tomato plants exposed to different concentrations of salicylic acid under light or dark conditions. Plant Physiol. Biochem. 108, 266–278. https://doi.org/10.1016/j.plaphy.2016.07.020

Tanumihardjo, S.A., McCulley, L., Roh, R., Lopez-Ridaura, S., Palacios-Rojas, N., Gunaratna, N.S., 2020. Maize agro-food systems to ensure food and nutrition security in reference to the Sustainable Development Goals. Glob. Food Sec. 25, 100327. https://doi.org/10.1016/j.gfs.2019.100327

Tari, I., Szalai, G., Lôrincz, Z., Bálint, A., 2002. Changes in Thiol Content in Roots of Wheat Cultivars Exposed to Copper Stress. Biol. Plant. 45, 255–260. https://doi.org/10.1023/A:1015105025080

Tavu, L.E.J., Redillas, M.C.F.R., 2025. Oxidative Stress in Rice (*Oryza sativa*): Mechanisms, Impact, and Adaptive Strategies. Plants 14, 1463. https://doi.org/10.3390/plants14101463

Terzi, R., Kalaycıoglu, E., Demiralay, M., Saglam, A., Kadioglu, A., 2015. Exogenous ascorbic acid mitigates accumulation of abscisic acid, proline and polyamine under osmotic stress in maize leaves. Acta Physiol. Plant. 37, 43. https://doi.org/10.1007/s11738-015-1792-0

Tian, P., Feng, Y.-X., Li, Y.-H., 2024. SOS! Hydrogen Sulfide Enhances the Flavonoid Early Warning System in Rice Plants to Cope with Thiocyanate Pollution. Toxics 12, 591. https://doi.org/10.3390/toxics12080591

Tian, X., Li, M., Huang, X., Wirtz, M., Zheng, X., Fan, S., Tian, J., Liu, S., Liu, Z., Zhao, H., 2026. A GLUTAMATE CYSTEINE LIGASE Gene *StGSH1* Regulated by StERF10 Enhanced Glutathione Accumulation and Adaptation to Low Phosphorus Stress in Potato. Adv. Sci. 13. https://doi.org/10.1002/advs.202509143

Tóth, S.Z., 2023. The Functions of Chloroplastic Ascorbate in Vascular Plants and Algae. Int. J. Mol. Sci. 24, 2537. https://doi.org/10.3390/ijms24032537

Troyer, A.F., 1995. Early Illini Corn Breeders. Their quest for Quality and Quantity. Prof. of. 50t. ASTA Conference, pp. 56–67.

Tsai, Y.-C., Hong, C.-Y., Liu, L.-F., Kao, C.H., 2005. Expression of ascorbate peroxidase and glutathione reductase in roots of rice seedlings in response to NaCl and H_2O_2. J. Plant Physiol. 162, 291–299. https://doi.org/10.1016/j.jplph.2004.06.004

Van Aken, O., 2021. Mitochondrial redox systems as central hubs in plant metabolism and signaling. Plant Physiol. 186, 36–52. https://doi.org/10.1093/plphys/kiab101

Vanacker, H., Guichard, M., Bohrer, A.-S., Issakidis-Bourguet, E., 2018. Redox Regulation of Monodehydroascorbate Reductase by Thioredoxin y in Plastids Revealed in the Context of Water Stress. Antioxidants 7, 183. https://doi.org/10.3390/antiox7120183

Vrhovsek, U., Masuero, D., Gasperotti, M., Franceschi, P., Caputi, L., Viola, R., Mattivi, F., 2012. A Versatile Targeted Metabolomics Method for the Rapid Quantification of Multiple Classes of Phenolics in Fruits and Beverages. J. Agric. Food Chem. 60, 8831–8840. https://doi.org/10.1021/jf2051569

Waheed, A., Zhuo, L., Wang, M., Hailiang, X., Tong, Z., Wang, C., Aili, A., 2024. Integrative mechanisms of plant salt tolerance: Biological pathways, phytohormonal regulation, and technological innovations. Plant Stress 14, 100652. https://doi.org/10.1016/j.stress.2024.100652

Wang, C., Deng, Y., Liu, Z., Liao, W., 2021. Hydrogen Sulfide in Plants: Crosstalk with Other Signal Molecules in Response to Abiotic Stresses. Int. J. Mol. Sci. 22, 12068. https://doi.org/10.3390/ijms222112068

Wang, Z., He, F., Mu, Y., Zhang, L., Liu, Z., Liu, D., Yang, J., Jin, Z., Pei, Y., 2022. Identification and functional characterization of a cystathionine β-lyase (CBL) enzyme for H_2S production in Arabidopsis thaliana. Plant Physiol. Biochem. 182, 76–89. https://doi.org/10.1016/j.plaphy.2022.04.008

Wu, P., Xiao, C., Cui, J., Hao, B., Zhang, W., Yang, Z., Ahammed, G.J., Liu, H., Cui, H., 2021. Nitric Oxide and Its Interaction with Hydrogen Peroxide Enhance Plant Tolerance to Low Temperatures by Improving the Efficiency of the Calvin Cycle and the Ascorbate–Glutathione Cycle in Cucumber Seedlings. J. Plant Growth Regul. 40, 2390–2408. https://doi.org/10.1007/s00344-020-10242-w

Xie, D.-L., Zheng, X.-L., Zhou, C.-Y., Kanwar, M.K., Zhou, J., 2022. Functions of Redox Signaling in Pollen Development and Stress Response. Antioxidants 11, 287. https://doi.org/10.3390/antiox11020287

Xiong, J., Yang, Y., Fu, G., Tao, L., 2015. Novel roles of hydrogen peroxide (H_2O_2) in regulating pectin synthesis and demethylesterification in the cell wall of rice (*Oryza sativa*) root tips. New Phytol. 206, 118–126. https://doi.org/10.1111/nph.13285

Xiong, Y., Lei, Q.-Y., Zhao, S., Guan, K.-L., 2011. Regulation of Glycolysis and Gluconeogenesis by Acetylation of PKM and PEPCK. Cold Spring Harb. Symp. Quant. Biol. 76, 285–289. https://doi.org/10.1101/sqb.2011.76.010942

Xu, E., Brosché, M., 2014. Salicylic acid signaling inhibits apoplastic reactive oxygen species signaling. BMC Plant Biol. 14, 155. https://doi.org/10.1186/1471-2229-14-155

Yang, N., Wang, Y., Liu, X., Jin, M., Vallebueno-Estrada, M., Calfee, E., Chen, L., Dilkes, B.P., Gui, S., Fan, X., Harper, T.K., Kennett, D.J., Li, W., Lu, Y., Ding, J., Chen, Z., Luo, J., Mambakkam, S., Menon, M., Snodgrass, S., Veller, C., Wu, Shenshen, Wu, Siying, Zhuo, L., Xiao, Y., Yang, X., Stitzer, M.C., Runcie, D., Yan, J., Ross-Ibarra, J., 2023. Two teosintes made modern maize. Science (80-.). 382. https://doi.org/10.1126/science.adg8940

Yang, R.S., Xu, F., Wang, Y.M., Zhong, W.S., Dong, L., Shi, Y.N., Tang, T.J., Sheng, H.J., Jackson, D., Yang, F., 2021. Glutaredoxins regulate maize inflorescence meristem development via redox control of TGA transcriptional activity. Nat. Plants 7, 1589–1601. https://doi.org/10.1038/s41477-021-01029-2

Yang, W., Wen, D., Yang, Y., Li, H., Yang, C., Yu, J., Xiang, H., 2024. Metabolomics and transcriptomics combined with physiology reveal key metabolic pathway responses in tobacco roots exposed to NaHS. BMC Plant Biol. 24, 680. https://doi.org/10.1186/s12870-024-05402-z

Ye, J., Coulouris, G., Zaretskaya, I., Cutcutache, I., Rozen, S., Madden, T.L., 2012. Primer-BLAST: A tool to design target-specific primers for polymerase chain reaction. BMC Bioinformatics 13, 134. https://doi.org/10.1186/1471-2105-13-134

You, X., Zhang, F., Liu, Z., Wang, M., Xu, X., He, F., Wang, D., Wang, R., Wang, Y., Wang,

G., Chu, C., Wang, G.-L., Ning, Y., 2022. Rice catalase OsCATC is degraded by E3 ligase APIP6 to negatively regulate immunity. Plant Physiol. 190, 1095–1099. https://doi.org/10.1093/plphys/kiac317

Zanganeh, R., Jamei, R., Rahmani, F., 2021. Response of maize plant to sodium hydrosulfide pretreatment under lead stress conditions at early stages of growth. Cereal Res. Commun. 49, 267–276. https://doi.org/10.1007/s42976-020-00095-0

Zarbakhsh, S., Saleem, A., Fayezizadeh, M.R., Hafeez, M.B., 2025. Interplay between γ-aminobutyric acid metabolism and other crucial amino acid pathways in modulating plant growth and stress conditions. Plant Stress 16, 100883. https://doi.org/10.1016/j.stress.2025.100883

Zhang, H., Wang, M.J., Hu, L.Y., Wang, S.H., Hu, K.D., Bao, L.J., Luo, J.P., 2010. Hydrogen sulfide promotes wheat seed germination under osmotic stress. Russ. J. Plant Physiol. 57, 532–539. https://doi.org/10.1134/S1021443710040114

Zhang, J., Zhang, Y., Song, S., Pan, Y., Wang, H., 2024. Involvement of reactive oxygen species in zinc-deficiency induced inhibition of crown root growth in maize plant. Plant Soil 501, 455–470. https://doi.org/10.1007/s11104-024-06529-6

Zhang, Ke, Wang, F., Liu, B., Xu, C., He, Q., Cheng, W., Zhao, X., Ding, Z., Zhang, W., Zhang, Kewei, Li, K., 2021. ZmSKS13, a cupredoxin domain-containing protein, is required for maize kernel development via modulation of redox homeostasis. New Phytol. 229, 2163–2178. https://doi.org/10.1111/nph.16988

Zhang, Yan, Xu, J., Li, Ruofan, Ge, Y., Li, Y., Li, Ruili, 2023. Plants' Response to Abiotic Stress: Mechanisms and Strategies. Int. J. Mol. Sci. 24, 10915. https://doi.org/10.3390/ijms241310915

Zhang, Yanqin, Yun, F., Man, X., Huang, D., Liao, W., 2023. Effects of Hydrogen Sulfide on Sugar, Organic Acid, Carotenoid, and Polyphenol Level in Tomato Fruit. Plants 12, 719. https://doi.org/10.3390/plants12040719

Zhao, X., Wang, S., Guo, F., Xia, P., 2024. Genome-wide identification of polyamine metabolism and ethylene synthesis genes in *Chenopodium quinoa* Willd. and their

responses to low-temperature stress. BMC Genomics 25, 370. https://doi.org/10.1186/s12864-024-10265-7

Zhao, X., Zhang, Y., Zhang, X., Shan, C., 2023. Putrescine improves salt tolerance of wheat seedlings by regulating ascorbate and glutathione metabolism, photosynthetic performance, and ion homeostasis. Plant, Soil Environ. 69, 512–521. https://doi.org/10.17221/312/2023-PSE

Zheng, K., Martinez, M. del P., Bouzid, M., Balparda, M., Schwarzländer, M., Maurino, V.G., 2025. Regulation of plant glycolysis and the tricarboxylic acid cycle by posttranslational modifications. Plant J. 122. https://doi.org/10.1111/tpj.70142

Zhong, W., Dong, L., Zhang, G., Li, Z., Wang, Q., Jackson, D., Yang, F., 2025. *CUC* genes control boundary domains for shoot meristem maintenance and organ initiation in maize. New Phytol. 248, 706–720. https://doi.org/10.1111/nph.70441

Zhou, H., Chen, Y., Zhai, F., Zhang, J., Zhang, F., Yuan, X., Xie, Y., 2020. Hydrogen sulfide promotes rice drought tolerance via reestablishing redox homeostasis and activation of ABA biosynthesis and signaling. Plant Physiol. Biochem. 155, 213–220. https://doi.org/10.1016/j.plaphy.2020.07.038

Zhou, H., Huang, J., Willems, P., Van Breusegem, F., Xie, Y., 2023. Cysteine thiol-based post-translational modification: What do we know about transcription factors? Trends Plant Sci. 28, 415–428. https://doi.org/10.1016/j.tplants.2022.11.007

A2: Supplementary figures and tables

Supplementary table- 1- List of primers

Gene Name	Gene ID	Forward sequence	Reverse sequence	Primer efficiency
cAPX1.1: cytosolic ascorbate peroxidase 1.1	100285887	5'-TGATGCCACTAAGGGTTCT-3'	5'-ATCACTCCAGGATAGGGTCT-3'	1.99
cAPX1.2: cytosolic ascorbate peroxidase 1.2	103639279	5'-TTCAGCTCCCAAGTGACAAA-3'	5'-TCTAGGCAAACGGAAAATGG-3'	2.045
cAPX2: cytosolic ascorbate peroxidase 2	542476	5'-CTCAGGCAGGTTTTCTCCAC-3'	5'-GGATCAGAGAGGAGGGCTTT-3'	1.998
cAPX4: cytosolic ascorbate peroxidase 4	100193965	5'-GAGGTCTGGATTCGATGGTG-3'	5'-CTGATTTGGATGGTGCTGTG-3'	2.004
cDHAR2: cytosolic dehydroascorbate reductase 2	100273125	5'-CAATGTCCATGCCTACACCA-3'	5'-CAGGTAGCACCAAAGCACAA-3'	2.021
cGR: cytosolic glutathione reductase	100273659	5'-TGTATGGGCTGTGGGTGATG-3'	5'-ATCAGGCTTAACTTGCTGGC-3'	2.041
chAPX7: chloroplastic ascorbate peroxidase 7	100283135	5'-TGCTAAGCTGAGCGATCTTG-3'	5'-TACTCCGCCCTGATCTTTTG-3'	2.036
chDHAR1: chloroplastic dehydroascorbate reductase 1	100382696	5'-CATCAAGACTAAGCCCACCAA-3'	5'-TAGAAACATGGCCACCACAA-3'	1.928
chGlu-Cys ligase: chloroplastic glutamine-cysteine ligase	100381846	5'-AACTGGAGAATTGGCACGGAG-3'	5'-ATCAAATCTCTCAGCGAGCC-3'	2.036

chGR: chloroplastic glutathione reductase	541986	5'-CGTGCTTCGTGGATGTGTTC-3'	5'-CCAATCATGCTTCGGATCAGTC-3'	1.988
cMDAR1: cytosolic monodehydroascorbate reductase 1	100501585	5'-TACTCCCGATCATTCGACCT-3'	5'-GGCAATGACCTTGTTCTCGT-3'	1.837
cMDAR:2 cytosolic monodehydroascorbate reductase 2	100382120	5'-TCAAGGAGCAGAATCCAACA-3'	5' -GCCCTATGTAACCACCTCCA-3'	1.993
cMDAR3: cytosolic monodehydroascorbate reductase 3	100279805	5'-CAGCTCTGTGTATGCCGTTG-3'	5'ATCGATGTCCCTCGTCTTTG-3'	2.045
gECS: gamma-glutamylcysteine synthetase	542026	5'-AGCCATATCTGGACAGATAC-3'	5'-AACCCAAATGAGTCGTCAAAG-3'	1.991
mAPX5: mitochondrial ascorbate peroxidase 5	100193740	5'-GATGCTGTGCTGTTTGAGGA-3'	5'-ACAGGGCACGCTAAGAAAAA-3'	2.015
mAPX6: mitochondrial ascorbate peroxidase 6	100194161	5'-GCAGGGATTCTCTTTGGATG-3'	5'-GCCACTGTGTCGGTTCTTTT-3'	2.023
mDHAR3: mitochondrial dehydroascorbate reductase3	100285047	5'-CGAGGAAAAATGGATTGGTG-3'	5'-TGTTCCATCGCTTGGATCTT-3'	2.01
mMDAR4: mitochondrial monodehydroascorbate reductase	100272772	5'-GTGCAAAGAAGGTGGTGGTT-3'	5'-TTCTTAGCAAGCGAGGGTGT-3'	1.999
P5CR: δ1-pyrroline-5-carboxylate reductase	606449	5'-TGCCCTTGGTCTTGCATCTC-3'	5'-TACCTGCTGGAGAAGTAACCTG-3'	2.028

pAPX3: peroxisomal ascorbate peroxidase	100282326	5'-CCAGATCTGCGAATAAACACAA-3'	5'-AAATACATGTGCACAGAACTGAAA-3'	1.986
ZmABAox1a: Zea mays abscisic acid oxidase 1a	AC194862.4	5'-ATGCTCGTGCTCTTCCACCACCT-3'	5'-TATACCGCCATACCATATCCATCCGCC-3'	2.02
ZmABAox3a: Zea mays abscisic acid oxidase 3a	103647484	5'-ACAGAAAGGGGCGTGAGACCGA-3'	5'-AGGCGAGCAAAGAAGAATTTCAA-3'	2.067
ZmACCO: Zea mays 1-aminocyclopropane-1-carboxylic acid oxidase	542136	5'-TCTACAACCCAGCCAACG-3'	5'-TCTCCCTGTTTATTTATGCC-3'	1.972
Zmactin1	100282267	5'-GATTCCTGGGATTGCCGAT-3'	5'-TCTGCTGCTGAAAAGTGCTGAG-3'	2.088
ZmACS: Zea mays 1-Aminocyclopropane-1-carboxylate synthase	103646045	5'-GCGTGCCCGTACATCCGT-3'	5'-CTGCTTGCGTGCTTTTGACT-3'	2.05
ZmAD: Zea mays arogenate dehydrogenase	100284089	5'-AGTGTCCCTCCGAAACCTA-3'	5'-GCCCTCAGTGAAGTGCC-3'	1.925
ZmADC: Zea mays arginine decarboxylase 1	103638134	5'-GCTACGGCTCAAGGTACCAG-3'	5'-CCGAACTCCACAATGTCCTC-3'	2.071
ZmASS: *Zea mays argininosuccinate synthase*	100274106	5'-CCGCTTCACTCTGTTCTAA-3'	5'-GGGTTTGGTCGCTACTCC-3'	2.008
ZmATF: Zea mays aminotransferase y4uB	100282236	5'-AACCCAGGCGATACGAGATG-3'	5'-TGCTGTGCCCCTTAAACCCA-3'	2.074
ZmCBL: Zea mays cystathionine beta-lyase	100281708	5'-ATGTCTCCAGTGCTCTCCC-3'	5'-CCGACCCTTCAGCATTTTG-3'	2.032

ZmGAPDH: Zea mays glyceraldehyde-3-phosphate dehydrogenase	542367	5'-GAATCAACGGCTTCGGAAGGAT-3'	5'-CCTCAGGGTTCCTGATGCCAAA-3'	2.013
ZmGS3: Zea mays Glutamine synthetase 3	542215	5'-CCCGTGCTGTCACTTTTTGT-3'	5'-CTACACCTATGGCGAAGGC-3'	2.061
ZmL-C-Des: Zea mays L-cysteine desulfhydrase	100193096	5'-TCTACAATGTCACGGAGGAG-3'	5'-GAGCAGGAGAAACCATCAAG-3'	2.079
ZmNCED: Zea mays nine-cis epoxycarotenoid dioxygenase	103626043	5'-CTTTGAGACTTTCCGAGCAG-3'	5'-AGGGAGGATAGGAAGGTAAACA-3'	2.025
ZmNNR1: Zea mays nitrate reductase 1	542278	5'-GGAGGAGGGGTGGAAGTA-3'	5'-TGGCAAGTCGGCTGGTTTAT-3'	2.074
ZmPAO1: Zea mays polyamine oxidase 1	541983	5'-CCAGCAGCAGGAGAGGTTAC-3'	5'-GCGTCAGGGTACTGCTTCTC-3'	2.089
ZmPAO2: Zea mays polyamine oxidase 2	103642073	5'-CACACACACCATCCGCTATT-3'	5'-CATCAGCAGCAGCAAGACC-3'	2.089
ZmPAO3: Zea mays polyamine oxidase 3	103631626	5'-AAAGCCACACACACCATCTG-3'	5'-CAGCAGCAGCAAGACCTGTA-3'	2.088
ZmSAMDC2: Zea mays S-adenosylmethionine decarboxylase 2	542733	5'-TGTGGCTACTCCATGAATGC-3'	5'-CGTAACTGGCGTAGCTGAAA-3'	2.085
ZmSAT3: Zea mays serine acetyltransferase 3	542499	5'-GTAATCCTCCTCGACCACG-3'	5'-GCCTTCTTCCCACCAATCA-3'	1.819
ZmSPDS: Zea mays spermidine synthase	100282933	5'-TGTTCAATTCCATCCCCTAAA-3'	5'-TCCACTGAACTGTGTCTGGAA-3'	2.069

ZmSPMS: Zea mays spermine synthase	732743	5'-ATCCTCGTGTCCGACTTCA-3'	5'-CATCATATTTTCCTTCAGGGAGA-3'	2.049
ZmVP14-1: Zea mays viviparous14-1	100281391	5'-TCCACGACTTCGCCATCACC-3'	5'-CGTCTTCTCCTTGTCCAGCACC-3'	1.999
ZmVP14-2: Zea mays viviparous 14-2	732819	5'-TTCTCGGAGGAGGAACAGAGGA-3'	5'-CCAACTGTAACTCTGGTGTGCG-3'	2.035

Supplementary table 2- Hormone analysis

Targeted phenolics UPLC-US-MS/MS method details - According to Vrhovsek et al 2012. and Pál et al. 2019, with modifications:			
Preparation:	Spike with internal standard at 20 ng/mL level. Extract 0.2g fresh weight with 2x1 ml MeOH:Water=2:1 (v/v%), liquid-liquid partition with n-hexane, centrifuge, collect lower MeOH:Water phase, filter, inject		
UPLC:	**Waters Acquity I-class**		
Column:	Waters HSS T3 column (1.8 µm, 100 mm × 2.1 mm) at 40°C		
inj vol.:	2 µl	**Autosampler temperature:**	10 °C

Gradient conditions			
A: Water (0.1 v/v% formic acid)	**B: Acetonitrile (0.1 v/v% formic acid)**		
Time (min)	Flow rate (mL/min)	A%	B%
0	0.4	95	5
3	0.4	80	20
4.3	0.4	80	20
9	0.4	55	45
11	0.4	0	100
13	0.4	0	100
13.01	0.4	95	5
15	0.4	95	5

Detector 1:	**PDA - 210-700 nm; 20 scans/sec**
Detector 2:	**Xevo TQ-XS with Unispray source**
Resolution:	Unit mass (+/- 0.8 Da)
Impactor voltage:	2 kV
Polarity:	UniSpray Positive

Desolvation temperature:	550 °C
Nebulizer gas:	6.5 bar N_2
Desolvation gas flow:	1000 L/h N_2
Cone gas flow:	450 L/h N_2
Collision gas flow:	0.15 mL/min Argon 5.0

Component name	**Unispray Impactor voltage polarity**	**quant. MS/MS transition**	**Pred.RT (min)**	**RT found (min)**	**Cone voltage (V)**	**Collision energy (eV)**	**Calibrated to**
[2H6](+)-cis,trans-abscisic acid Internal standard	negative	269.1 > 159.1	7.13	7.15	20	10	external
2,6-dihydroxybenzoic acid	positive	153 > 109	3.59	3.40	26	14	external
3,4-dihydroxybenzoic acid	positive	153 > 81	2.12	2.15	24	20	external
4-hydroxybenzoic acid (pHBA)	negative	137 > 93	2.84	2.87	20	12	external
abscisic acid	negative	263.1 > 153	7.18	7.19	20	10	external
apigenin	negative	269 > 117	8.31	8.32	42	34	external
chlorogenic acid	negative	353 > 191.1	2.84	2.83	36	22	external
chlorogenic acid related unknown isomer	negative	353 > 191.1	3.30	3.30	36	22	external
cinnamic acid	positive	131 > 103	7.57	7.55	40	12	external
coniferyl alcohol	positive	163 > 131	4.04	4.09	12	10	external
cryptochlorogenic acid	negative	353 > 173	2.93	2.92	34	14	external
dihydro kaempferol	negative	287 > 259	6.12	6.12	20	14	external
dihydro-phaseic acid	negative	281.14 > 237.2	3.56	3.56	25	12	external
ferulic acid 1 (trans isomer)	positive	195 > 145	4.54	4.56	12	16	external
ferulic acid 2 (possible cis isomer)	positive	195 > 145	4.67	4.69	12	16	ferulic acid 1 (trans isomer)
ferulic acid 3 (possible cis isomer)	positive	195 > 145	4.87	4.90	12	16	ferulic acid 1 (trans isomer)
IAA - Indole3AA	positive	176.1 > 130.1	6.05	6.01	25	14	external
isorhamnetin-3-O-glucoside	positive	479 > 317	5.78	5.79	16	14	isorhamnetin-3-rutinoside
isorhamnetin-3-rutinoside	positive	625 > 317	5.42	5.45	18	20	rutin pos
jasmonic acid	negative	209.12 > 58.9	8.30	8.28	22	12	external
jasmonicAc-Isoleucine/leucin sum	negative	322 > 130	9.95	9.94	25	22	external
kaempferol	negative	285 > 187.1	8.47	8.46	50	26	external
kaempferol-3-O-glucoside	positive	449 > 287	5.51	5.55	16	14	kaempferol-3-O-rutinoside
kaempferol-3-O-rutinoside	positive	595 > 287 and 595 > 85	5.14	5.17	18	20	external
luteolin	positive	287 > 135	7.43	7.40	52	32	external
luteolin-7-O-glucoside	negative	447 > 285	4.67	4.70	46	24	luteolin
luteolin-8-C-glucoside	positive	449 > 413	3.80	3.77	36	30	luteolin
naringenin	negative	271 > 150.9	8.23	8.20	46	18	external
neochlorogenic acid	negative	353 > 191	2.24	2.24	26	18	external

p-coumaric acid neg	negative	163 > 93	4.04	4.08	20	26	external
phaseic acid	negative	279.12 > 139	5.24	5.24	25	12	external
quercetin	negative	301 > 150.95	7.41	7.41	42	24	external
quercetin-3-O-glucoside	positive	465 > 303	4.56	4.58	18	12	quercetin-3-O-glucuronide
quercetin-3-O-glucuronide	positive	479 > 303	4.51	4.52	20	18	external
robinin isomer?	positive	741 > 287	na	4.00	22	38	robinin
rutin (quercetin-Glc-Rha)	negative	609.1 > 300.1	4.22	4.27	90	38	external
salicylic acid neg	negative	137 > 93	5.81	5.83	20	12	external
sinapic acid (trans)	negative	223 > 208	4.67	4.63	14	10	rutin neg
syringetin-3-O-glucoside + syringetin-3-O-galactoside	positive	509 > 347	5.80	5.83	16	14	apin
syringic acid	positive	197 > 182	3.35	3.44	22	14	external
vanillic acid	positive	169 > 93	3.28	3.28	18	14	external
vanillin	positive	153 > 93	4.07	4.10	20	16	external
vanillin isomer	positive	153 > 93	na	3.82	20	16	vanillin
FOLLOWING COMPOUNDS HAVE BEEN SURVEYED BUT NOT DETECTED IN SAMPLES							
3-hydroxybenzaldehyde	positive	123 > 95	4.00	<LOQ	20	10	external
1,3-dicaffeoylquinic acid	negative	515 > 353	3.45	<LOQ	34	20	not calibrated
1,5-dicaffeoylquinic acid	negative	515 > 191	5.22	<LOQ	26	28	not calibrated
2,4-dihydroxybenzoic acid	positive	153 > 109	3.29	<LOQ	24	14	external
2,5-dihydroxybenzoic acid	positive	153 > 109	2.89	<LOQ	26	16	external
3,5-dihydroxybenzoic acid	positive	153 > 109	2.11	<LOQ	26	14	external
4-hydroxycoumarin	positive	163 > 91	6.04	<LOQ	42	18	not calibrated
4-hydroxystilbene	negative	195 > 93	10.70	<LOQ	44	26	not calibrated
4-methylumbelliferone	positive	177 > 121	5.87	<LOQ	34	20	not calibrated
6-methoxyflavone	positive	253 > 108	10.64	<LOQ	16	38	external
acetovanillone	positive	167 > 43	4.59	<LOQ	20	12	external
alpha-viniferin	negative	677 > 437	8.65	<LOQ	48	30	not calibrated
ampelopsin D + quadrangularin A	negative	453 > 359	6.74	<LOQ	42	18	not calibrated
ampelopsin H + vaticanol C-like isomer	negative	905 > 811	8.03	<LOQ	52	30	not calibrated
anthranilic acid	positive	138 > 65	3.96	<LOQ	14	26	not calibrated
apigenin-7-O-glucoside	positive	433 > 271	5.73	<LOQ	24	20	rutin pos
apiin	positive	565 > 271	5.45	<LOQ	26	30	external
astringin	negative	405 > 243	3.57	<LOQ	36	20	external
baicalein	positive	271 > 123	8.8	<LOQ	46	32	external
benzoic acid	negative	121 > 77	5.51	<LOQ	22	12	external
caffeic acid	positive	181 > 145	3.25	<LOQ	16	16	external
caffeic acid + catechin condensation product	negative	451 > 341	5.53	<LOQ	34	18	not calibrated
caftaric acid	negative	311 > 149	2.31	<LOQ	18	10	external
catechin gallate	negative	441 > 289	4.36	<LOQ	34	18	external
catechol	negative	109 > 81	2.88	<LOQ	36	12	external
cathecin	negative	289 > 203	2.83	<LOQ	32	20	external
chrysin	negative	253 > 143	10.19	<LOQ	44	30	external

cis-e-viniferin	negative	453 > 347	7.97	<LOQ	48	22	trans-e-viniferin
cis-gm-viniferin	negative	453 > 347	8.50	<LOQ	46	20	trans-e-viniferin
cis-piceid	negative	389 > 227	5.94	<LOQ	28	20	trans-piceid
cis-resveratrol	negative	227 > 185	7.55	<LOQ	40	22	trans-resveratrol
coniferyl aldehyde	negative	179 > 119	5.71	<LOQ	22	14	not calibrated
daidzein	negative	255 > 199	6.95	<LOQ	30	24	external
daphnetin	positive	179 > 123	3.24	<LOQ	36	22	external
E-cis-miyabenol	negative	679 > 345	8.28	<LOQ	54	30	not calibrated
ellagic acid	negative	301 > 145	4.36	<LOQ	52	34	external
epicatechin gallate	negative	441 > 289	4.33	<LOQ	34	18	external
epicathecin	negative	289 > 203	3.31	<LOQ	34	20	external
epigallocatechin	negative	305 > 125	2.56	<LOQ	32	22	external
epigallocatechin gallate	negative	457 > 169	3.42	<LOQ	32	16	external
eriodictyol	negative	289 > 153	7.29	<LOQ	30	24	external
esculetin	positive	179 > 133	3.49	<LOQ	34	22	external
esculin	positive	341 > 179	2.42	<LOQ	24	18	external
eupatorin-5-methylether	positive	359 > 329	8.90	<LOQ	12	18	not calibrated
fertaric acid	negative	325 > 193	3.15	<LOQ	20	16	not calibrated
fraxin	positive	369 > 207	3.09	<LOQ	32	20	external
galangin	negative	269 > 171	10.3	<LOQ	48	32	external
gallic acid	positive	169 > 79	1.41	<LOQ	28	22	external
gallocathechin	negative	305 > 125	1.98	<LOQ	32	26	external
gallocathechin gallate	negative	457 > 169	3.59	<LOQ	26	20	external
hesperetin	positive	303 > 153	8.52	<LOQ	32	26	external
hesperidin	positive	611 > 449	5.89	<LOQ	18	10	external
isohopeaphenol	negative	905 > 359	7.61	<LOQ	48	38	not calibrated
isorhamnetin	positive	317 > 302	8.72	<LOQ	44	26	external
isorhapontin	negative	419 > 241	4.74	<LOQ	30	36	not calibrated
kaempferol-3-O-glucuronide	positive	463 > 287	5.50	<LOQ	18	16	kaempferol-3-O-rutinoside
laricitrin	positive	333 > 318	7.50	<LOQ	44	26	not calibrated
m-coumaric acid neg	negative	163 > 93	4.76	<LOQ	20	26	external
methyl gallate	positive	183 > 124	2.94	<LOQ	32	22	external
morin	positive	303 > 153	6.81	<LOQ	38	32	external
Myricetin	negative	317 > 150.9	6.30	<LOQ	20	24	external
myricitrin	positive	465 > 319	4.30	<LOQ	14	10	external
naringenin-7-O-glucoside	negative	435 > 273	6.23	<LOQ	16	14	not calibrated
o-coumaric acid neg	negative	163 > 93	5.76	<LOQ	20	26	external
pallidol	negative	453 > 359	6.07	<LOQ	32	14	not calibrated
phloretin	negative	273 > 167	8.29	<LOQ	32	18	external
phloridzin	negative	435 > 273	6.21	<LOQ	32	16	external
picetannol	negative	243 > 159	5.01	<LOQ	40	28	external
procyanidin A2	negative	575 > 285	4.70	<LOQ	42	30	external
procyanidin B1	negative	577 > 289	2.49	<LOQ	32	26	external

procyanidin B2 + B4	negative	577 > 289	3.06	<LOQ	30	24	external
procyanidin B3	negative	577 > 289	2.72	<LOQ	34	22	procyanidin B1
pterostilbene	negative	255 > 240	10.60	<LOQ	40	18	external
quercetin	positive	303 > 153	7.41	<LOQ	50	34	external
quercetin-3,4'-diglucoside	positive	627 > 303	3.62	<LOQ	18	32	quercetin-3-O-glucuronide
quercetin-3-Glc-Ara	positive	597 > 303	4.07	<LOQ	20	22	quercetin-3-O-glucuronide
quercetin-3-O-galactoside	positive	465 > 303	4.25	<LOQ	18	12	quercetin-3-O-glucuronide
quercetin-3-O-glucose-6'-acetate	positive	507 > 303	5.74	<LOQ	20	16	quercetin-3-O-glucuronide
quercetin-3-O-rhamnoside	positive	449 > 303	5.61	<LOQ	16	10	quercetin-3-O-glucuronide
quercetin-3-sulfate	negative	381 > 301	4.55	<LOQ	24	18	not calibrated
quercetin-4'-O-glucoside	positive	465 > 303	5.70	<LOQ	18	12	quercetin-3-O-glucuronide
rhamnetin	positive	317 > 123.01	9.54	<LOQ	48	42	external
robinin	positive	741 > 287	3.81	<LOQ	22	38	external
rosmarinic acid	negative	359 > 161	6.11	<LOQ	30	18	external
sakuranetin	negative	287 > 119	10.24	<LOQ	32	30	external
salicin	positive	309 > 185	2.28	<LOQ	38	16	external
scopoletin	positive	193 > 133	4.53	<LOQ	34	20	external
sinapyl alcohol	negative	193 > 161	4.11	<LOQ	14	10	not calibrated
sinensetin	positive	373 > 343	9.91	<LOQ	8	28	external
syringaldehyde	positive	183 > 123	4.38	<LOQ	20	12	external
syringetin	positive	347 > 153	8.57	<LOQ	40	28	not calibrated
taxifolin	negative	303 > 125	4.76	<LOQ	20	20	external
trans-coutaric acid	negative	295 > 163	2.88	<LOQ	20	12	not calibrated
trans-e-viniferin	negative	453 > 347	8.13	<LOQ	52	22	external
trans-gm-viniferin	negative	453 > 347	8.65	<LOQ	48	22	trans-e-viniferin
trans-piceid	negative	389 > 227	4.25	<LOQ	28	18	external
trans-resveratrol	negative	227 > 185	6.59	<LOQ	38	18	external
trilobatin	negative	435 > 273	6.74	<LOQ	36	18	not calibrated
umbelliferone	positive	163 > 107	4.41	<LOQ	32	20	not calibrated
Z-miyabenol C	negative	679 > 345	8.91	<LOQ	54	36	not calibrated

Supplementary Figures

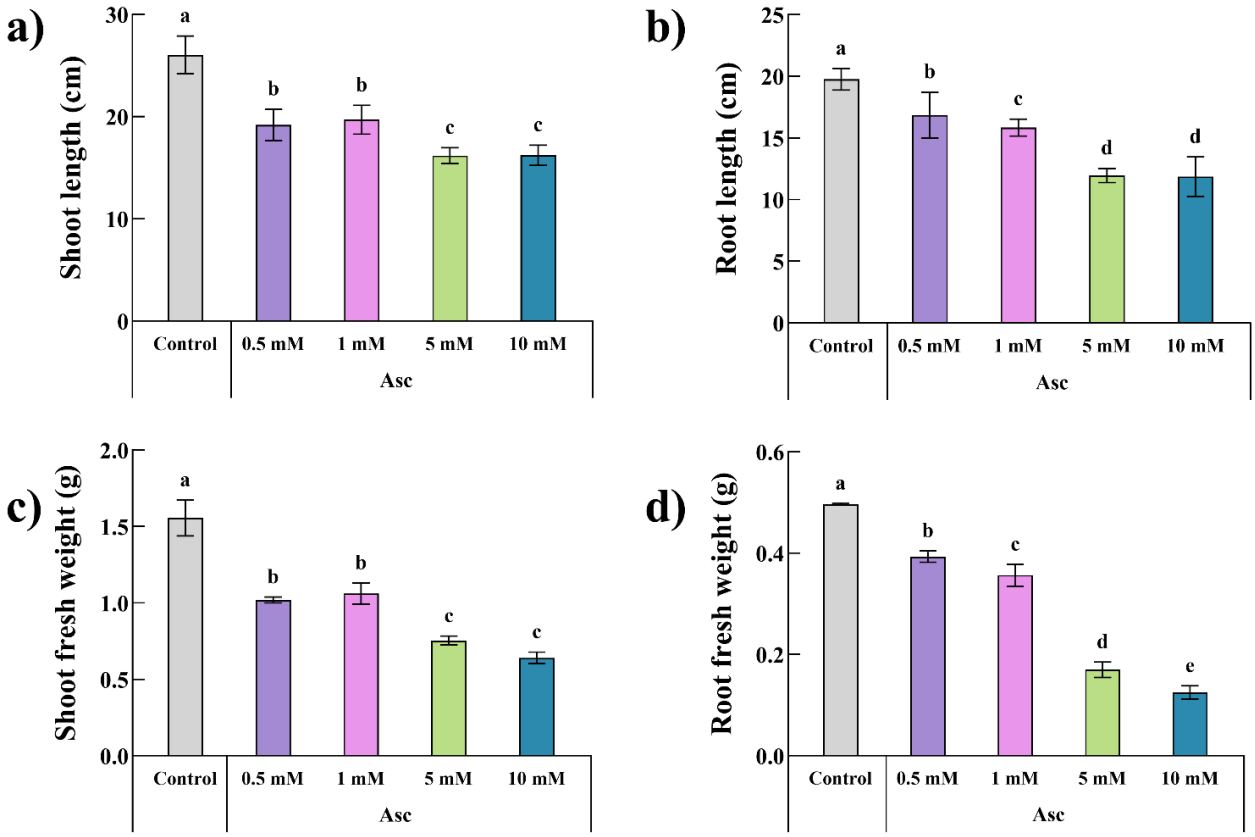

Supplementary Figure 1: The effect of various concentrations (0.5 mM, 1 mM, 5 mM, and 10 mM) of Asc on (a) Shoot length, (b) Root length, (c) Shoot fresh weight, and (d) Root fresh weight, along with the respective control after 3 days of the treatment to determine the final concentration. Values marked with different letters are significantly different from each other at $p \leq 0.05$ levels (One-way ANOVA followed by Fisher's Least Significant Difference (LSD) Test for the data obtained with three biological replicates each).

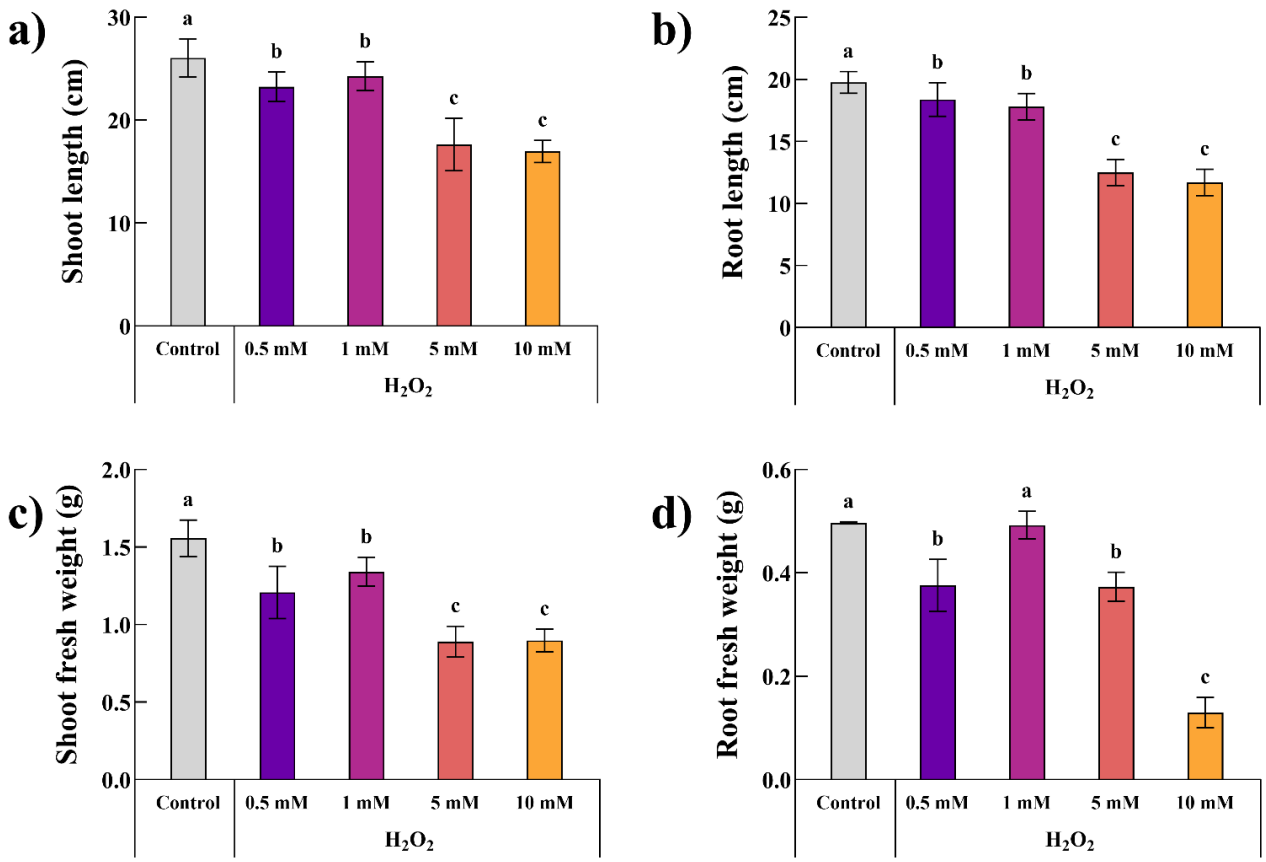

Supplementary Figure 2: The effect of various concentrations (0.5 mM, 1 mM, 5 mM, and 10 mM) of H_2O_2 on (a) Shoot length, (b) Root length, (c) Shoot fresh weight, and (d) Root fresh weight, along with the respective control after 3 days of the treatment to determine the final concentration. Values marked with different letters are significantly different from each other at $p \leq 0.05$ levels (One-way ANOVA followed by Fisher's Least Significant Difference (LSD) Test for the data obtained with three biological replicates each).

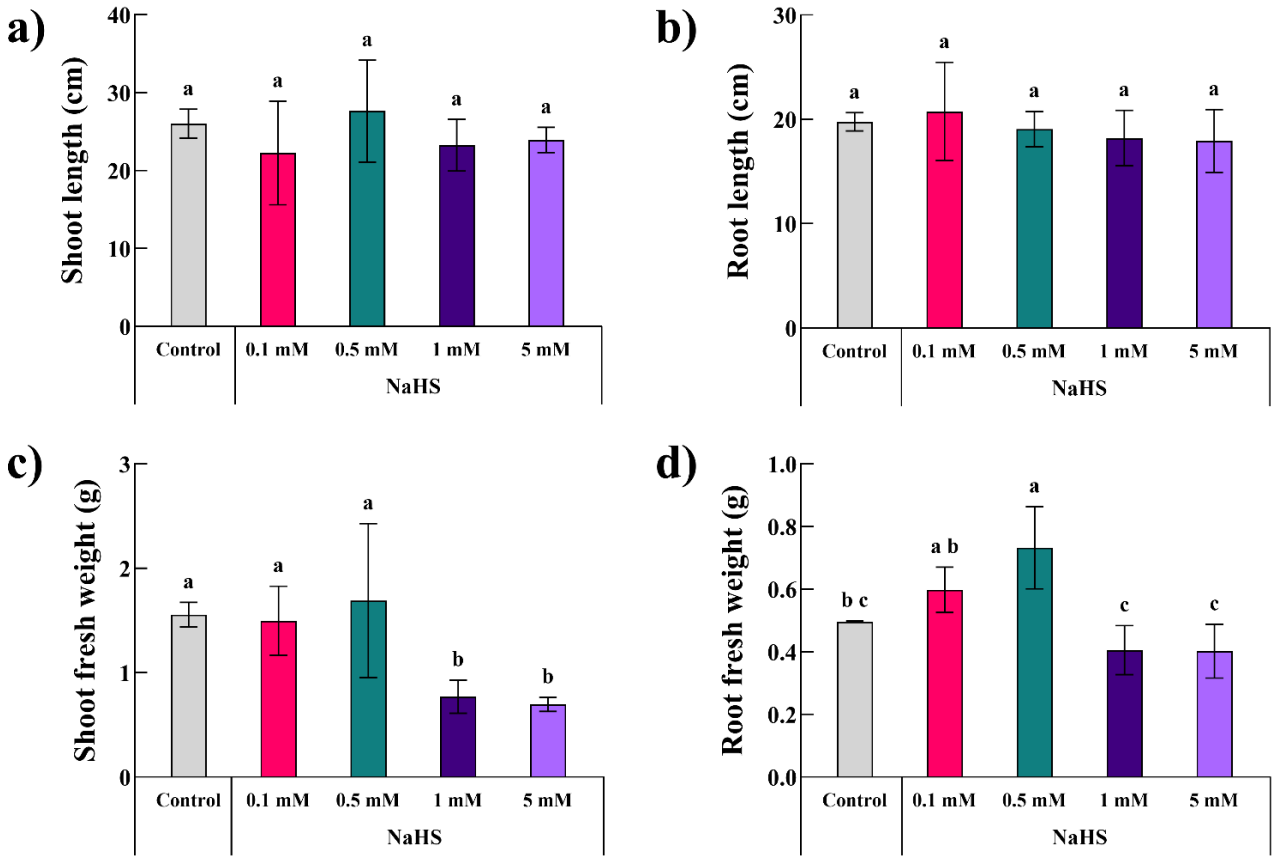

Supplementary Figure 3: The effect of various concentrations (0.1 mM, 0.5 mM, 1 mM, and 5 mM) of NaHS on (a) Shoot length, (b) Root length, (c) Shoot fresh weight, and (d) Root fresh weight, along with the respective control after 3 days of the treatment to determine the final concentration. Values marked with different letters are significantly different from each other at $p \leq 0.05$ levels (One-way ANOVA followed by Fisher's Least Significant Difference (LSD) Test for the data obtained with three biological replicates each).

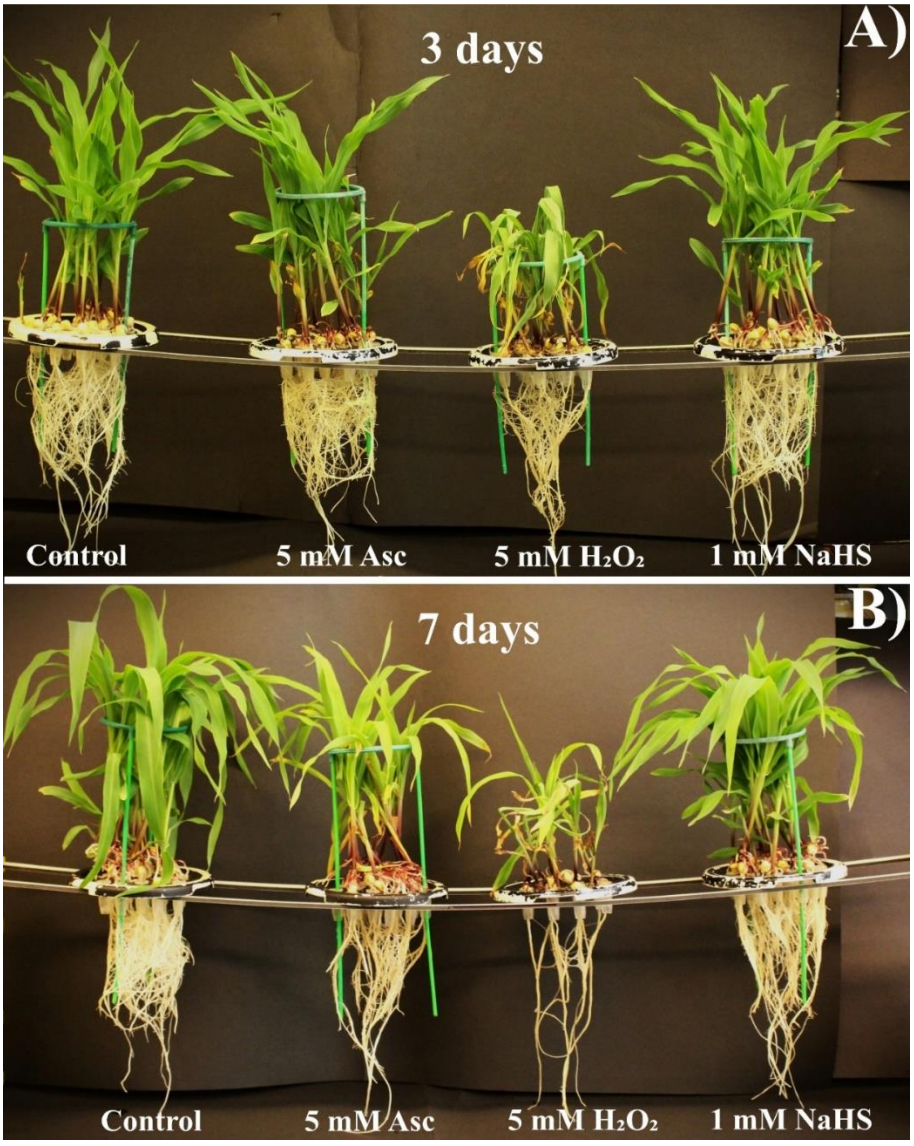

Supplementary figure 4: The effect of 5 mM ascorbate (Asc), 5 mM hydrogen peroxide (H_2O_2), and 1 mM sodium hydrosulfide (NaHS) treatment on plant morphology after 3 days (A) and 7 days (B) of the treatment along with the respective controls.

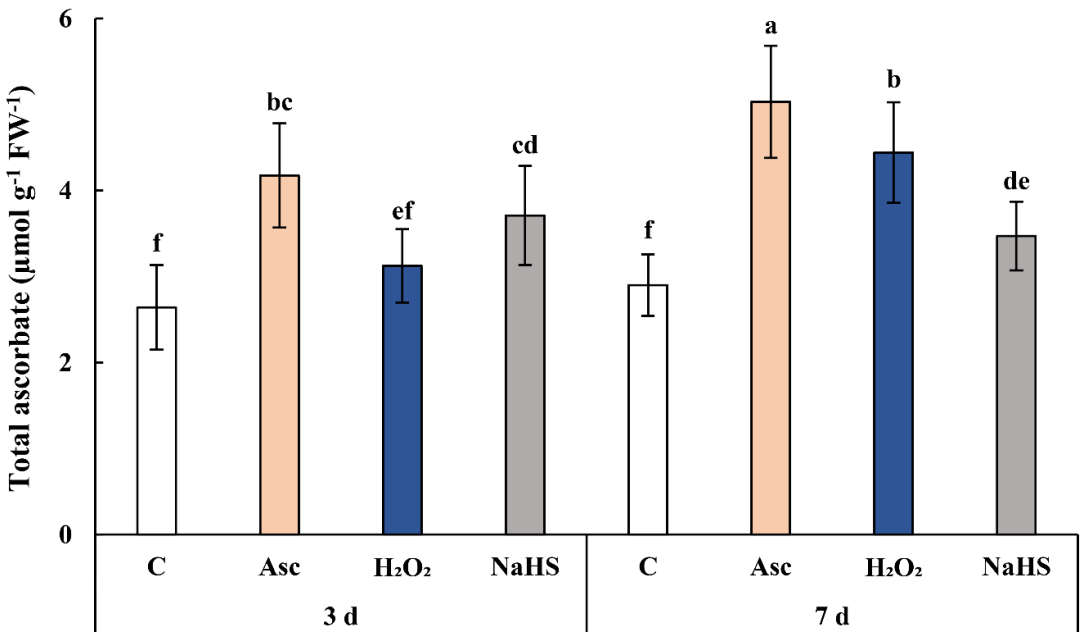

Supplementary figure 5: The effect of 5 mM ascorbate (Asc), 5 mM hydrogen peroxide (H_2O_2), and 1 mM sodium hydrosulfide (NaHS) on total ascorbate levels, after 3 and 7 days of the treatment along with the respective controls (C). Values marked with different letters are significantly different from each other at $p \leq 0.05$ levels (one way ANOVA followed by Fisher's LSD post hoc tests for the data obtained by three independent experiments with three parallels each).

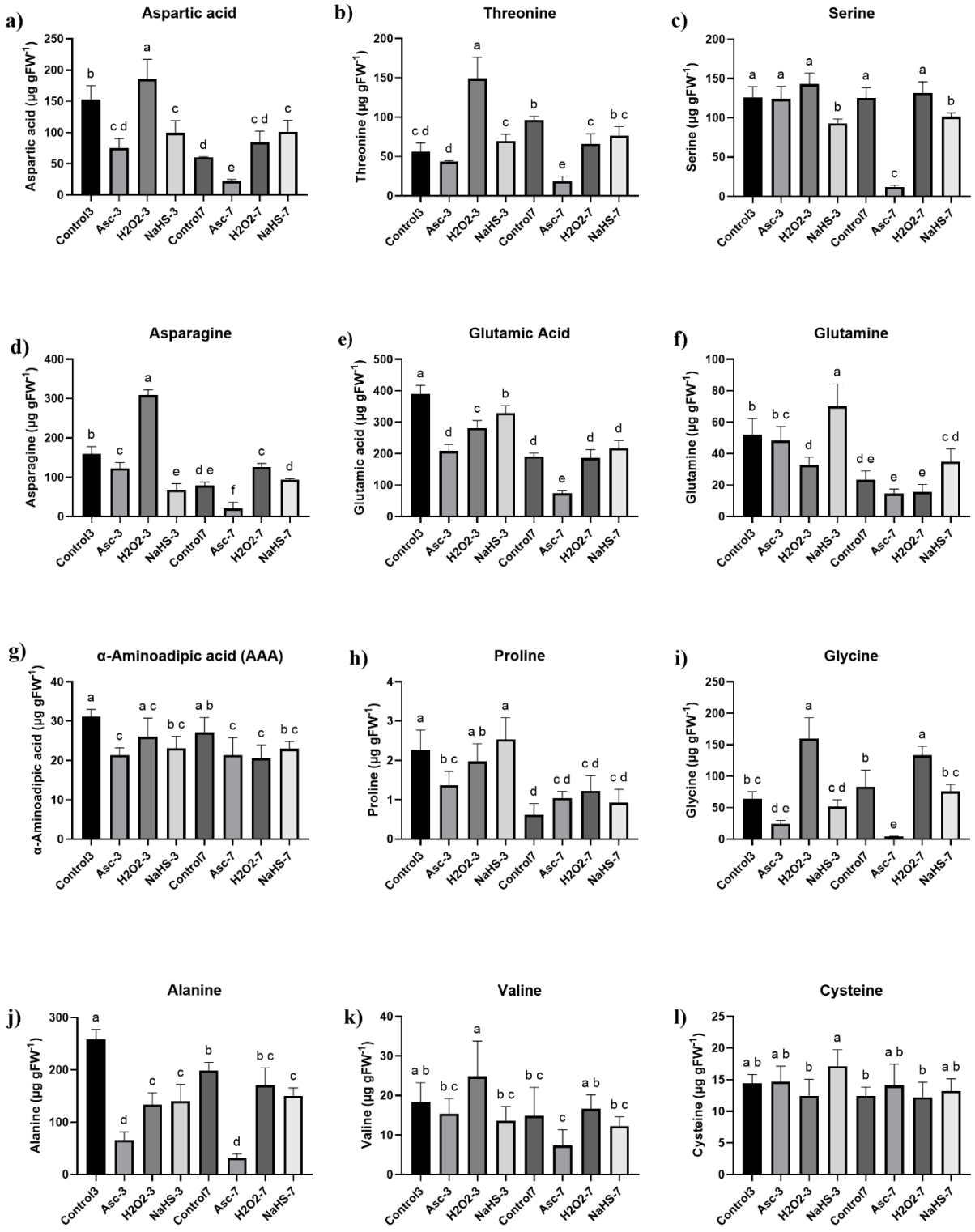
a)
Aspartic acid
Aspartic acid (µg gFW-1)
b)
Threonine
Threonine (µg gFW-1)
c)
Serine
Serine (µg gFW-1)
d)
Asparagine
Asparagine (µg gFW-1)
e)
Glutamic Acid
Glutamic acid (µg gFW-1)
f)
Glutamine
Glutamine (µg gFW-1)
g)
α-Aminoadipic acid (AAA)
α-Aminoadipic acid (µg gFW-1)
h)
Proline
Proline (µg gFW-1)
i)
Glycine
Glycine (µg gFW-1)
j)
Alanine
Alanine (µg gFW-1)
k)
Valine
Valine (µg gFW-1)
l)
Cysteine
Cysteine (µg gFW-1)
Control3
Asc-3
H2O2-3
NaHS-3
Control7
Asc-7
H2O2-7
NaHS-7

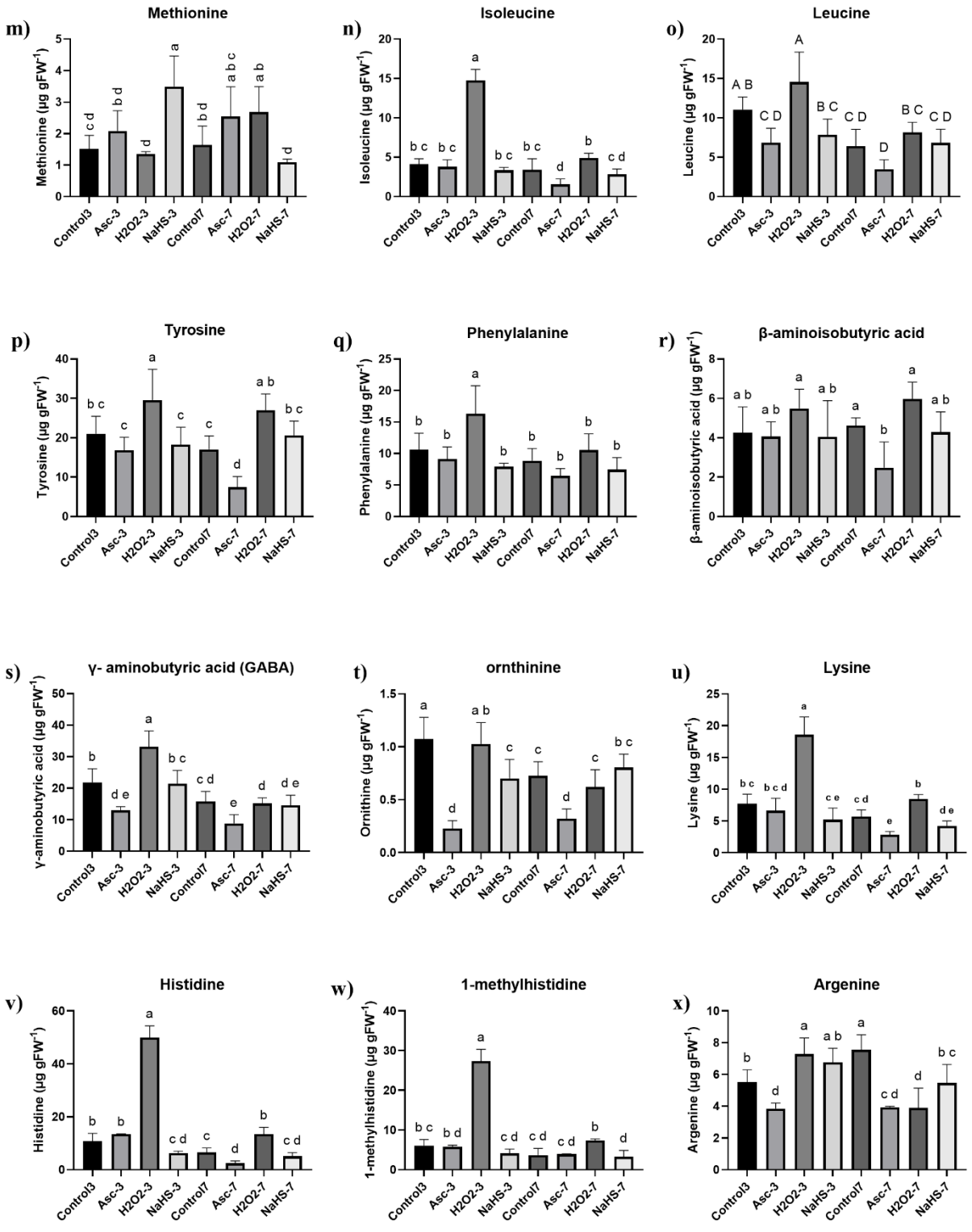

Supplementary figure 6: The effect of 5 mM ascorbate (Asc), 5 mM hydrogen peroxide (H_2O_2), and 1 mM sodium hydrosulfide (NaHS) treatment on individual amino acids, (a) Aspartic acid,

(b) threonine, (c) serine, (d) Asparagine, (e) glutamic acid, (f) glutamine, (g) alpha-aminoadipic acid, (h)proline, (i)glycine, (j) alanine, (k) valine, (l) cysteine, (m) methionine, (n) isoleucine, (o) leucine, (p) tyrosine, (q) phenylalanine, (r) β-aminoisobutyric acid, (s) gamma-aminobutyric acid, (t) ornithine, (u) lysine, (v) histidine, (w) 1-methylhistidine, and (x) arginine after 3 and 7 days of the treatment along with the respective controls (C). Values marked with different letters are significantly different from each other at $p \leq 0.05$ levels (One-way ANOVA followed by Fisher's Least Significant Difference (LSD) Test for the data obtained with three biological replicates each).

A3: List of scientific activities

Articles published in peer-reviewed scientific journals

Serving as a basis for the PhD-thesis:

1. **Singh, K.**, Jobbágy, K., Kulman, K., Pál, M., Benczúr, K., Mednyánszky, Z., Simon-Sarkadi, L., Gulyás, Z., Polgári, D., Riyazuddin, R. and Kocsy, G., 2025. Specific redox regulation of carbohydrate, organic acid, amino acid and polyamine levels in maize seedlings. *Plant Stress*, p.101100. https://doi.org/10.1016/j.stress.2025.101100
2. **Singh, K.**, Asghar, M.A., Jobbágy, K., Kulman, K., Szalai, G., Hamow, K.Á., Soltész, A., Polgári, D., Gulyás, Z. and Kocsy, G., 2025. Different modulation of the redox homeostasis and hormone levels by ascorbate, hydrogen peroxide and hydrogen sulfide in maize. *Physiologia Plantarum*, *177*(2), p.e70215. https://doi.org/10.1111/ppl.70215

Other articles:

3. **Singh, K.**, Gulyás, Z., Athmer, B., Kovács, B., Mednyánszky, Z., Galiba, G., Stein, N., Simon-Sarkadi, L. and Kocsy, G., 2024. Comparative study of free amino acids at metabolite and gene expression levels in *Triticeae* during cold acclimation. *Journal of Plant Biochemistry and Biotechnology*, *33*(4), pp.558-569. https://doi.org/10.1007/s13562-024-00912-1

4. **Singh, K.**, Gupta, R., Shokat, S., Iqbal, N., Kocsy, G., Pérez-Pérez, J.M. and Riyazuddin, R., 2024. Ascorbate, plant hormones and their interactions during plant responses to biotic stress. *Physiologia Plantarum*, *176*(4), p.e14388. https://doi.org/10.1111/ppl.14388
5. Jobbágy, K., **Singh, K.,** Ahres, M., Soltész, A., Kocsy, G., Pál, M. and Gulyás, Z., 2026. Role of Polyamines in the Adaptive Osmotic Stress Response of the Goatgrass *Aegilops biuncialis* Vis. 382. *Journal of Agronomy and Crop Science*, 212(2), p.e70176. https://doi.org/10.1111/jac.70176
6. Jobbágy, K., **Singh, K.**, Kulman, K., Szalai, G., Molnár, I., Panda, S.K., Hamow, K.Á., Gulyás, Z. and Kocsy, G., 2025. Identification of unique osmotic response mechanisms in *Aegilops biuncialis* Vis. compared to *Triticum aestivum* L. Mv9kr1. *Plant Physiology and Biochemistry*, p.110477. https://doi.org/10.1016/j.plaphy.2025.110477
7. Kulman, K., Jobbágy, K., **Singh, K.**, Szalai, G., Pál, M., Benczúr, K., Pálmai, T., Borbély, P., Asghar, M.A., Soltész, A. and Lacek, J., 2025. Differences in the Improvement of Regeneration Ability of Wheat Calli by Ascorbate and H_2O_2 Through Modulation of Their Hormone and Metabolite Profile. *Journal of Plant Growth Regulation*, *44*(11), pp.6630-6646. https://doi.org/10.1007/s00344-025-11849-7
8. Jobbágy, K., **Singh, K.**, Kulman, K., Szalai, G., Pál, M., Molnár, I., Panda, S.K., Kocsy, G. and Gulyás, Z., 2025. Differences in the Metabolic Response to Osmotic Stress Between *Triticum aestivum* L. and Two Ecologically Disparate *Aegilops biuncialis* Vis. Genotypes Differing in Drought Tolerance. *Journal of Agronomy and Crop Science*, *211*(5), p.e70110. https://doi.org/10.1111/jac.70110
9. Gulyás, Z., Ahres, M., Pálmai, T., Kulman, K., Tahmasebi, Z., **Singh, K.**, Jobbágy, K., Tarkowská, D., Dobrev, P., Vanková, R. and Borbély, P., 2025. Blue or far-red light supplementation induced pre-hardening in the leaves of the *Rht12* wheat dwarfing line: hormonal changes and freezing tolerance. *Physiologia Plantarum*, *177*(2), p.e70112. https://doi.org/10.1111/ppl.70112
10. Riyazuddin, R., **Singh, K.**, Iqbal, N., Labhane, N., Ramteke, P., Singh, V.P. and Gupta, R., 2023. Unveiling the biosynthesis, mechanisms, and impacts of miRNAs in drought stress resilience in plants. *Plant Physiology and Biochemistry*, *202*, p.107978. https://doi.org/10.1016/j.plaphy.2023.107978

Book Chapters

1. Kocsy, G., Gulyás, Z., Kulman, K., Jobbágy, K., **Singh, K.**, Panda, S.K. (2025). Redox Regulation of the Response to Abiotic Stresses by MicroRNAs and Transcription Factors in Plants. In: Panda, S.K., Khan, M.A. (eds) Plant Functional Genomics for Abiotic Stress Resilience. Plant in Challenging Environments, vol 7. Springer, Cham. https://doi.org/10.1007/978-3-032-01704-8_4
2. **Singh, K.**, Abbas, S.H., Singh, S., Iqbal, N., Kocsy, G., Pérez-Pérez, J.M. and Riyazuddin, R., 2025. Deciphering the Plants' Response to Flood-Induced Hypoxia and Anoxia at the Molecular Level. In *Plant Flooding: Sensitivity and Tolerance Mechanisms* (pp. 93-112). Cham: Springer Nature Switzerland. https://doi.org/10.1007/978-3-031-83068-6_5
3. Iqbal, N., Nauman, M., Jamil, H.M.A., Kondak, S., **Singh, K.** and Riyazuddin, R., 2025. Effects of Flooding Stress on Plant Developmental Stages and Antioxidant Defense System and Its Alleviation Through Agronomic Measures. In *Plant Flooding: Sensitivity and Tolerance Mechanisms* (pp. 55-73). Cham: Springer Nature Switzerland. https://doi.org/10.1007/978-3-031-83068-6_3

Articles and abstracts published in conference books

1. **Singh K.**, Pál M., Kocsy G. (2023): Redox control of polyamine metabolism in maize. 3rd Plant Polyamine Research Workshop. 12-13 October 2023, Budapest and Martonvásár, Hungary. Book of Abstracts (2023), p. 28.
2. Jobbágy K., **Singh K.**, Kulman K., Szalai G., Pál M., Kocsy G. (2023): Effect of osmotic stress on antioxidants and polyamines in cereals. 3rd Plant Polyamine Research Workshop. 12-13 October 2023, Budapest and Martonvásár, Hungary. Book of Abstracts (2023), p.18.
3. **Singh K.**, Jobbágy K., Kulman K., Szalai G., Hamow, K.Á., Kocsy G. (2024): Redox modulation of hormones and metabolites in maize. FIBOK 2024, April, Martonvásár, Hungary. ISBN 978-615-6448-45-3.
4. Jobbágy, K., **Singh, K.**, Kulman, K., Szalai, G., Pál, M., Molnar, I., Kocsy, G. (2024): Changes of stress-responsive parameters in different cereal genotypes during osmotic stress. FIBOK 2024, April, Martonvásár, Hungary. ISBN 978-615-6448-45-3.

5. **Singh, K.**, Jobbágy, K., Kulman, K., Szalai G., Hamow, K.Á., Kocsy, G. (2024): Redox balance and growth modulation in maize under oxidative stress. XIV. Magyar Növénybiológiai Kongresszus: Összefoglaló kötet (2024) p. 93.

Oral and Poster presentations

1. **Singh, K.** (2024): Redox modulation of hormones and metabolites in maize at FIAtal NÖVénybiológusok ELŐadássorozatát PLANT BIOLOGISTS lecture series on March 2024, Debrecen, Hungary.
2. **Singh K.**, Pál M., Kocsy G. (2023): Redox control of polyamine metabolism in maize. 3rd Plant Polyamine Research Workshop. 12-13 October 2023, Budapest and Martonvásár, Hungary.
3. **Singh K.**, Jobbágy K., Kulman K., Szalai G., Hamow, K.Á., Kocsy G. (2024): Redox modulation of hormones and metabolites in maize. FIBOK 2024, April, Martonvásár, Hungary.
4. **Singh, K.**, Jobbágy, K., Kulman, K., Szalai G., Hamow, K.Á., Kocsy, G. (2024): Redox balance and growth modulation in maize under oxidative stress. XIV. Magyar Növénybiológiai Kongresszus: Összefoglaló kötet (2024).
5. Soltész, A., Jobbágy, K., **Singh, K.** and Gulyás, Z. (2025): Ectopic expression of wheat *TaCbf14* and *TaCbf15* genes in barley induces cold tolerance and reveals trichome- and anthocyanin-associated responses. 8th Conference on cereal biotechnology and breeding. 10-13 November 2025, Budapest, Hungary.
6. Jobbágy, K., **Singh, K.**, Kalapos, B., Farkas, Z., Ahres, M., Soltész, A., Galiba, G., Kocsy, G. and Gulyás, Z. (2025): Characterisation of auxin transport-related *HvACT1* and *HvGNOM* in barley. 8th Conference on cereal biotechnology and breeding. 10-13 November 2025, Budapest, Hungary.
7. **Singh, K.**, Jobbágy, K., Kulman, K., Szalai, G., Hamow, K.Á., Gulyás, Z., Kocsy, G. (2025): Redox-mediated changes in hormones and metabolites in maize seedlings. Plant Biology Europe 2025, 25-28 June 2025, Budapest, Hungary.
8. Kulman, K., Jobbágy, K., **Singh, K.**, Török, A.L., Cadar, O., Vanková, R., Szalai, G., Ahres, M. and Kocsy, G. (2025): Redox regulation of the response to cadmium in wheat. Plant Biology Europe 2025, 25-28 June 2025, Budapest, Hungary.

9. **Singh, K.** (2024): Specific redox regulation of carbohydrates, organic acids, amino acids, and polyamines levels in maize seedlings at FIAtal NÖVénybiológusok ELŐadássorozatát PLANT BIOLOGISTS lecture series on March 2026, Budapest, Hungary.

Mobility scholarships received

Pannónia Scholarship for Stipendium Hungaricum students for a short-term mobility research at Karl-Franzens-Universität Graz, Institut für Biologie, Graz, Austria. Financed by the Hungarian University of Agriculture and Life Sciences for the years 2025 (contract number: PANP-00005-001/2024/SMT-G-024) and 2026 (contract number: PANP-00005-001/2024/SMR-G-005).

“PROM - Short-term academic exchange” to the University of Lublin, Poland, financed by the National Agency for Academic Exchange and co-financed by the European Union (application number: PROM.IN.SD.2026:9).

10. ACKNOWLEDGEMENT

I am deeply thankful to God for blessing me with good health, intellectual ability, and determination, which have continuously motivated me throughout my research journey.

I am grateful for the opportunity to conduct my research at HUN-REN ATK, and for the constant support and encouragement from MATE and the Tempus Public Foundation. This support provided an enriching and stimulating research environment that greatly contributed to my academic and professional growth. I am profoundly indebted for this opportunity.

I extend my sincere appreciation to the many individuals whose guidance and support were instrumental in the successful completion of this project. Foremost among them are my supervisors, Dr. Gábor Kocsy and Dr. Dávid Polgári. Their guidance, patience, and encouragement steered me through this journey. I am also thankful to my fellow lab members- especially Dr. Zsolt Gulyás (Honorary PhD supervisor), Kristóf Jobbágy, Kitti Kulman, Dr. Mohamed Ahres, Dr. Zsuzsanna Farkas, Dr. Péter Borbély, and Zahra Tahmasebi, whose contributions and support were invaluable at every stage of my research.

I am forever in debt to Dr. Riyazuddin Riyazuddin, who has been a constant mentor not only in my scientific journey but also in life. His teachings on patience, perseverance, and hard work have been a guiding light during challenging times. Also, his scientific insights helped in improving the quality of this research. I also sincerely thank Dr. Kamirán Áron Hamow, Dr. Kinga Benczúr, Dr. Magda Pál, Dr. Zsuzsanna Mednyánszky, Dr. Lívia Simon-Sarkadi, and Dr. Gabriella Szalai for generously sharing their expertise. Their valuable contributions helped me complete the experimental work and conclude my PhD in a timely manner. I would also like to express my heartfelt thanks to Ms. Mónika Fehér for her unwavering support, from helping me settle into a new country to assisting with successful research in the laboratory.

I am profoundly grateful to my parents, my little brother, my family and friends (especially Akansha and Vrinda), whose love, encouragement, and understanding have been a constant source of strength throughout this journey.

Finally, I extend my sincere thanks to everyone who contributed to my academic journey.